CRANFIELD UNIVERSITY

Omkar Vitthal Gulavani

Non-linear Finite Element Analysis led design of a Novel Aircraft Seat against Certification Specifications (CS 25.561)

School Of Engineering

Master of Science by Research
Academic Year: 2010 - 2011

Supervisors: Dr Kevin Hughes and Professor Rade Vignjevic
January 2011

CRANFIELD UNIVERSITY

School Of Engineering

Master of Science by Research

Academic Year 2010 - 2011

Omkar Vitthal Gulavani

Non-linear Finite Element Analysis led design of a Novel Aircraft Seat against Certification Specifications (CS 25.561)

Supervisors: Dr Kevin Hughes and Professor Rade Vignjevic

January 2011

Executive Summary

Seeking to quench airliners' unending thirst for lightweight, reliable and more comfortable seating solutions, designers are developing a new generation of slim economy – class seats. Challenge in front of the designers is to carve out additional "living space", as well as to give a "lie – flat" experience to air travellers with strict adherence to safety regulations. Present research tries to address all these industry needs through an innovative and novel "Sleep Seat".

A generous angle of recline (40 degree), movement of "Seat Pan" along the gradient, fixed outer shell of backrest, and unique single "Forward Beam" design distinguishes "Sleep Seat" form current generation seats. It is an ultra-lightweight design weighing 8kg (typical seat weight is 11kg). It satisfies "Generic Requirements (GR2)" which ensures "Comfort in Air". It will be a "16g" seat, means it can sustain the "Emergency landing" loads as specified by "Certification Specifications (CS 25.561 and CS 25.562)". For present research, only CS 25.561 has been considered.

Since, the design of "Sleep Seat" is still in its conceptual phase, it is not possible to build the prototypes and their physical testing, due to costs and time involved. "Finite Element Analysis (FEA)" is a useful tool to predict the response of the structure when subjected to real life loads. Hence, the aim of research being undertaken is to develop a detailed FE model of the complete seat structure, which will help designers to identify potential weak areas and to compare different design concepts virtually, thereby reducing the development cycle time.

In order to avoid handling of large number of design variables; major load carrying members (called Primary Load Path) i.e. Forward beam and leg; are designed for the most critical "Forward 9g" loads; using FEA results as a basis. A robust framework to verify the FEA results is developed. "Sequential Model Development Approach"; which builds the final, detailed FE model starting from preliminary model (by continuously updating the FE model by addition of details that are backed up by pilot studies); resulted in a FE model which could predict

the stress induced in each of the components for applied CS 25.561 loads along with “Seat Interface Loads”. The “Interface Load” is the force exerted by the seat design on the floor and is one of the main contributing factors in seat design.

“Optistruct” is used as a solver for linear static FEA, whereas “Abaqus / Standard” is used for non-linear FEA. Stepwise methodologies for mesh sensitivity study, modelling of bolt-preload, representing bolted joint in FEA, preventing rigid body motion, and obtaining a converged solution for non-linear FEA are developed during this research.

Free-Shape Optimisation is used to arrive at a final design of Seat-leg. All the findings and steps taken during this are well documented in this report. Finally, a detailed FE model (involving all the three non-linearities : Contact, material and geometric) of the complete seat structure was analysed for the loads taken from CS 25.561, and it was found that design of “Forward beam” and leg are safe against CS 25.561.

Therefore, all the aims and objectives outlined for this research were accomplished. For future work, first area to look for, would be validation of present FEA results by experimental testing. FE model to simulate dynamic loads CS 25.562 can be developed followed by design improvements and optimisation.

Keywords:

Sleep Seat, CS 25.561, Non-linear FEA, Abaqus/Standard, Free Shape Optimisation

ACKNOWLEDGEMENTS

I would like to dedicate this research to my parents and to my younger brother, Ashish.

First of all, I am thankful to my childhood friend Ajay Patil, who helped me from the beginning to prepare a database of UK Universities enabling me to pursue my Masters and continued giving me support until my flight was booked to Cranfield.

I am thankful to Dr. Kevin Hughes for his guidance. He gave me the freedom to try my ideas and helped me in every possible way, even to the extent of sharing his office with me for which I am very grateful. In addition, I was inspired by his tremendous energy, flexible nature, humbleness and interests in many fields of engineering.

I consider myself fortunate to have had the chance to work under Professor Vignjevic Rade .His brilliance, innovative ideas and ability to foresee problems have been some of the major driving forces for this research.

I would like to express my gratitude to Mr. Jason Brown, for sharing his knowledge and guiding me towards the right path when the time demanded.

I would like to thank Mrs. Marion Bastable for helping me with all the paper work and offering valuable suggestions.

Had it not been for Eileen and Stephan Cave, my life after University hours would have been boring. Due to their caring and understanding nature, I did not miss my parents.

Last but not least, I am thankful to Mr. Dominic Robinson, CEO of BlueSky Designers Limited, UK for sharing all the information related to the design and development of the “Sleep Seat”. Because of his manufacturing expertise, I was introduced to the latest practices and technologies used in the aerospace industry.

TABLE OF CONTENTS

LIST OF FIGURES

LIST OF TABLES

1 Introduction

Aviation remains the safest mode of transport in today's world. There are currently more than 17,700 passenger aircraft in commercial passenger service in the world [1]. As per the world annual traffic report, it is envisaged that air traffic will double in 15 years [1]. In 2010, all airliners are estimated to carry approximately 4.5 trillion of world traffic based on RPK (Revenue passenger Kilometres) index.

On one hand, growing the number of air-travellers paints a very cheerful picture for the airliners offering an opportunity for expanding their business portfolio, whereas on the other hand; increasing fuel prices, economic downturn and increased competition from regional aircraft operators are minimising profit margins. In order to attract more customers, airlines are providing more comfort "In Skies" e.g. Air New Zealand has offered "lie-flat" experience in economy class segment for its Sky-Couch [2]. In order to balance increasing consumer demands and decreasing profit margins; airliners want to "Fit In" as many travellers as possible, without sacrificing comfort and safety. "Fit In" involves increasing number of seats in the present aircraft designs, thereby reducing the seat pitch. As passengers spend most of their time in their seats during travel any decrease in seat pitch will lead to passenger discomfort and reduction in survivable space around them in post crash situation. So, safety becomes paramount in such situations.

Aviation governing bodies like the Federal Aviation Authority (FAA) and the European Aviation Safety Agency (EASA), aircraft manufactures and universities have been constantly involved in activities, which ensure the dream of "Safe-Flying" and maintain uniform safety standards across the globe. The European Commission has drawn the following design objectives for improving survivability in the event of crash [3],

- Designing built-in crashworthiness, so that the forces transmitted to occupants are within human tolerance limit,

- Developing structural components that determine the manner in which the fuselage deforms and dissipates energy during a crash,
- Creating the airframe structure that maintains a living space around the occupant and generates very low impact forces induced in occupants throughout the crash event.

Hence, the daunting task for today's designers is to design a slim and lightweight seat that will offer more comfort to air traveller and will be reliable. With the help of slim designs, the number of seats in an aircraft can be increased, without reducing the seat pitch.

1.1 New Product Development (NPD) using Finite Element Analysis (FEA)

All aircraft seats must be tested in order to meet either FAA regulations or Certification Specifications (CS). Certification tests require the most critically loaded seat to withstand dynamic inertia loads in two directions with seat pre-deformation and static loads in different directions, summing up to eight or nine tests [16], [38]. As per the requirement, the seat design must be proved with physical (experimental) test data. Disadvantages of experimental testing are,

- Usually for testing, the number of samples required is less as compared to those in mass production. Manufacturing, Quality Control Costs and time involved; per test sample is quite high as those are made from general manufacturing processes and machines by skilled workers and without any automated techniques. Cost of test set-up, skilled manpower, overheads and consumable items, data acquisition equipments, inspection and documentation and cost of jigs and fixtures add together to thousands of dollars.

- Physical tests are destructive in nature. So, one does not want to run unnecessary tests. In addition, one does not want to run the tests blindly without really knowing what is going on i.e. without initial estimates. Moreover, for each test, new seat structure is required so the additional

cost of the seat escalates the overall testing cost rapidly. Hence, physical testing is extremely expensive and time consuming.

- Physical test is basically a “Pass or Fail” ritual. It does not give a chance to the designer to study precisely the sequence of failure or the weakest link before failure.

- Overall, if a design fails to meet the performance standards for any of the tests, then all the tests need to be repeated with new design; making it further costly. This can shatter the aircraft delivery schedule. A recent example is the delayed delivery of Boeing 777-300 ER and of Airbus A380, A330-300 due to problems during certification of seats manufactured by Japanese Seat maker Koito Industries [4].

- For a global player, like B/E Aerospace, aircraft are built in United States, Germany or France [5]. The overall aircraft is built based on specific schedule, which requires that sub-systems such as seats should arrive at a specific time. If the Certification programme is delayed due to test failures then the entire process of airplane assembly stops and huge investments are at stake. Therefore, the enormous pressure builds up to be successful in next test.

The only possible solution to reduce the time and money involved in physical testing is to use Virtual Product Development (VPD) tools such as Finite Element Analysis (FEA) that simulate the testing scenario and predict the static and dynamic behaviour of the structure. FEA is a numeric technique for predicting the behaviour of the structure when subjected to natural factors such as loads, vibrations and heat. It is a very powerful tool for virtual prototyping, which shortens the build-test-break cycle from months to weeks of computer calculations. It also allows designers to quickly compare number of design options that was not possible earlier due to time and budget. It prevents dangerous under-designed products as well as costly over-designed parts. Recent developments in High Performance Computing (HPC) and simulation software have made it possible to analyse complex models at low costs.

Nowadays, FEA tools are not only used for post design predictions but also to derive the optimum design concepts. Though the need of physical testing has not been completely eliminated, number of prototypes built and tested before mass production has been dramatically reduced. For B/E aerospace, simulation tools have helped to reduce the number of trials of physical testing just to one, which in turn has saved one-week time of product development and a whopping $35000 per test [5]. In case, when a seat has failed to satisfy the test criteria, FEA has helped them to determine the causes and to suggest design revisions and their “Pass rate” on second tests is 100% [5]. Thus, FEA helps to,

- Compare “What if” design combinations without fabricating test samples and subsequent testing.
- Generate sufficient data to estimate “How close to failure” or “How much Over-engineered” a particular component or the entire assembly is. This is an incredible aspect if compared with “Pass or Fail” test result.
- Verify impact of a design change on performance on the same day thereby reducing the “Product Lead time”. Thus, it becomes easier to meet the delivery schedules, which increases “Customer Satisfaction”.
- Save lot of unnecessary physical tests (once good co-relation has been achieved in between FEA and testing) and repetition of tests.
- Assist physical testing by giving an insight for “What to look for during testing”.

Going further, FAA has released Advisory Circular (AC) 20-146 on May 19th, 2003, which sets forth acceptable means to demonstrate compliance to “Parts 25 – 25.562” and “Technical Standard Order (TSO) C127/C127a; by “Computer Modelling Analysis Techniques”. This is a major step towards “Certification By Analysis (CBA)”, the ultimate goal of which would be to replace physical testing by virtual simulation thereby significantly reducing the costs and time consumed during Certification [38].

On a similar note, the main role of current research undertaken is to develop a FEA methodology, which will compare different design concepts of an aircraft seat and will aid to arrive at a feasible and reliable design concept, in a faster and economical way.

1.2 Theme behind present Research

Any New Product Development (NPD) starts with a particular theme, which is derived from personal experiences, market survey, brand establishment, industrial culture or improvement over existing products. The theme behind design and development of new seat is: writing a new chapter of “comfort in air”, propelling “airliners profit” through cost effective solutions, and boosting confidence of the air traveller through safer designs. Keeping this in mind, following key areas would be addressed by new design.

- Seat should provide generous angle of recline for greater comfort.
- Seat design should be such that, area in front of the passenger should always remain constant irrespective of activities of front passenger. When passenger sitting in the front, reclines his/her seat, passenger at the back gets irritated due to invasion of his/her space.
- Common problem faced by tall passengers is that they cannot flex their legs due to undercarriage of the front seat. New design should try to maximise the legroom.
- An airliner would love to keep the number of parts in the seat assembly to its bare minimum. Therefore, part count in new design should be reduced thereby minimising cost and hasten during assembly.
- Fuel prices are ever increasing and there is an additional pressure to cut carbon emissions. Ultra lightweight seat designs can contribute in reducing the fuel consumption.

- Gone are the days of mass production. Present era is of limited edition with a range of different designs of passenger flights. New seat should be suitable for any business model i.e. Scheduled, Charter flights in aviation and for national and international rail travel applications.

- From safety aspect, new seat should be a “16g seat” which will satisfy the structural requirements as specified by CS 25.561 and CS 25.562.

To summarise, new seat should - be lightweight, increase passenger comfort and fulfil “16g” requirements.

1.3 Objective and Scope Of project

Objective of the project is - Analysis-led design of a novel aircraft seat to demonstrate compliance with Crash Safety Certification requirements. Focus will be to achieve “9g” compliance.

Scope of the project encompasses,

1. Review existing literature concerning design of aircraft seats / different configurations. This aspect will not only consider the crash certifications, but additional safety design features a seat must incorporate.

2. This research will develop a practical modelling methodology that can be used to assist designers in assessing the suitability of a chosen seat configuration, through a sound understanding / application of the FE Method, together with demonstrating a critical assessment of the quality of the numerical results through appropriate verification methods.

3. FE Models developed will be piecewise, as design of leg is critical for static 9g load case. This task will involve mesh sensitivity studies, prudent choice of element formulation, techniques for modelling bolt behaviour / preload and non-linear contact.

4. Analysis led design of leg/seat track interface to investigate reaction loads generated and integrity of seat track. Develop detailed non-linear FE Model(s) that represent the load path of the seat for 9g load cases.

5. Additional design work may be required if poor performance is demonstrated, which may be through manual design modifications, or the use of commercial optimisation tools.

6. Develop a full-scale FE Model of the complete seat and demonstrate compliance for static load case.

1.4 Industrial Partner – BlueSky Designers Limited, England

BlueSky Designers Limited (here onwards called as “BlueSky) based at Surrey Research Park, Guildford- England, is developing this innovative seat. The company is spearheaded by Mr. Dominic Robinson [6].

The 600 series -Stella designed by BlueSky has been acclaimed as “The most exciting development in aviation in over 30 years”. Company has received many awards including “British Invention of the Year’s prestigious Diamond Award – 2006”, “International Invention of the Year’s prestigious World Obelisk runner up– 2006” and also a research grant from SEEDA from 2008 to 2010 [6]. Recently, company has won “Supplier’s Innovation Challenge for 2010” under “Aero-Structures” category [7].

1.5 Structure of the Report

Chapter 2 takes an overview of different terminologies used in aviation safety, historical development of aviation safety, contribution of seat design in reducing the causalities in case of accidents, safety and comfort requirements desired from design of a seat. It identifies “Certification Specifications (Cs 25.561)”, as a design guideline for “Sleep Seat”.

Chapter 3 describes the components involved in the design of “Sleep Seat”, novelty of design and how it meets the comfort standards specified by Generic Requirements (GR2).

Chapter 4 presents the overall project plan for the design and development of “Sleep Seat”. It explains the development of analytical calculations (spreadsheet) and findings of “Mesh Sensitivity Study” performed for “Forward Beam”. It also states how the spreadsheet was used to transfer the inertia loads (according to CS 25.561) from “Global Co-ordinate system” to equivalent forces and moments in “Local Co-ordinate system” of “Forward beam”.

Chapter 5 presents results of “Mesh Sensitivity Study” done for leg and advantages of ordered node-numbering scheme. It boosts confidence in the FEA procedure being developed in this research, by showing that the FEA results obtained so far, satisfy critical quality checks.

Chapter 6 revolves around the procedure derived for simulation of “Bolt Pre-load” using Abaqus / Standard.

Chapter 7 gives the background of “Seat Interface Loads” and FEA methodology developed for their calculation. Important FE features such as “Structural Idealisation”, effect of initial penetrations and clearances on the results and ways to deal with “Rigid Body Motion” have been discussed at length in this chapter.

Chapter 8 gives the design activities carried out for “Forward beam”, reinforcing inserts and leg. It shows how the “Boeing Specifications” have been incorporated in the design of leg. This chapter concludes the development of detailed FE model of “Primary Load Path” (involving contact, material and geometry non-linearity) which was the main objective of this research.

Chapter 9 outlines the steps involved in “Free Shape Optimisation” technique used to arrive at a final design of leg. In addition, it gives the description of the non-linear FEA of the complete seat and discusses FEA results.

Chapter 10 is the concluding chapter, which shows that the objective of the research has been met. Future activities for this project (not part of this project) have been briefly presented.

Appendix Sections A-J are used to give details at various stages.

Please note that, a concluding paragraph has been provided at the end of each chapter.

2 Literature Review

It is of utmost importance to review the previous work done in the structural design of a seat. It can help to: avoid repetition of the mistakes done earlier, foresee the problematic areas or unresolved issues, identify the necessary regulations and canvass the overall picture containing the steps involved in the development. There is no straightforward information available on passenger aircraft seat design. Hence, the database was prepared through journal papers, accidents investigation reports published by FAA and EASA, magazines in aviation field. For FEA, help manuals of commercial software and books on FEA were studied. Overall, literature survey has been split in five sections.

- Definition of general terms
- Overview of aircraft accident scenario
- Seat and safety arrangements
- Crashworthiness design principles
- Seat and Comfort

2.1 Definition of general terms

This section takes an overview of general terms used in aircraft safety. Brief introduction to the classification of aircrafts and various terms used in aircraft accidents is provided in coming sub-sections.

2.1.1 Classification of aircraft

An aircraft is a vehicle, which can fly being supported by the air. It counters the gravitational force by using either static or the dynamic lift of an airfoil, or in a few cases the downward thrust provided by jet engines [8].

Impact characteristics such as mass and velocity vary from one aircraft to another, which influences the post-crash scenario. Therefore, for the purposes

of crash-risk assessments, aircrafts are divided in following categories (only fixed-wing aircrafts are considered) [9],

LIGHT CIVIL AIRCRAFT (Category 1) - It falls under Civil Aviation Authority (CAA) classification. Maximum take-off weight authorized (MTWA) is limited to 2.3 tonnes (te). Category 1 also includes military light aircraft with a limit of 2.3 te MTWA.

SMALL TRANSPORT (Category 2) - Civil and military transport aircraft with a range of 2.3 te to 20.0 te MTWA. “Sleep Seat” is being developed for the civil aircraft that fall under this category.

MILITARY COMBAT AND JET TRAINERS (Category 3) – Military aircrafts with MTWA up to 40 - 50 te.

LARGE TRANSPORT AIRCRAFT (Category 4) - any other aircraft, civil or military that is not covered under Category 1, 2, and 3.

2.1.2 Classification of accidents

These definitions have been taken through “Annual Safety Review Report (2006)” of EASA [10]. Only those parts of definition, which are related to seat structure and occupant protection, are produced here.

An accident is an occurrence associated with the aircraft operation, which takes place between the time of boarding and time of disembarking [10], due to which

- All on-board passengers are lost as the aircraft goes missing or is completely inaccessible (Catastrophic).
- The aircraft sustains the damage and failure is limited only to aircraft body. Forces transmitted to occupant are minimal causing minor injuries (Nonfatal).
- A person is fatally or seriously injured due to direct contact with any part of aircraft (Survivable Case).

In general, aircraft accidents can be classified as Catastrophic, Nonfatal and Survivable. In catastrophic accidents in which aircraft is destroyed, protective measures are of no use. In Nonfatal accidents, cabin, seats are still functioning, and all the travellers survive crash force. Thus, protective measures may contribute but it is not an absolute requirement. In survivable type of accidents, cabin structure and seats maintain their integrity with rest of the structure. Causalities are consequences of fire, drowning or other post crash incidents. If restraint systems are designed properly, occupants are subjected to loads below human tolerance limits and can evacuate the damaged aircraft easily. Therefore, in survivable accidents, protective measures play a major role, as they can make the difference between life and death or serious injury. Seat developers are mainly interested in the data from such accidents.

2.2 Overview of aircraft accident scenario

Therefore, next task would be to collect the information on accident statistics, when accident occurs and severely damaged parts in case of crash. This exercise would help to locate the problematic areas and to quantify the safety requirements.

2.2.1 Historical development of aviation safety

Since 1945, ICAO (International Civil Aviation Organization) has been publishing accident rates for accidents involving passenger fatalities (excluding acts of unlawful interference with civil aviation like suicide, terrorism and sabotage) for scheduled commercial transport operations [10], [11]. Figure 2-1 is based on accident rates published in the Annual report of the Council of ICAO.

Figure 2-1 Global rate of accidents involving passenger fatalities per 10 million flights, scheduled commercial transport operations, excluding acts of unlawful interference [11]

The rate for fatal accidents in scheduled operations (excluding acts of unlawful interference) per 10 million flights, ranged from nineteen (1988) to twenty-one (1993) and showed no improvement from 1987 to 1993. From that year, the rate dropped continuously, such that in 2003, it reached its lowest value of three. After increases in 2004 and 2005, the rate dropped in 2007 to four [11].

However, from 2007 onwards, aviation sector underwent many changes in terms of government regulations, cap on emission controls, more demanding travellers in terms of comfort in air, stringent safety regulations and cost cutting measures required due to recession[10], [11]. As the number of air travellers is increasing, the demand for new aircraft is high. Due to strict safety regulations, it becomes very important to ensure complete protection in survivable accidents.

Figure 2-2 shows the phase of flight during accidents, for the year 2005 [12].The phase of flight is the time point during the operation of an aircraft at which the first occurrence of an accident takes place [12].

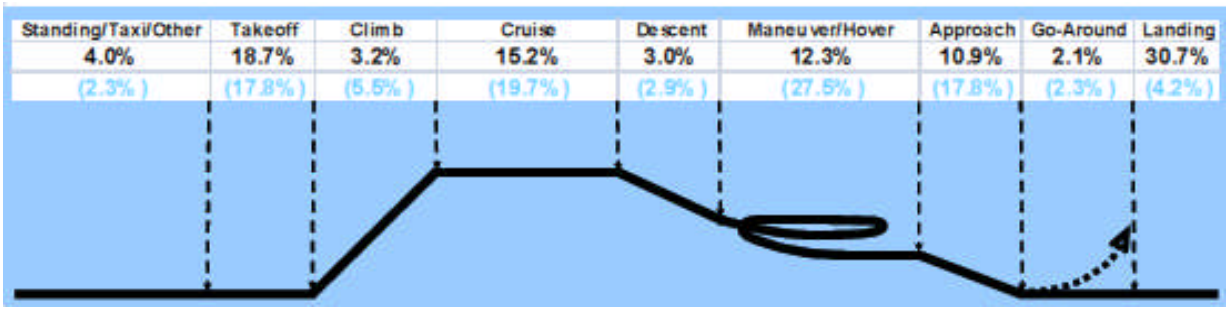

Figure 2-2 Accident Aircraft Phase of Flight during First Occurrence, 2005 [12]

Referring to Figure 2-2, about half of all accidents (49.4%) occurred during either takeoff or landing, despite the relatively short duration of these phases compared to the entire profile of a normal flight. This high number of accidents reflects the increased workload during takeoff and landing. Aircraft systems are also stressed during takeoff and landing with changes to engine power settings, the possible operation of retractable landing gear, flaps, spoilers and changes in cabin pressurisation. The situation may become worse during an emergency landing! This gives us an idea to design the occupant safety systems taking into consideration the loads due to emergency landing. Once it has been figured out the worst loading scenario, it is important to look into the failure modes of an aircraft. This will provide an insight into the most critical parts from a safety point of view.

Figure 2-3 shows that the dominant category regarding the number of fatalities is SCF – NP i.e. “system and component failure or malfunction of non- power plant” [11]. It emphasises the need to design more reliable seats and occupant protection systems.

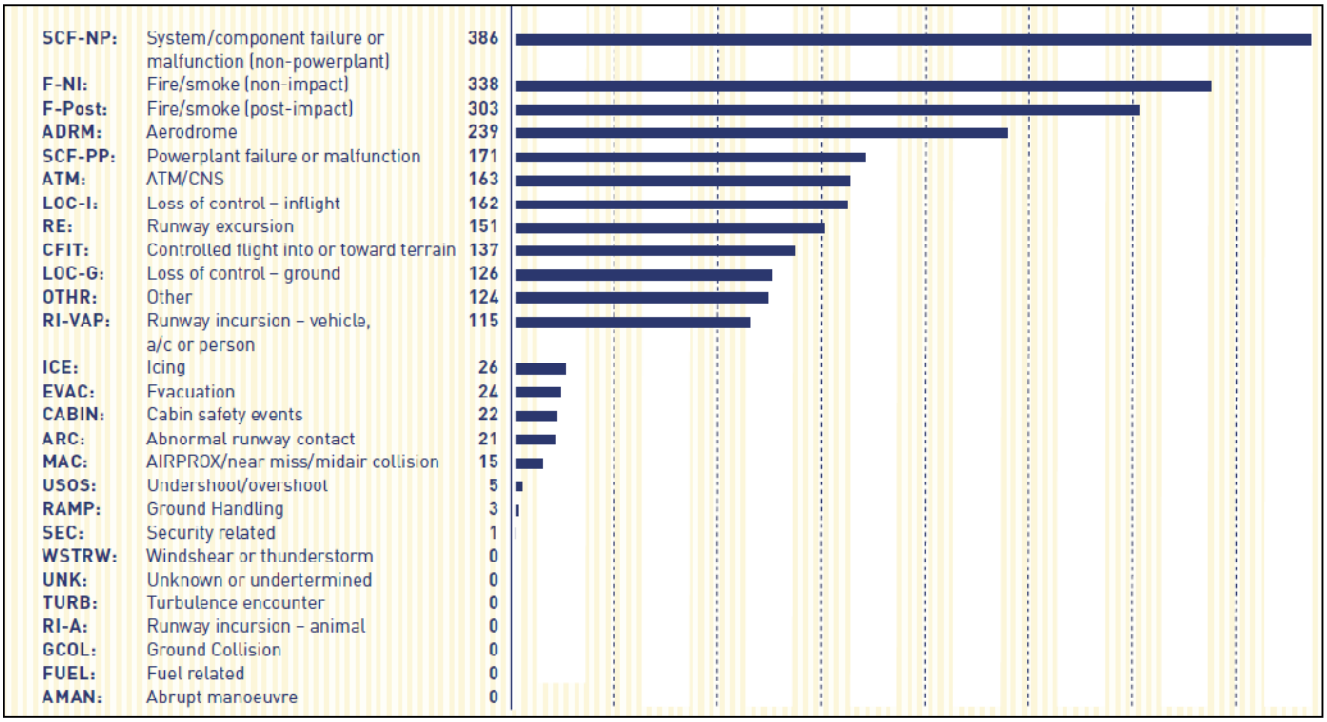

Figure 2-3 Fatalities per accident category, aircraft registered in EASA Member State used in public transport operations or general aviation, turbine powered, fixed wing aircraft, over 5,700 kg MTOM [11]

Next part is to collect the survival factor data. As most of the investigations conducted for aircraft crashes, focus on causes of accidents, survival factors data is limited. It mainly addresses inertial or accelerative injuries to organs (such as heart, lung, liver and pelvic). Weignmann published one of the most detailed data of injury listings in 2002 [13]. This study includes 559 autopsies from 498 accidents. All the autopsies were of male pilots (i.e. 95th percentile) and more than 50 % of them were over 45 years of their age. Figure 2-4 presents the normalised list of injuries specific to body parts.

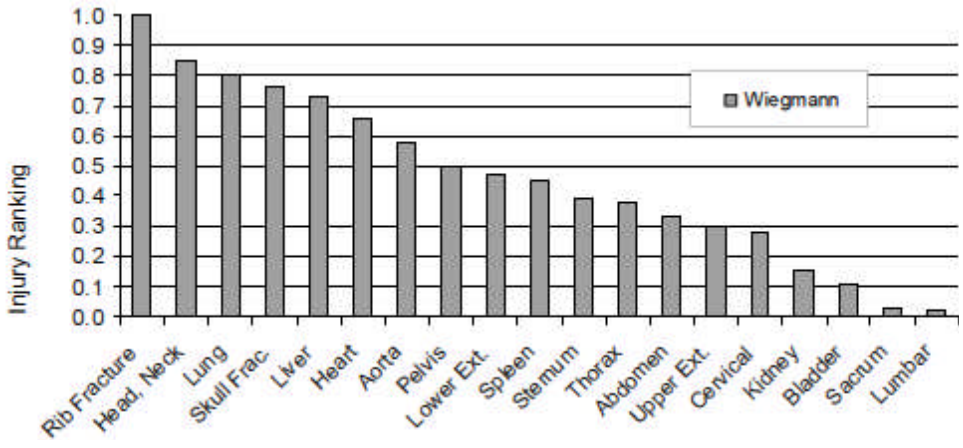

Figure 2-4 Injury Ranking for n=559 Autopsies of fatal accidents [13]

It can be inferred from Figure 2-4 that injuries to head, neck, chest and pelvic are most critical one and result in casualties. Hence, it is important to convert this data into quantitative data that can be used in developing safety regulations for occupant protection.

With the historical development of aviation safety, it is clear that seat plays a dominant role in post-crash safety of a passenger. Due to the latest safety regulations and increasing demand for comfort, it is of utmost importance to come up with a new design of seat that will is lightweight, more comfortable and safer!

2.3 Seat and Safety

In aircraft operations, personal safety is of vital importance. Man and machine interfaces such as seats, play a very important role in making flying safer. The term “Air safety” encompasses the theory, investigation and categorisation of crash mechanisms, and prevention of accidents through defining regulations, personnel education and training.

Various independent agencies investigate aviation accidents, determine the probable causes of the accidents, issue safety recommendations, and evaluate the effectiveness of safety regulations issued by local Government. Naturally, different countries have their own set of safety standards to make the flying safer and comfortable in their own terms. When one thinks of legal rules in terms of flight passenger safety, one is typically concerned with a number of regulations by the US aviation board, the FAA, and its European equivalent, EASA. Such an existence of various regulations confuses designers, when it comes to the designing of an occupant safety system for an airliner operating across the continents.

EASA is the centrepiece of the European Union’s strategy for aviation safety [14]. It develops common safety and environmental rules for European countries (EU). In addition, it monitors the implementation of standards through inspections and offers technical expertise, training and research [14].

In order to establish uniform standards in European and US aviation sector, Certification Specifications (CS) and the Federal Aviation Regulations (FAR) agree in content, up to some extent [15]. The CS / FAR encompasses works of all relevant governing bodies in international commercial aviation containing airworthiness requirements, procedures for pilot training, material testing methods and crew licensing considerations. CS has been followed as a guideline for safety in this research.

As seen in the Section 2.2.1, majority of the aircraft accidents happen in the emergency landing conditions and seat failure mainly leads to the head, neck and lung injuries. Naturally, the need to address these points is reflected in the CS sections 25.561 and CS 25.562 safety regulations [16].

CS sections 25.561 and 25.562 gives, static and dynamic loads during emergency landing conditions respectively [16]. Details are given in “Appendix A”. This research mainly focuses on “9g” static loads in forward direction, as per CS 25.561 Clause B.3.i.

2.4 Crashworthiness Design Principles

In post crash scenario, an intact protective fuselage around the occupant does not alone ensure improvement in the survivability, if occupants receive fatal injuries inside the shell [17]. Hence, measures must be provided such that the occupants remain secure in their seats and the seats in turn attached to the floor. In addition, occupant when subjected to crash pulse, should not strike any sharp objects while remaining integrated to his/her seat. This is called as “Delethalisation” [18]. The objectives of delethalisation are [18],

- ✓ To provide a system that maintains the occupant decelerations below the human tolerances limits.
- ✓ To retain the occupant in his/her seat (Occupant retention).
- ✓ To maintain integrity of the seat with the main airframe after crash.

- ✓ To prevent the occupant from striking with nearby interior structure or being struck by loose objects leading to injuries.

2.4.1 Occupant Retention

Occupant retention is the most significant contributor for increasing delethalisation. In FAR25, large civil type of aircraft, retention of the passengers along with protection against longitudinal retention is of utmost important [18].

The most survivable plane accidents do not produce airplane longitudinal decelerations of magnitudes that would seriously affect the passengers![18] However, occupants are subjected to major or fatal injuries, seat belts fail, or seat attachments fail. The answer to this mismatch lies in the study that shows that occupant decelerations do not necessarily coincide with airplane decelerations.

2.4.2 Slack and Stiffness of Seat

The factor that causes difference between decelerations experienced by fuselage and that by occupant is the “Slack” between the occupant and restraining structure [18]. Longitudinal slack is the effect of a loose seat belt where as vertical slack is produced due to thick and soft seat cushion. Due to presence of slack, a relative velocity is developed between the seat and occupant, produces a very high Kinetic Energy (KE). Rigid restraining structure and limited deceleration distance may magnify an occupant’s deceleration [18].

In order to reduce the consequences of slack, KE of the occupant resulting from relative velocity of occupant with respect to seat or floor, must be absorbed by restraint systems and by providing additional deceleration distance.

Seat structure itself can be used for energy absorption [18]. The idea behind this method is to use ductile materials for seat components, which absorb the energy through progressive plastic collapse. It does not suffer from restrictions such as, valid for only one time application, or operation resulting in increasing slack or adding additional weight to the seat structure. The logic is to design a

seat such that it starts deforming plastically, after occupant reaches a deceleration above “9g”, thereby seat belt or seat attachments do not experience any further decelerations until full collapse of seat [17], [18]. Therefore, principle behind the successful seat design is that the seat structure should be rigid until “9g” after which, additional KE is absorbed through plastic deformation increasing deceleration distance.

After going through crashworthiness principles, one natural question is how much it will add towards cost and weight of airplane. Due to ever-increasing fuel prices and cutthroat competition due to globalisation, airliners are under immense pressure to reduce the aircraft development costs. At the same time, safety regulations are stringent, and tougher than ever. A designer has to find a golden mean to come up with a low cost, weight efficient and yet safe and reliable design of a seat. Crashworthy principles help to improve occupant survivability without any significant increase in weight or cost [18]. Seat construction using ductile metals does not cause a weight penalty. Further use of FEA enables to compare different design concepts before actual physical testing and thereby reducing the cost.

2.5 Seat and Comfort

Seats are the most critical component in the plane as 90-95 % of a passenger’s flying time is spent in the seat. In early 1930’s; commercial aircrafts had fewer seats due to undeveloped technology to propel bigger flights and large mass. Hence, seats were spacious, luxurious and comfortable [2]. However, introduction of the Boeing 737 in 1968 opened the doors for masses. Later on concept of “Economy Class” pitched in, in order to “fit as many passengers as possible”. This resulted in reduction of seat pitch and in turn in comfort. However, from year 2000, trend is back towards offering passengers more room and more comfort, thanks to stiff competition between airliners [2].

Passenger comfort mainly depends on correct seat width, seat recline, sufficient leg room, comfortable cushion, correct angle and position of the footrest from seat, correct height, angle and material of armrest and headrest and most

importantly adequate lumbar support. All these parameters require use of anthropometrical data for the targeted end users.

CS 25.785 defines the requirements for the design of aircraft seats mainly addressing issues of structural integrity and safety. However, it does not touch any area related with passenger comfort [20]. However, Civil Aviation Authority (CAA) prescribes minimum dimensions for seated passengers through CAP (Civil Aviation Publications). CAP 747, Section 2 Part 3 “Generic Requirement Number 2” (GR2) issued on November 30, 2009 (formerly known as Airworthiness Notice, AN64); specifies three critical dimensions [19], [20]. GR2 is applicable to all UK registered aeroplanes over 5700 kg MTWA, operated for the purposes of Commercial Air Transport and configured to carry 20 or more passengers.

These requirements take into account the normal design extremes for all occupied zones (namely the anthropometric data for the 5^{th} percentile female to the 95^{th} percentile male). Buttock – knee length has been identified as a critical dimension along with the minimum distance between two seats and the vertically projected distance between the seat and any seat or fixed structure immediately in front of the occupant. These three dimensions are considered a minimum realistic standard, which can be uniformly adopted and are used as a criterion for determining the acceptability of any seating configuration [19].

2.5.1 GR2 requirements [19]

Please refer Figure 2-5 for minimum dimension requirements.

Dimension A, is the minimum distance between the datum point and the rear of the front seat or any other fixed structure in the front, measured in the both vertical and longitudinal arcs. It shall be twenty-six inches.

A datum point is located in the centre of the seat back at a height of three inches above the mean uncompressed seat cushion height.

Dimension A is also measured from any point on the seat back within the span of half “Y” (as shown in Figure 2-5) symmetric about the centre line, at a height of three inches above the mean uncompressed seat cushion to the seat or any other structure in the front, within vertical and horizontal arcs of twelve inch radius. Both the measurements of “A” are limited up to twenty-five inches above the carpeted floor level.

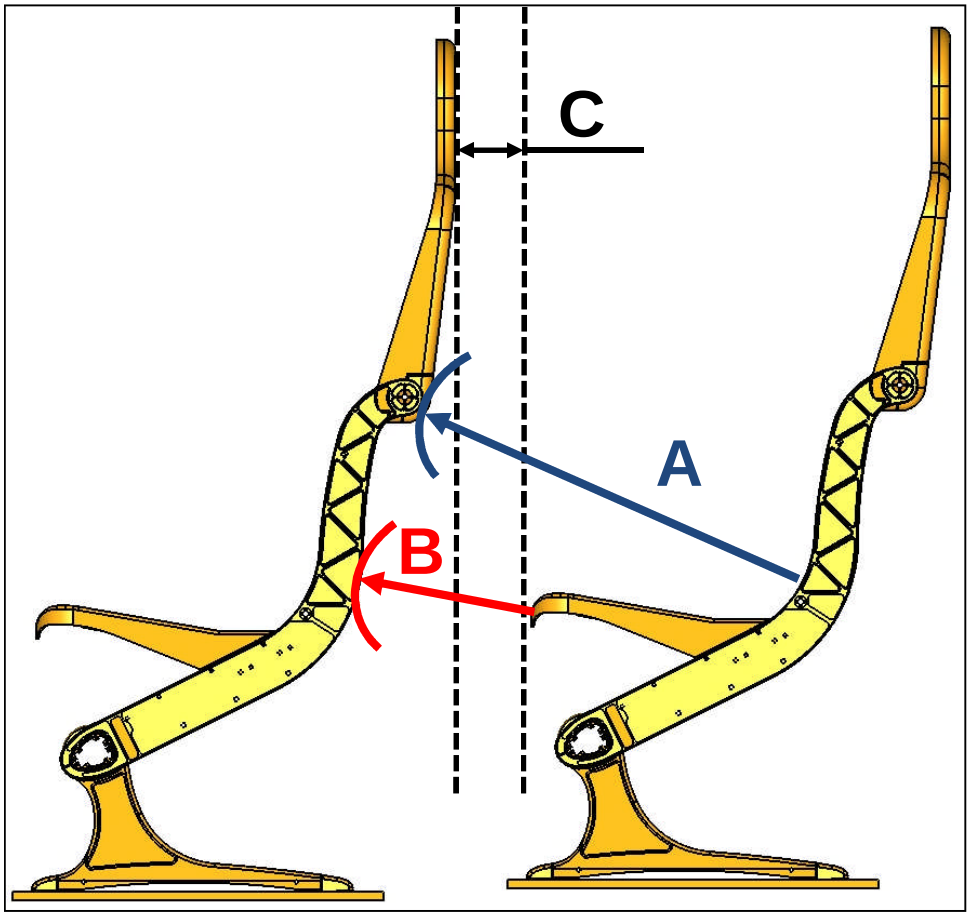

Figure 2-5 GR2 requirements of a seat. Dimensions A, B and C [19]

Dimension B, is the minimum distance between a seat and the seat or any other fixed structure in the front, measured between the full width of the forward edges of the seat cushion or the seat armrests and the rearward part of the seat or any other structure in the front, in both vertical and horizontal unlimited arcs. It shall be seven inches.

Dimension C, is the minimum vertically projected distance between seat rows or between a seat and any other fixed structure in the front. The procedure to

establish “C” is same as that for “B”, except the condition of projected distance. It shall be three inches.

Following points should also be considered during the measurement of “A”,”B” and “C” [19],

- In-flight reading material, cabin safety leaflets and sick bag will be in place.
- Food tray will be in its stowed (take-off and landing) position.
- Seat will be in upright (take-off and landing) position and armrests will be full down.

Apart from body dimensions, other factors such as location of entertainment consol, location and intensity of reading light, height of the seatback and location of life jacket (easily accessible yet positioned out of site) defines “Comfort of a Seat”.

2.5.2 Anthropometric Study done by JAA in 2011 [20]

Anthropometric data of the population changes over time. European and US populations have shown increase in overall body dimensions e.g. In Europe and North America, an average secular increase of 10 mm per decade has been seen [20]. By 2020, number of old people will be same as that of younger ones. Age affects the body dimensions as well as the abilities to sustain the fatigue by sitting caused due to long duration flights.

Effect of all these factors namely, out of date anthropometric data and increasing body dimension has resulted in passenger discomfort and in inadequate brace position during emergency landing.

Hence, Joint Aviation Authorities (JAA) took an overview of relevance of GR2 specifications with respect to today’s population and health problems associated with prolonged sitting. This was funded by CAA [20]

Findings and conclusions from JAA report are [20],

- Design extreme should cover the 1%ile to 99%ile range.
- Dimension A should be increased to 28.2 inches (to accommodate 95%ile European passenger) or to 29.4 inches to accommodate 99%ile world passenger.
- At present, GR2 requires measurements to be made with all the seats in full upright position. However, in order to increase comfort in economy class, airliners are increasing reclining angles in rear direction. This gives false representation of “Dimension A”. Hence, it should be measured with the front seat in fully reclined position.
- Dimension B should be 9-10 inches at armrest level and should be 8.3 inches at cushion level.
- Dimension C should be increased to twelve inches, for the ease of movements of a 95%ile passenger between the rows of the seat.
- New minimum dimensions for the depth and width of the seat along with armrest should be introduced.
- As the older population is increasing, enough care should be taken during new seat development allowing easy handling of the seat for older people.

The present research will try to consider these findings during design of “Sleep Seat”. The reason being, if in near future, GR2 requirements are tuned to JAA findings, the design will not be “outdated” or will not require “re-work” to be able to cope with new comfort dimensions.

Conclusion from Chapter 2

Chapter 2 was the literature review. Review of aviation safety concluded that 49.4% of accidents occur during either takeoff or landing and failure of seat structure is the dominant reason for causalities. Crashworthy design principles showed that “Slack” between occupant and seat enhances the severity of decelerations experienced by passenger. Solution lies in, successful design of a seat, which is rigid until “9g” after which starts deforming plastically, absorbing the remaining Kinetic Energy. It helped to identify, Certification Specifications CS 25.561 as safety regulations and Generic Requirements (GR2) as comfort guidelines to be used in designing of “Sleep Seat”. In the end, suggestions given by JAA to update GR2 requirements based on their study published in 2001 have been given. These modifications would be considered in “Sleep Seat”. An existing seat design (9g certified in 1991) was studied. However, lot of deviations from latest regulations were found. Hence, details are not provided here.

First point from the scope of the project (Section 1.3) i.e. “Review existing literature concerning design of aircraft seats / different configurations. This aspect will not only consider the crash certifications, but additional safety design features a seat must incorporate”, was met with this study.

3 Description of “Sleep Seat”

This chapter provides nomenclature of “Sleep Seat”, introduction of various parts, functioning of seat and novelty of design. The new seat was coined as “Sleep Seat” to highlight that the comfort starts from name itself [6].

The main components of “Sleep Seat” are: Boomerang, Seat pan, single forward beam, and leg (Figure 3-1). Please note that representative “Anchor Blocks” (Figure 3-1) are shown, since their design is not yet finalised.

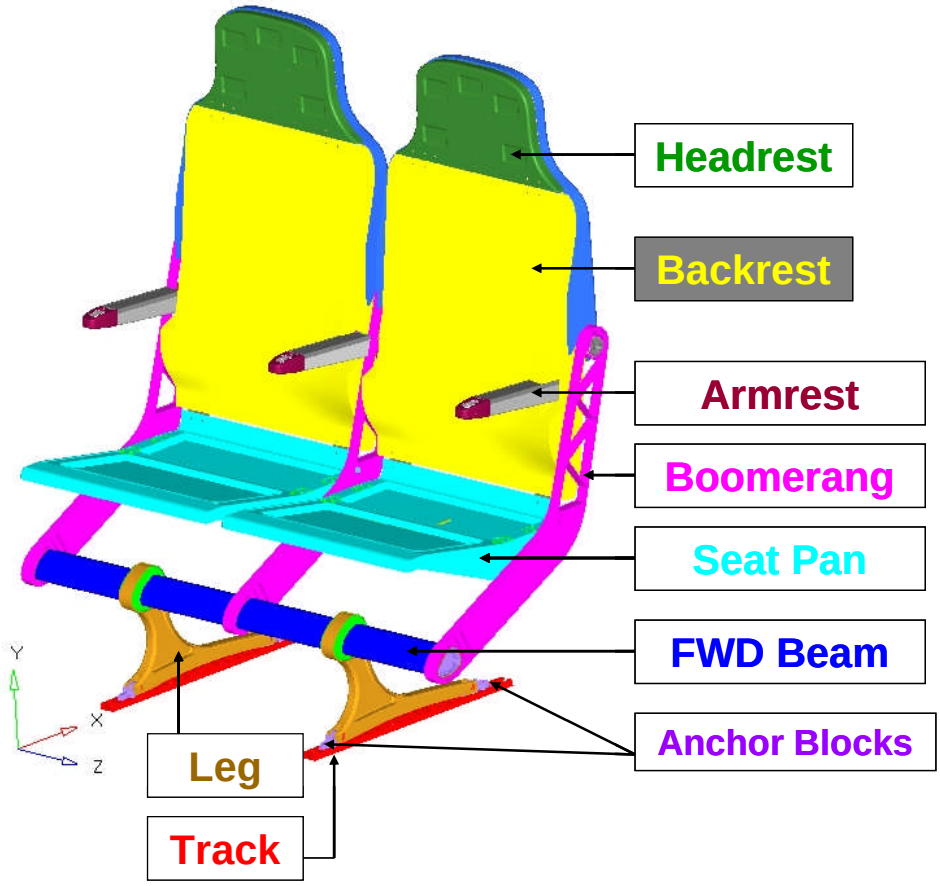

Figure 3-1 Nomenclature of Sleep Seat (Courtesy BlueSky) [6]

Armrest, seat pan and seat belt (not shown in figure) are mounted on boomerang. The Seat-pan moves along the gradient through guided track that is fixed to boomerang as shown in Figure 3-2.

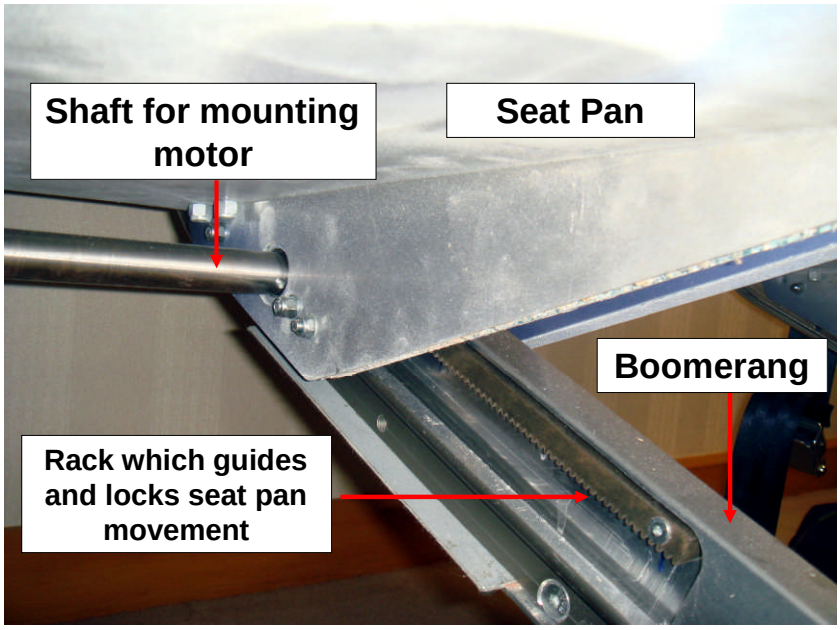

Figure 3-2 Provision for movement of seat pan along the gradient

All three boomerangs are bolted to “Forward Beam (FWD beam)”. FWD beam is then assembled with seat legs through C-clamps. Reinforcing inserts have been provided in the FWD beam at its meeting points with boomerang and leg. These inserts provide local stiffening and help to spread the load over larger area. Width of the leg is 30mm and that of C-clamps is 10mm each. Therefore, the overall width of the leg assembly at the interface with FWD beam is 50 mm as shown in Figure 3-3. Seat structure is attached with the track through anchor blocks, which are attached to the leg through pin joint. This connection between leg and blocks enables relative pitch and roll movement between seat structure and the seat track, which is extremely useful to prevent damage of the seat structure during pre-deformation requirement, as per CS 25.562 (explained in detail in Section 8.3.1).

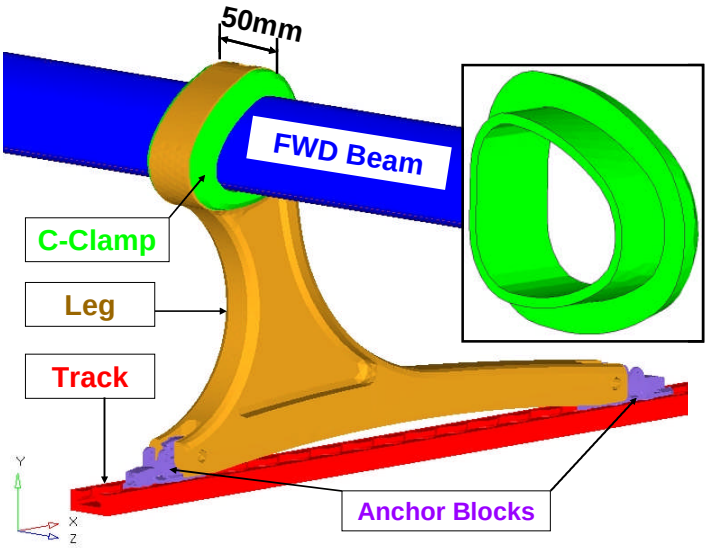

Figure 3-3 FWD beam and leg sub-assembly, Leg C-Clamp (in sight)

The Sleep seat will come in double and triple configurations (an input from BlueSky). It will have three different designs based on the movement of seat pan.

- *Basic Economy Seat* will focus on regional short haul (2-3 hours) flights. In this version, seat pan will not have any movement and hence this will be a fixed-position seat without any reclining.
- *Normal Economy Seat* will offer three-inch forward motion of seat pan thereby providing more legroom. This is aimed at medium haul (5-6 hours) flights.
- *Premium Economy Seat* will cater the needs of international flights of long duration (> 6 hours). It will enable, seat pan movement of three inches in forward direction along with six inch in downward thereby generating a luxurious recline of 40 degrees [7].

The potential buyers for “Sleep Seat” include A 330/A340, Boeing 737, 767, Thomas Cook and Delta airlines. The designs will be modified as per the needs

of different airliners e.g. more outboard, different seat spacing, different seat track spacing.

Based on the requirement from BlueSky; dual seat configuration from “Basic Economy Class”, which is symmetric in terms of passenger seating; has been considered for the present research. This would reduce the FE modelling effort required and help analysts to concentrate on developing a robust FE model that can predict the performance of seat when subjected to loads according to CS25.561. Once the FE procedure is satisfactory, actual track spacing and layouts (aircraft specific) would be considered.

3.1 Novelty of Design

3.1.1 Comfort and Safety

- This innovative architecture will have a single actuator to move the seat pan three-inch forward and six-inch downward, creating an unrivalled space for leg spread. This will also create 40 degree generous recline of the backrest within a fixed outer shell which does not protrude into the space of the passenger seating behind! Because of this innovative seat, passenger will be entertained with increased level of comfort on medium to long hauls [6] [7].

- Conventional seats have twin beams at shin level under the seat pan that restricts access to the valuable space under seat. Sleep seat features a unique single FWD beam design, which eradicates this undercarriage thereby maximising the space in the tight confines of economy [6]. It will also significantly reduce the part count, hasten during assembly and costs.

- Sleep seat is an ultra lightweight design. Basic Economy class model will weigh less than 8kg (typical seat weighs around 11kg) and Premium model will be just under 12kg [6].

- With little alterations, Sleep seat can be used for Economy class (both basic and premium), regional business in aviation sector as well as for national and international rail travel applications.

- Sleep seat will be a “16g” seat that means it will satisfy the structural requirements as specified by CS 25.561 and CS 25.562.

3.1.2 Compliance with GR2 requirements and JAA findings

Table 3-1 shows the values of “Three Critical Dimensions (A, B and C)” as defined in GR2 [19].The dimensions on actual seat data are given in Appendix B.

Critical Dimension	GR2 Requirement (compulsory)	JAA Recommendations (optional)	"Sleep Seat" Actual
A	26	28.2	28
B_A	7	9-10	12.8
B_c		8.3	9.9
C	3	12	4.5

Dimension B –
B_A ➡ At Arm Rest Level
B_C ➡ At Seat Cushion Level
All dimensions are in inch.

Table 3-1 Compliance with GR2 [6], [19], [20]

It can be seen that,

- Sleep seat satisfies the GR2. In addition, Dimensions A and B_A and B_C meet the JAA findings which will prepare the design for future modifications.

- Another interesting fact, is that “Dimension A” will be measured when the passenger in front is fully reclined. This gives the “True” representation of “Dimension A”, which is achieved due to “fixed-backrest” design [6] [20].

Conclusion from Chapter 3

Chapter 3 introduced the actual design of “Sleep Seat”. It explained the functioning of various parts and innovative features of “Sleep Seat”. With lot of market potential, it is worth to engineer this product. Design completely meets the dimensions specified by GR2 and partially by JAA findings, confirming that comfort part is captured. Next step would be, to see that the seat structure has sufficient strength to withstand static loads as specified in CS 25.561.

Please note that due to “Non-Disclosure Agreement” signed between Cranfield University, UK and BlueSky, details such as dimensions and mass of each component, mechanisms and attachment of leg with track (anchor blocks – Figure 3-1) can not be presented in the report.

In next Chapter, approach to be followed during execution of project and background calculations done have been presented.

4 Project Plan and Analytical Calculations

Since the Sleep Seat design is in its conceptual stage, there are too many design variables comprising of design of individual components and their influence on each other. Hence, a systematic approach for component design is essential.

In addition, during the first design cycle, when designs of almost all the components are not fixed; it is appropriate to consider only main components with equivalent loads. This enables designers to focus their efforts and gives freedom to FEA side to do extensive research on appropriate element choice and boundary conditions. As the design progresses, complexities can be added to previously developed robust FE models, ultimately leading to a detailed FE model (Sequential Modelling Approach).

With this line of thinking, the overall design process is divided into SIX stages (called as “Toll Gates (TG)” shown in Figure 4-1).

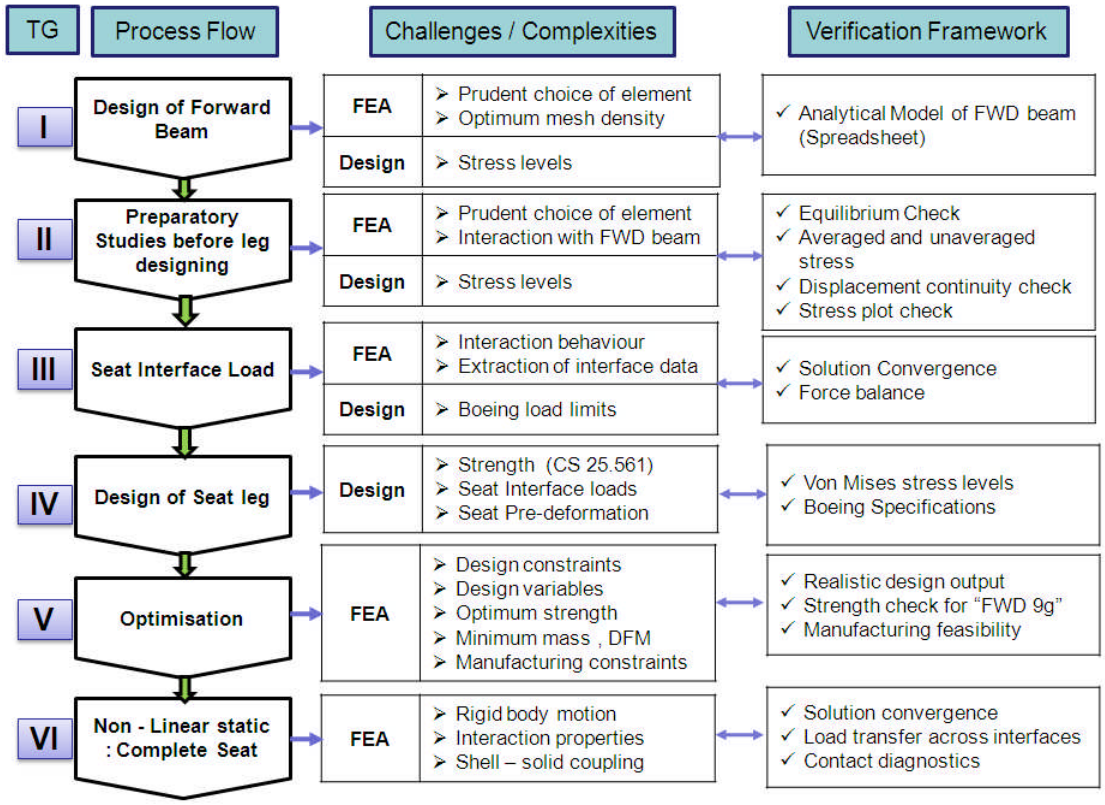

Figure 4-1 Project Plan

Process flow indicates milestones in the execution of project. Major challenges and complexities have been identified at each stage. Challenges have been classified into two sections i.e. FEA complexities and potential design challenges. It will help to clearly classify different phenomenon into their respective segments and will narrow down global (macro level) activities into well-defined detailed objectives. In conceptual design stage, such a differentiation between various aspects helps to avoid otherwise chaotic mixing of various parameters, which develop un-necessary complications thereby blocking the flow of project.

FEA has migrated from the complicated research themes of postdoctoral studies into day-to-day product development cycle. Now days, it is very user-friendly and graphically attractive to use an FEA software even for an inexperienced engineer. Potential damage in this scenario is a smooth journey from “Uninformed” to “Misinformed” about the model behaviour due to inappropriate assumptions made or unrealistic expectation from FEA. Keeping this in this mind, verification framework has been developed at each stage considering FEA checks, analytical methods and experience (Figure 4-1). This will help to critically assess the output at each stage. If FE methodology at a particular stage satisfies these checks, then it will be adopted for evaluating future design concepts.

4.1 Analytical Calculations

Analytical calculations help for initial size estimation. Therefore, it was decided to use them as a conceptual design tool and a base for FE calculations. Once the sufficient confidence is established in FE models then FEA results would be used as a design-base.

Next question was which loads to consider and which parts to consider for the calculations.

4.1.1 Total loads considered

The total weight considered for the CS 25.561 consists of an occupant weight 77 kg, seat structure weight 8.22 kg (for basic fixed economy seat including restraints, cushions, food trays, all electronics and avionics items), life vest 0.9 kg per passenger and in-plane literature weight of 1.36 kg per passenger. Therefore, the total weight is 87.48 kg [35]. This weight is then multiplied by corresponding “g” factor in the respective direction. E.g. for “Forward 9g” load case, total seat weight of 87.48 kg is multiplied by a factor of (9.81*9) resulting in 7723.6 N of force for each seat. Load application point has been explained in Section 4.3.

4.1.2 Identification of Critical Load Case

A closer look at the inertial loads specified in CS 25.561 (Appendix A) reveals that, 9g load in forward direction is the most critical load by magnitude. In addition, it will create very large moment, which will be reacted by studs in the track introducing maximum vertical loads in them. It will also produce maximum loads in FWD beam and in the throat area of the leg (Figure 8-4). Looking at the dynamic loads as per CS 25.562, a pulse with a peak of 16g is also applied in forward direction. Therefore, safe seat design against “Forward 9g” loads (i.e. 9g inertial load applied in Forward direction) is a decisive factor for the success of the project. Since, scope of this research is concerned only with CS 25.561; “Forward 9g” has been identified as the critical load case.

Next critical load would be 6g inertial load in downward direction, which is uniformly distributed over the seat pan.

4g load in lateral direction will create out of plane bi-axial bending in boomerang. It will also experience out-of-plane loads at seat pan attachment points due to “Downward 6g” load.

The loads specified in CS 25.561 focus on different parts e.g. “Forward 9g” plays major role in the design of leg, “Downward 6g” is important for the Seat-Pan and “Side 4g” for the boomerang. If all these load cases are considered,

the complete seat structure along with all types of non-linearities needs to be involved, which will create large number of design variables. Since, it would be difficult to handle such a problem size in the beginning, the most critical load cases i.e. “Forward 9g” and “Downward 6g” have been considered.

4.1.3 Parts To be Considered during analysis

Decision of, which parts to consider in FEA is strongly driven by what information is sought; degree of accuracy required and anticipated computational cost and capabilities of FE solver (ultimate design tool to be used).

Since certification of a Passenger-Seat is a very cost – intensive process, the modular assembly of seat structure is a basic design principle [15]. Now-a-days, airliners want to use different seat configurations on different seat track layouts. This is accomplished mainly by shifting seat spreading and using different seat legs for different seat track spacing. Therefore, identification of main structural components that carry the load from passengers to aircraft floor is an important task (also called as “Primary Load Path - PLP”). Figure 4-2 shows, the components of “Sleep Seat” involved in the load path.

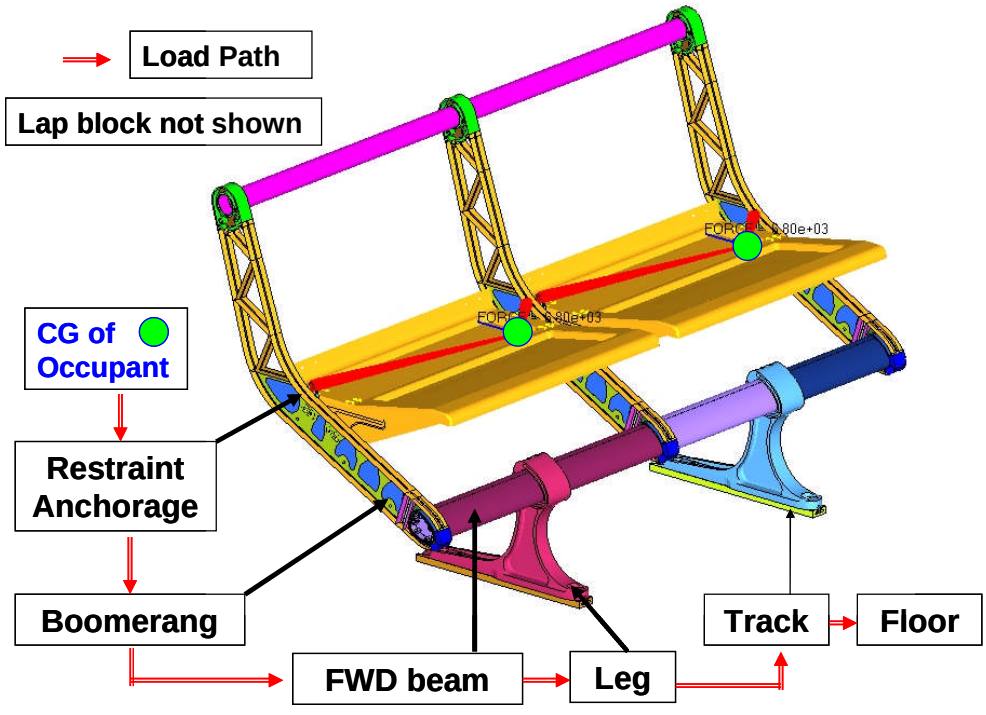

Figure 4-2 Load path for the Sleep seat

In Sleep seat, loads from all the boomerangs are accumulated at “FWD beam” which are then transferred to the seat track via legs. Thus, FWD beam and seat leg form the PLP. Hence, successful design of these components during the initial design phase, will guarantee adequate structural strength and functionality of seat.

Hence, during the initial FE Analysis, extensive research has been done on different designs of leg and FWD beam and their performance from structural point of view against applied “Forward 9g” load (CS 5.561).

4.2 Development of Spreadsheet for Preliminary Sizing

Figure 4-3, shows schematic diagram of PLP and loads acting on it (Forward 9g and Downward 6g). Using this “Free Body Diagram (FBD)” all analytical calculations were developed using Engineer’s theory of bending and Microsoft Excel (Spreadsheet) [22]. Please note that the spreadsheet was developed by CISM (Crashworthiness, Impact and Structural Mechanics Group), Cranfield University prior to this research [21]. It has been added in this report, as it was the starting point for this research.

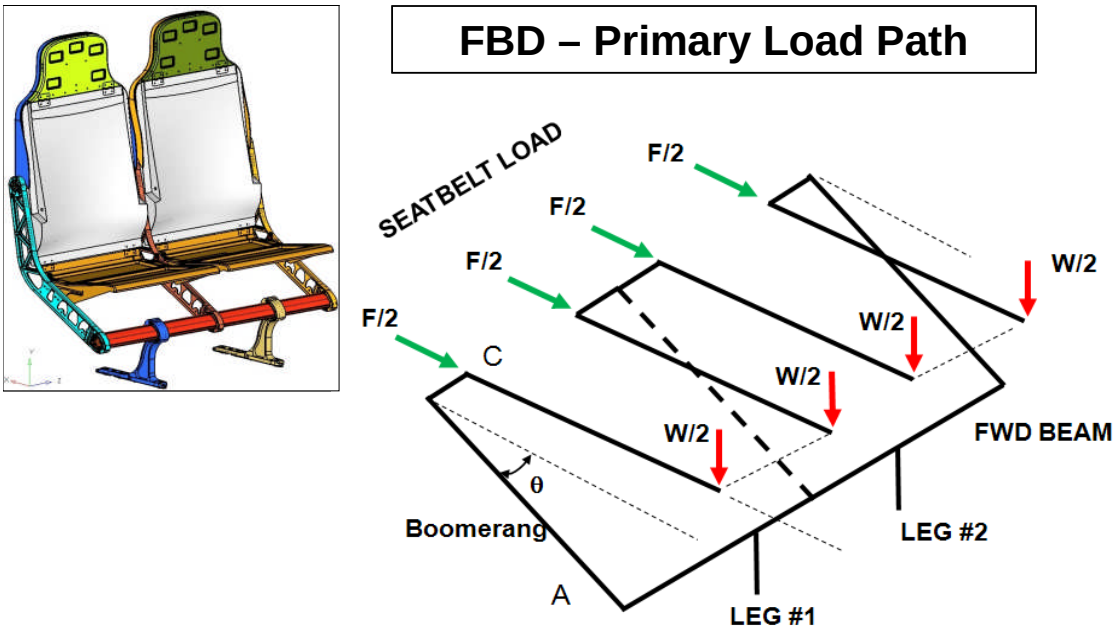

Figure 4-3 Free Body Diagram of FWD Beam and Leg Assembly. Courtesy CISM, Cranfield University [22]

Looking at Figure 4-3 following assumptions can be made,

- Offset from seat supports to boomerang can be ignored, as its effect on overall stress distribution will be minimum considering dimensions involved.
- Idealised support conditions i.e. simply supported at legs (no rotational reactions)
- Symmetry can be extracted.
- Additional stresses due to torque M_C are not considered.

Then Simplified FBD becomes as shown in Figure 4-4.

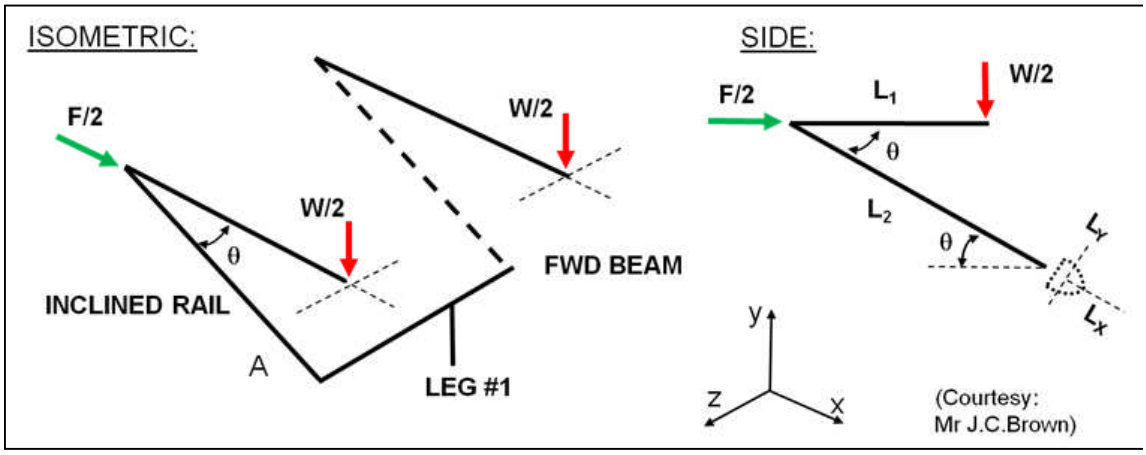

Figure 4-4 Simplified FBD for FWD beam and leg assembly [22]

The strategy used was to solve for Shear Force (SF) and Bending Moment (BM) Distribution as a function of distance along the beam [21]. After estimating the SF and BM in each of the members, spreadsheet was extended to identify the normal stresses in the FWD beam, that result from in-plane bending loads due to “Forward 9g” and “Downward 6g” loads. The analytical calculations performed (here onwards termed as “Spreadsheet”) have been given in Appendix C.

4.3 Usefulness of Spreadsheet

- The load application point for static loads (CS 25.561) is determined using National Aerospace Standard (NAS 809) [23]. Downward load is evenly distributed over the seat pan.

- For Forward and Side loads, load point is 10.5 inches up from the base of body block and 8.5 inches forward from the back of the block and is in the mid plane of side boomerangs [23]. The load imposed by the occupant should be applied through a lap block or a dummy, which is restrained in the seat, by seat belt, which is attached to its anchor point. However, FE modelling of body block, loading mechanism and their attachments brings in lot of contact non-linearities. Therefore, for the present research, Multipoint Constraints (MPC) have been used to transfer the load from application point to the seat belt attachment points in boomerang. The 10.5-inch up and 8.5 inch forward dimensions have been taken from Seat Reference Point (SRP) (Figure 4-5). This has been communicated with BlueSky and is satisfactory.

- Initially, as only PLP is simulated, it was necessary to transfer loads (as specified in CS 25.561) from “Load Application Point (in Global Co-ordinate system)” to the ends and centre of FWD beam (i.e. Local Co-ordinate System) in equivalent forces and moments. Spreadsheet enabled such a load transfer (Figure 4-5).

- A quick and simple conceptual design tool that provides information on, influence of design changes e.g. thickness of beam, on stress levels.

- Different airlines have different seat leg spacing. Change in bending stress induced in the FWD beam due to different leg spacing can be readily accounted using spreadsheet thereby providing preliminary sizing of cross-section of FWD beam.

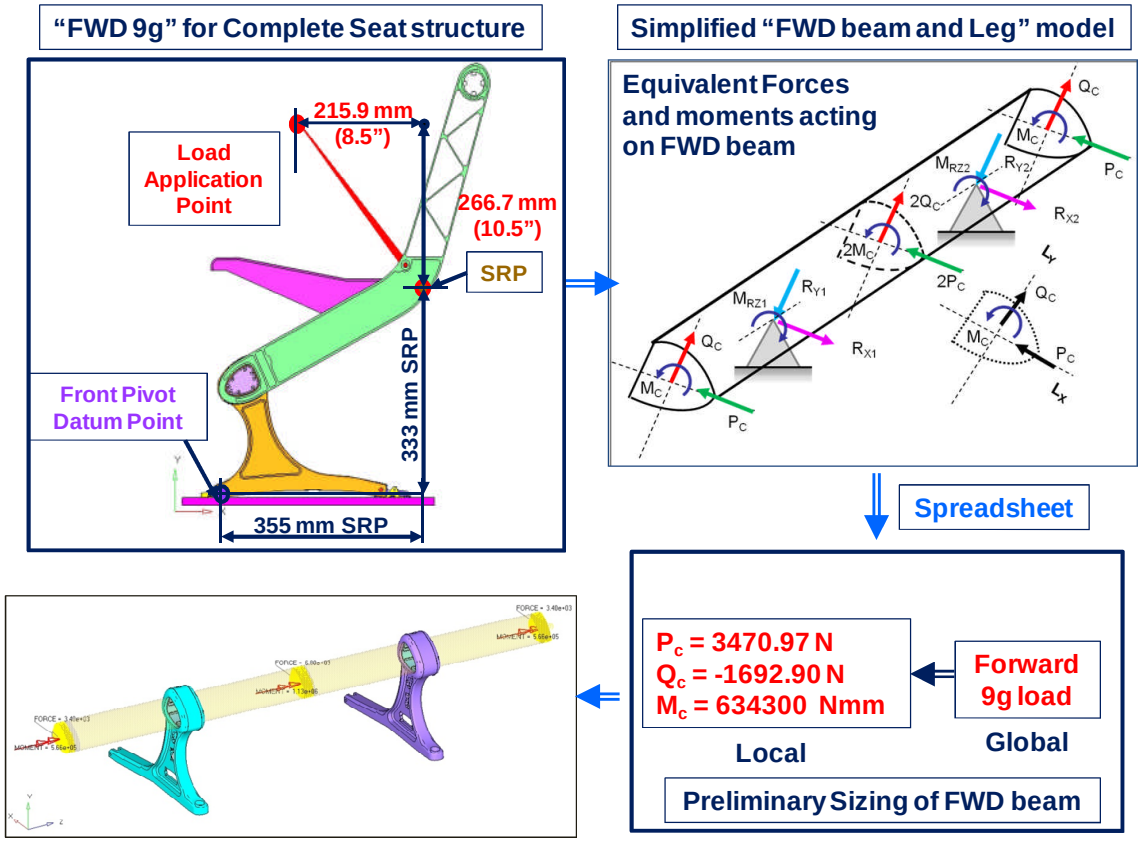

Figure 4-5 Resolving loads from global co-ordinate system to local co-ordinate system of "FWD beam and leg" using spreadsheet [22]

- A tool to verify the FEA results of FWD beam

Figure 4-6 shows, bending stresses in the FWD beam estimated using spreadsheet for "Forward 9g". According to "Tension-Compression" behaviour of the beam, stresses are calculated at six different locations (Figure 4-6). These values would be compared with the stress values obtained from FEA of FWD beam. Thus, spreadsheet formed the base for the mesh sensitivity study of FWD beam.

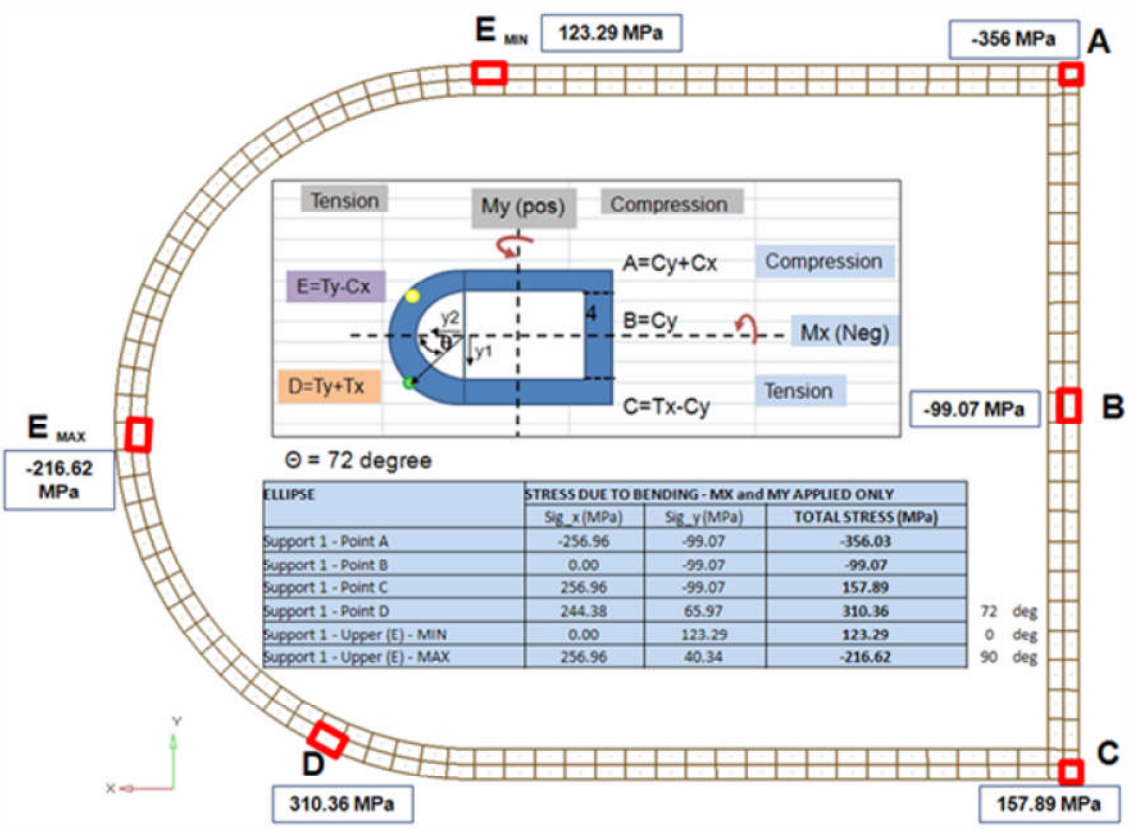

Figure 4-6 Bending stress estimated using spreadsheet at six different locations

In this section, analytical model of FWD beam was developed and BM, SF and bending stresses in the FWD beam were calculated. Next task would be to develop an equivalent FE model of FWD beam and to verify the results from spreadsheet. In this regard, identification of software packages for building FE models and solving FEA problems was done first.

4.4 Altair Hypermesh for Pre-processing

Pre- processing involves generating FE models for the given CAD (Computer Aided Designing) geometries, their assembly, definition of material properties and sections and representation of loads and support conditions. A product of

Altair Hyperworks, Hypermesh was chosen for this due to its advantages, which are listed below [24], [25],

- Hands-on experience during author's professional career
- Supports a number of CAD and FE file formats which increases efficiency and interoperability
- Advanced features to manipulate/clean-up the geometry, which enables meshing of highly complex models. Powerful technique for mid-surface generation
- An easy-to-use and highly interactive graphical user interface
- Semi-automatic functions generating quality mesh with minimal user input
- Built-in optimisation tools as topology, free shape (with Optistruct as a solver).

Please note that, reference 24 is available only for commercial clients (e.g. Cranfield University) of Altair Hyperworks.

4.5 Optistruct for Linear Static Analysis

Optistruct, a FE package offered by Altair Hyperworks, was selected to deal with linear structural analysis with following reasons [24],

- Finite elements of Optistruct are benchmarked with NAFEMS (National Agency for Finite Element Methods and Standards) and some of the peculiar problems requested by industry.
- Along with the simulation of structural behaviour, Optistruct has powerful size and shape optimisation techniques that can accelerate the design process. Therefore, linear static FEA can be seamlessly extended for structural optimisation in future.

- Has built-in design interpretation software called “Ossmooth”, which recovers and smoothens a modified geometry resulting from optimisation that can be readily used in any other external CAD package.

- Since Hypermesh and Optistruct are products of same parent company (Altair Hyperworks), preparation of input deck for structural analysis and its extension for optimisation is not very demanding.

- Post processing of the FEA results can be done effectively using other Altair products such as HyperView, HyperGraph and HyperStudy. So all file formats are fully supported.

It would be difficult to judge, accuracy of FEA results of FWD beam subjected to “Forward 9g” loads (loads same as those used in Spreadsheet), if elements and meshing pattern is decided arbitrarily. A systematic approach to decide these factors has been followed and explained in coming section.

4.6 Mesh Sensitivity Study – Background and Importance

Sensitivity is the response of an FE model to the changing environment, which can be change in loads, support conditions, mesh density, element types or many other parameters. Sensitivity study is a self-validation tool, to check the robustness of the assumptions made during FE modelling [26]. It may affect the stress levels experienced by the model or may change the load path.

Mesh is a discrete representation of the continuous real world component being analysed. It comprises of elements connected at nodes. Response of the structure i.e. field variable is defined in terms of nodal degrees of freedom (dofs). The type of element used determines these nodal dofs, continuity conditions and subsequent extrapolation of results from integration points to nodes (using shape functions). Hence, before any simulation study, an engineer must decide on type of element to be used for FE modelling of various parts involved. In Addition, FEA is “computationally intense”, a CPU and disk-space consumer, and the star player is the mesh [26]. Following factors help to decide type of element to be used,

- Geometry and subsequent details to capture
- Type of loading, physical phenomenon to be captured and theory behind.
- Expected behaviour of the structure and built-in capabilities of element.
- Assumptions and restrictions of a particular FEA package.
- Anticipated output from the FEA e.g. field variable or its gradient
- Ratio of accuracy to per unit of computational expense.
- Method of connections, special phenomenon required such as preloads, release and support conditions to be applied.
- In-house component and “Aero-space Certified (3rd party)” part.

After selection of element type, precision of an analysis also depends on the size and position of elements. A satisfactory FEA is one that converges to the exact solution of the mathematical model. It can be achieved by refining the mesh. On one hand, denser the mesh greater is the number of dofs, which in turns increases the computational time. On the other hand, if coarse mesh is used then results suffer from discretisation errors and the model fails to capture the real behaviour of the structure.

Therefore, it is very important to build the model that balances number of dofs and solution accuracy. In order to define a proper mesh, some estimation of parameters (e.g. stress, displacement) within the components is essential.

An exercise to decide type and size of element to be used and the mesh density (i.e. number of elements) to be incorporated; is commonly known as “Mesh Sensitivity Study”.

4.6.1 A thought before start-up of Mesh Sensitivity study

The area of interest of this research is the structural response of the entire seat when subjected to static inertia loads as specified by CS 25.561. Loads

constitute bending, torsion and combination of both. Primary aspect to be evaluated is the stress (gradient of field variable i.e. of displacement) pattern and values in different structural components. Since this is a design project, emphasis should be made to quickly predict the behaviour of seat when subjected to loads for different designs of individual components. Therefore, number of simulations to be run is quite high. Major parts included in the analysis would be seat leg, FWD beam, boomerang, seat track and seat mounting assembly. Geometry of the leg, boomerang and seat mounting assembly is complicated and their interaction will lead to non-linear solution. Due to many number of parts considered, their 3D representations required, non-linear (all three i.e. contact, material and geometry) nature of the solution and number of design iterations required, computational cost and data storage cost is significant. Hence, emphasis should be made to find optimum balance between solution accuracy and CPU memory. Therefore, an extensive effort has been taken in the initial phase of the project, to identify a suitable element type and density of the mesh to be used for FE modelling of various components of seat. Findings are given in coming sections categorised as per the component.

4.6.2 Mesh Sensitivity Study for FWD beam

In current project, first component identified for mesh sensitivity study is the FWD beam as,

- It is a critical component since all the loads are transferred to beam from boomerangs.
- Bending stresses have been already calculated using spreadsheet developed earlier (Section 4.3, Figure 4-6). Therefore, means of a comparison for accuracy FEA results has already been well established.
- Good agreement between spreadsheet and FEA will be a major achievement. It will boost the confidence in FE model and in

spreadsheet, which, can be effectively used for initial sizing of the FWD beam.

Following parameters were identified for the comparison purpose,

- Compare the FEA stress (normal bending stress) results with those calculated by spreadsheet.
- Computational time and model size.

Model Set Up - Portion of FWD beam between boomerang and leg was used for mesh sensitivity study as it acts as a cantilever beam subjected to bending from boomerang and clamped to the leg, at the other end. The cross-section considered (Figure 4-7), force applied (equivalent to “Forward 9g” in local co-ordinate system of FWD beam) and location of force application point in FE model is identical to that used in spreadsheet for consistency.

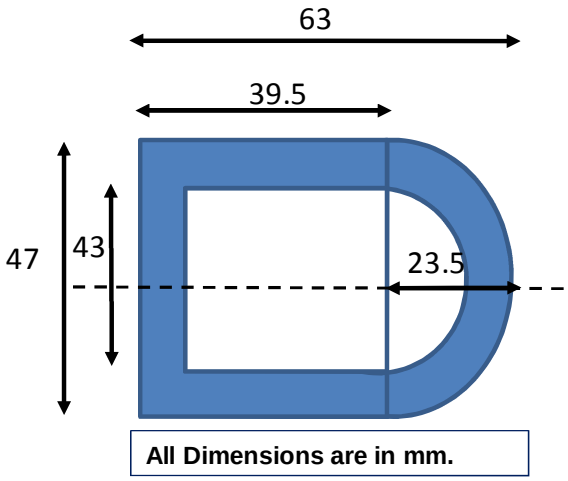

Figure 4-7 Cross-section of the FWD beam

The nodes on the clamped surface have been restrained for all the dofs. This overestimates the stiffness at support and gives very high stress values at constrained nodes. In order to avoid such an unphysical response, stresses at the restrained edge have been ignored.

The load is applied at the “Centre of Mass (COM)” of the cross-section at the end. Concentrated force is a convenient fiction, since all real forces are spread

over an area greater than zero [27]. Therefore, MPC elements have been used to transfer the loads from a load application point in FWD beam to the area where boomerang will be bolted to FWD beam (Figure 4-8). This helped to spread the load over a considerable area, avoiding unrealistic high stresses in the vicinity of loading points. Force Applied:

– X component = -2649.06N
– Y component = +5431.38N

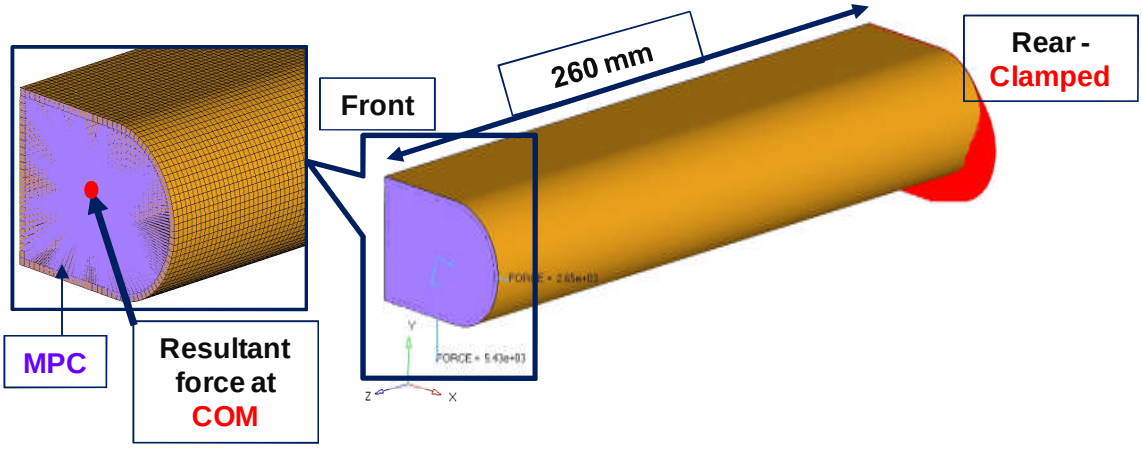

Figure 4-8 Load and Support Conditions Considered (Forward 9g)

Next task is to build the FE model of FWD beam with different element configurations used in Optistruct and Abaqus / Standard. The main variants were,

- Order of Element – First Order (Optistruct – (HEX 8, Tetra6), Abaqus - C3D8), Second Order (HEX 20)
- Elements through thickness – One element or Two elements
- Aspect Ratio (AR) – Uniform AR of 1:1 or varying AR of 3:1 (non-critical area) and 1:1 (in critical area to recover stresses).
- Special element configuration C3D8I (Abaqus/ Standard Only)

Using these combinations, eight different FE models of FWD beam were built and analysed. The results are summarised in Table 4-1 and compared with those from spreadsheet (Figure 4-6).

Meshing style	Number of elements through thickness	Element Type	Number of nodes	Number of Elements	Input File size, mb	Memory Required, mb	Maximum disc space used, mb	Solution time, sec	Normal bending stress (MPa)						Vertical Tip Deflection, mm	Remarks	Conclusion
									A	B	C	D	Emin	Emax			
Uniform mesh (Aspect Ratio (AR) close to 1)	1	Hex 8	30804	15300	3.75	302	62	8	-374	-95	168	302	200	-200	3.78	Constant Stress element. Can not capture bending properly.	Option ruled out
		Hex 20	107610	15300	109	290	2003	194	-376	-96	168	303	109	-201	3.81	Computationally expensive (solution time and disc space required).	Option ruled out
		Tetra 6	31570	96348	7.9	268	50	8	-406	-60	188	238	82.5	-234	3.7	No control over 3D mesh generation. OverStiff.	Option ruled out
		C3D8	30804	15300	2.5	74	372	17	-372	-102	162	302	105	-204	3.74	Constant Stress element. Can not capture bending properly.	Option ruled out
		C3D8I	30804	15300	2.5	174	580	25	-367	-109	161	310	132	-216	3.81	Computationally expensive but gives good results with less elements.	Selected for Abaqus FE models.
	2	Hex 8	47113	31201	6.49	113	595	51	-361	-101	156	310	126	-216	3.81	Good Co-relation with spreadsheet. Due to large number of elements costly CPU time.	Can be used for FWD beam but need to invistigate the possibility to reduce elements/CPU time.
		Tetra 6	32404	99349	8.28	277	53	9	-356	-56	187	267	76.8	-236	3.7	Poor Tetra-collpase (0.09). Overstiff.	Option ruled out
Dense in stressed region (AR 1) and coarse in other areas (AR 3)	2	Hex 8	19656	12896	2.7	234	48	7	-361	-101	156	310	126	-219	3.81	Good Co-relation with spreadsheet. Optimum CPU time.	Selected for Optistruct FE model of FWD beam

Table 4-1 Comparison of results for Mesh Sensitivity Study of FWD beam (Forward 9g load)

4.6.3 Key findings from mesh sensitivity study of FWD beam

- FE model with one constant strain element (HEX8, C3D8) through thickness is stiff and cannot predict bending stress accurately.
- Model with tetrahedral elements (Tetra 6 – one or two elements through thickness) are over-stiff. In addition, there is no control over 3D mesh generation using 2D Tria3 elements. In order to maintain good element quality (e.g. tetra-collapse); mesh needs to dense increasing computational time.
- Model with second order element (HEX 20, one element through thickness) gives acceptable results. However, the solution time (194 sec) and disc space requirement (2003 Mb) prohibit its use. If this modelling technique is used for the complete seat, then the input file size and processing time may not justify the accuracy of results. Therefore, FE models using second order Tetra elements (another element type) have not been built and this technique is not taken forward.
- Two HEX8 elements through thickness (with uniform AR 1:1) give results that are in good agreement with those from spreadsheet. A further investigation was done to reduce the number of elements. Simulation with varying AR (3:1) gave the same results as those with uniform AR (1:1) with significant savings in solution time (86%) and in maximum disc space required (91%). Therefore, it was decided to use two Hex8 elements through thickness with AR 1:1 in critical areas and 3:1 in non-critical areas; for FE modelling of FWD beam for Optistruct solver.
- In addition, one C3D8I (linear hex element with incompatible modes used in Abaqus/Standard) gives satisfactory results. Due to addition of extra internal dof, it is more expensive than the regular linear brick element (C3D8). However, they are significantly more economical than second-order Hex 20 elements (87% time saving). From literature review, it was observed that as these elements degrade from their quadrilateral shape (e.g. trapezoidal shaped C3D8I), the performance is reduced considerably. Hence, it was decided to use two regular shaped C3D8

element through thickness with varying AR (maximum of 3:1); for FE modelling of FWD beam for Abaqus / Standard solver.

Conclusion from Chapter 4

Chapter 4 outlined overall project plan to be followed. It identified “Forward 9g” and “Downward 6g” as critical load cases to focus on. In order to reduce the number of design parameters, it was decided to concentrate on successful design of the components from “Primary Load Path” i.e. FWD beam and leg.

Actual design work started with the analytical calculations for preliminary sizing of FWD beam. Later on, excellent co-relation was observed between bending stress induced in FWD beam (Forward 9g load); calculated by spreadsheet and that from FEA results of “Mesh Sensitivity Study” of FWD beam. This stamped the usefulness of spreadsheet for preliminary sizing of FWD beam and use of brick elements (two through thickness) with aspect ratio of 3:1.

For pre-processing, Hypermesh was chosen; while “Optistruct” was selected as a solver for linear static FEA.

5 Preparatory studies for design of leg

Next component in the “Primary Load Path (PLP)” is seat leg. Before straightway using FEA for the design of leg, it is important to study different aspects involved such as mesh sensitivity study of leg, development of verification framework for FEA results, methods to represent interaction between leg and FWD beam, and type of joint to be used.

Coming Chapters also demonstrate the “Sequential Development” of the detailed FE model of PLP

5.1 Strategy for leg Designing

First FEA is rarely satisfactory as it is a provisional one. A mature and detailed FE model evolves after “Sequence of models”; each one of them contains refinements suggested by results supplied by previous models and the last one includes all the necessary details, optimum mesh and boundary conditions. Such a systematic approach builds the confidence in the final results. In many cases, this approach takes less time and effort as compared to that required to build a detailed FE model right from the beginning [27]. Moreover, if the design itself is poor, precious time is unnecessarily spent on correcting a detailed FE model. A classic example of this is the designing of leg variant V#1, during this research. Preliminary linear static analysis for “Forward 9g” loads showed that the design is far away from the expected strength (Discussed in detail in Section H.1). A detailed FE model would have hogged huge amount of work and time, only to discover that leg is under-designed!

Figure 5-1 shows the strategy outlined for the development of a detailed FE model for PLP starting from the scratch.

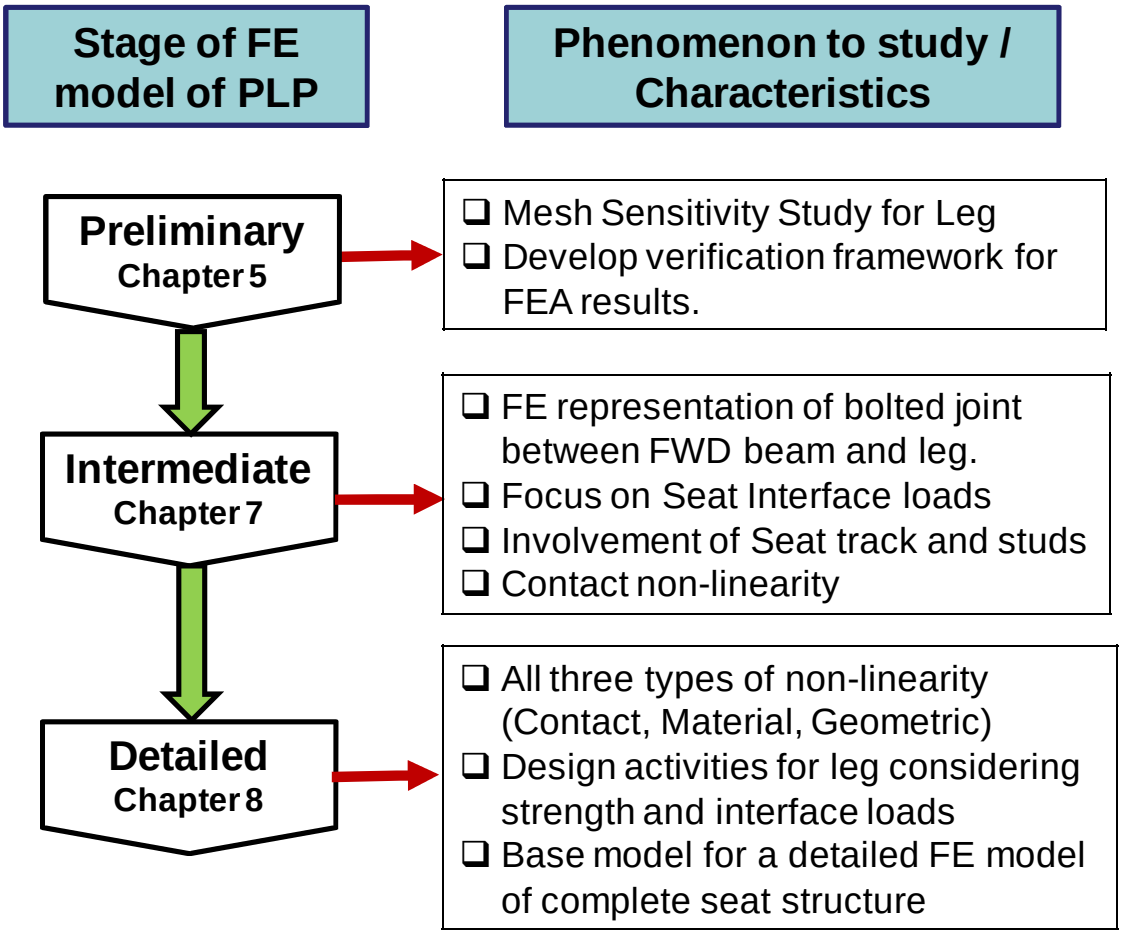

Figure 5-1 Sequential Development Approach for FE model of "Primary Load Path"

In this chapter, mesh sensitivity study for leg and sanity checks performed for assessing quality of FEA results of preliminary model of “FWD beam and leg” are explained in detail.

5.2 Mesh Sensitivity Study for Leg

The load case used was “Forward 9g” and the spreadsheet was used to convert the loads from Global Co-ordinate system to the local co-ordinate system of FWD beam (Appendix J).

5.2.1 Loads and Support Conditions

Leg is attached to the seat track using three studs and a locater pin. Locator pin also acts as a shear pin. Inclusion of seat track, studs and shear pin would demand modelling of contact non-linearity that brings in problems such as non-convergence and rigid body motion. It was not advisable to spend time in debugging these issues and a quick estimate of the strength of leg was a priority. Therefore, seat track, studs and shear pin were not included in the analysis and their representative support conditions were used (Figure 5-2). The peripheral surface of each stud protruding out of the lower foot-section of leg was constrained for vertical and lateral direction. Outer surface of the hole in the leg where shear pin is located was constrained for longitudinal direction.

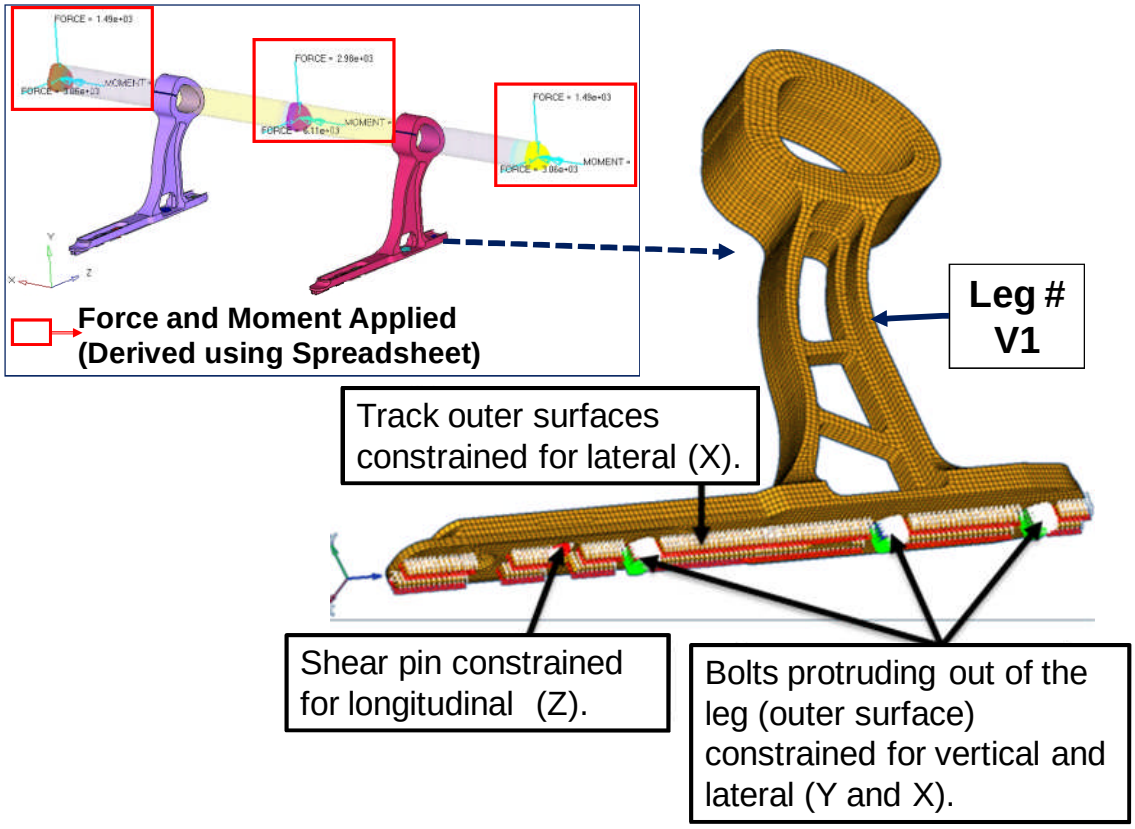

Figure 5-2 Loads (Forward 9g) and Support Conditions for Preliminary FE model of "FWD beam and leg"

The reaction forces introduced in each of the studs and constrained locations of track have been recovered using “SPCFORCE” control card of Optistruct [24]. These reaction forces are used for “Force Equilibrium check”, as discussed in coming Section 5.4.1, Figure 5-6.

The attachment between leg and beam (discussed in detail in Section 6.1) was captured using coincident nodes between interacting surfaces of FWD beam and leg. This helped to make the FEA a linear static one and hence, Optistruct was used as a solver.

5.2.2 FE Modelling Strategy for Leg

The leg design (named as Leg Variant V#1) used for mesh sensitivity study was given by BlueSky and weighted around 800g.As a starting point, leg modelling was done using brick (hexahedral) elements with a global element size of 2.5 mm. This resulted in 28927 number of nodes and 21506 number of elements and took about five man-days of modelling effort. Results interpretation from this preliminary model revealed that the current leg design is too weak to sustain the “Forward 9g” loads (Appendix H.1). This suggested that design modifications were required. Thus, finalising leg design was going to be an iterative process and each time FE model would be required to be built for a new leg design (here onward called as Variant). Considering strict time-line, spending five or six man-days (depending on complexity of leg geometry) just for FE modelling of leg was not a good option when the whole purpose of initial study was to compare the different design concepts QUICKLY, so that the designer gets an overall idea of load transfer and possible locations of high stress.

Compared to brick modelling of leg, use of tetrahedral elements was a very attractive and time saving option with following thinking,

- In an early design phase, feasibility of the design to sustain the loads is checked at global level. Therefore, precise values of stress and strain are not sought and their constant values per element are admissible

provided sufficient number of elements are used to capture the geometry.

- Modelling of necessary details in a complicated shape like leg favours use of large number of lower order elements rather than higher order elements [27].

- Geometrically versatile, simper elements (lower order, constant strain tetrahedral) provide reasonable estimation of stress per unit of time and computational expense [27].

Therefore, the strategy behind mesh sensitivity study of leg was to obtain the size of linear tetrahedral element that would give the comparable and acceptable results to those obtained from model with brick elements (base line results).

5.2.3 Result discussion of Mesh Sensitivity Study for Seat Leg

Starting from global element size (tetrahedral) of 10mm until 3mm (stepwise decrease of 1mm), FE models were built for leg and FEA for simplified model of "FWD beam and leg" was done. Results were compared with each other (not presented here as similar to FWD beam mesh sensitivity study). It was observed that results, which were within acceptable limits with base line results; were obtained with a tetrahedral element size of 4mm (Figure 5-3). This FE model of leg had 14861 number of nodes and 49057 number of elements.

Configuration	I – Tetrahedral Elements	II – Hexahedral Elements
Von Mises stress Plot for Leg #V1	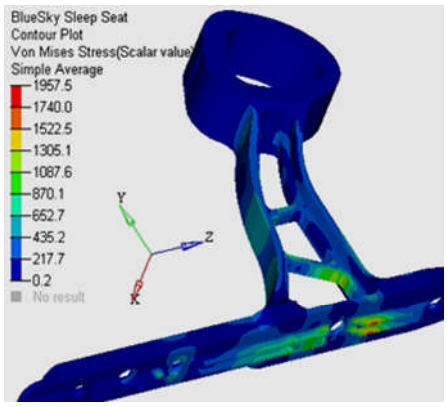	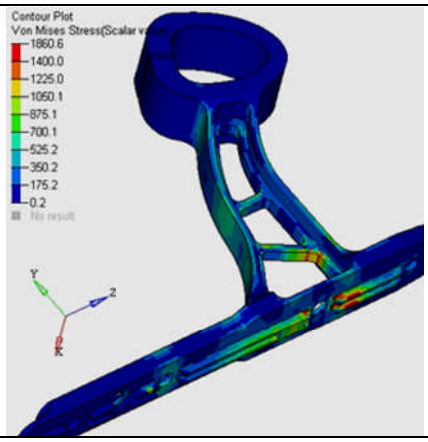
Number of Degrees Of Freedom	44583	86781
Maximum Von Mises stress (MPa)	1700	1800
Solution Time (Second)	4206	7167
FE Modelling Time	6 Hours	5 Days

Figure 5-3 Comparison between tetrahedral (LHS) and Hexahedral (RHS) elements for leg ("Forward 9g")

Interpretation of results shown in Figure5-3 can be done as follows,

- For both the configurations, maximum von Mises was observed at the same location i.e. at the underside of the foot-section of leg. Overall distribution of the stress contour remains same for both the configurations. A variation of 5.5% in the maximum von Mises stress observed between both the configurations is not significant.

- The greatest advantage of using tetrahedral elements can be seen when pre-processing time required for FE modelling of leg is compared. A massive 85% reduction in the time is obtained with tetrahedral elements, which is crucial in cutting the overall design time of the seat. In addition, 40% of solution time was saved with Configuration I.

Therefore, it was decided to **use linear tetrahedral element (with global element size of 4mm) for FE modelling of leg** as this saves considerable time and gives reasonably good estimate of behaviour of leg after load application. A care has been taken, to model walls of the leg with at least two elements through thickness.

During preliminary FEA of PLP, another interesting observation was made regarding detrimental effect of non-ordered node numbering on the solution time and file size.

5.3 Effect of ordered node numbering on solution time

Figure 5-4 shows, different node numbering schemes for the rod element and associated global stiffness matrix, K_e (assuming AE/L = 1, A – cross-sectional area, E- modulus of elasticity and L –length of individual element). Rod element is made up of six elements each of length L. In Case 1, node numbers are in order while in Case 2 arbitrary node numbering system has been chosen [28].

Two cases with different node numbering Scheme	Global Stiffness matrix
Case 1 : Ordered node numbering 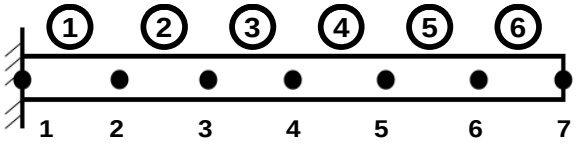 	$\begin{bmatrix} 1 & -1 & 0 & 0 & 0 & 0 & 0 \\ -1 & 2 & -1 & 0 & 0 & 0 & 0 \\ 0 & -1 & 2 & -1 & 0 & 0 & 0 \\ 0 & 0 & -1 & 2 & -1 & 0 & 0 \\ 0 & 0 & 0 & -1 & 2 & -1 & 0 \\ 0 & 0 & 0 & 0 & -1 & 2 & -1 \\ 0 & 0 & 0 & 0 & 0 & -1 & 1 \end{bmatrix}$
Case 2 : Non - Ordered node numbering 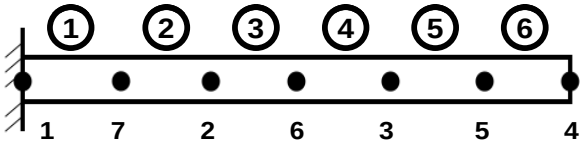 	$\begin{bmatrix} 1 & 0 & 0 & 0 & 0 & 0 & -1 \\ 0 & 2 & 0 & 0 & 0 & -1 & -1 \\ 0 & 0 & 2 & 0 & -1 & -1 & 0 \\ 0 & 0 & 0 & 1 & -1 & 0 & 0 \\ 0 & 0 & -1 & -1 & 2 & 0 & 0 \\ 0 & -1 & -1 & 0 & 0 & 2 & 0 \\ -1 & -1 & 0 & 0 & 0 & 0 & 2 \end{bmatrix}$

Figure 5-4 Stiffness matrices with different node numbering

Elements of i^{th} column of a stiffness matrix represent the force required to cause a deformation state ((translation or rotation) such that i^{th} dof gets a value of unity and all other, dof become zero [28]. With this interpretation of K_e, following observations can be made,

- All the non-zero coefficients in Case 1, are clustered around the leading diagonal, while in Case 2 they are spread over and picture is bit chaotic. Apart from considering upper or lower triangular matrix for storage not much can be made in Case 2.

- Assuming use of Gauss Elimination method to solve [Ke]{d} = {F} and exploiting symmetry, Ke in Case 1 can be written and stored as,

$$K_e = \begin{bmatrix} \mathbf{1} & \mathbf{2} & \mathbf{2} & \mathbf{2} & \mathbf{2} & \mathbf{2} & \mathbf{1} \\ \mathbf{-1} & \mathbf{-1} & \mathbf{-1} & \mathbf{-1} & \mathbf{-1} & \mathbf{-1} & \mathbf{0} \end{bmatrix}$$

Where,

{d} – Nodal dof vector,

{F}- Nodal load vector.

With this K_e, need of computer memory dramatically goes down. When very big FE models with thousands of elements, are analysed benefits are many fold. Thus ordered node numbering schemes lead to optimum size arrays for storage and are computationally economical. An exercise was carried out to check the effect of node numbering on solution time and disc space requirement for a linear static analysis of “FWD beam and leg” (preliminary model) subjected to “Forward 9g”. Benefits of ordered node numbering can be readily seen as shown in Figure 5-5,

Effect of Node numbering on Linear Static Analysis (all other conditions same)			
Serial Number	**Parameter**	**Ordered Numbering**	**Non-ordered Numbering**
1	Solution time, S	60	64
2	Memory (RAM) , MB	980	985
3	Disc space for Scratch files,MB	1204	1210
Leg V#1, Forward 9g Load. **Nodes = 138673, Elements = 136798**	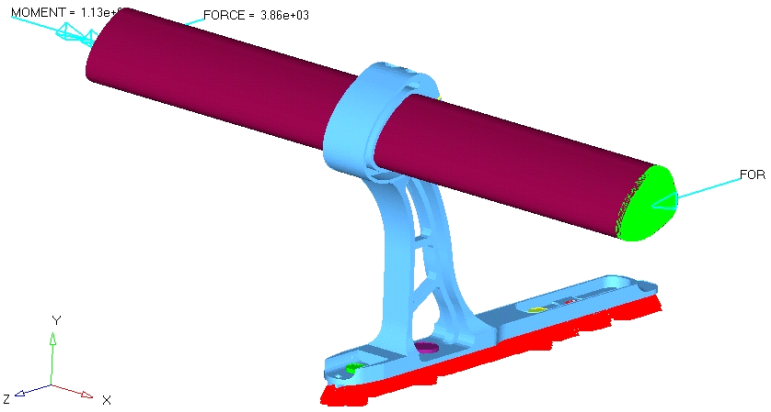		

Figure 5-5 Increase in solution time and disc space due to non-ordered node numbering for linear static analysis

Solution algorithm used Optistruct, Hardware details: 2 CPU: Intel(R) Core(TM) 2 Duo CPU T6600 @ 2.20GHz CPU speed 2200 MHz

The advantages of ordered node numbering schemes would be magnified when non-linear FEA of the complete seat will be performed (Solution time increases by 10% in case of non- ordered node numbering. Please refer Appendix D)

Node numbering schemes can also be effectively used to join different input decks e.g. a typical dynamic analysis of full-blown seats consists of seat superstructure, substructure, seat track assembly, contact definitions, and dummies. Keeping all these parameters in one file would make the file size very big also displaying, rotating such a file on computer will demand advanced graphics card and higher memory. Instead, a range of node numbers can be

assigned to each of the sub-assemblies of seat and separate files can be made. During solution phase, all the files can be linked together through a simple sub-routine. This will make the handling of the FE models much easier and at cheaper computer costs.

Preceding sections concluded “Pre-processing” and “Solution” stages in FEA for preliminary FE model of PLP. During interpretation of results, when analysts starts believing the FEA results, immediate question is “Why to believe FEA results?”. Therefore, it is of utmost important to develop procedures for initial checks of FEA results. In next section, framework developed for verifying the results from linear static analysis of “FWD beam and Leg” has been demonstrated.

5.4 Verification Framework

FEA provides an approximate technique to predict the behaviour of component under applied loading. This presents significant challenges for analysts to answer the critics “How do you know?” by computer-assisted engineering. Credibility lies at the heart of every simulation effort so; results should be checked with prior experience and engineering fundamentals.

For traditional problems, analytical calculations can be made using handbook formulae and a comparative study can be done between FE results and those from analytical calculations. For this research, this technique has been exploited for FWD beam as seen in Section 4.6.3. However, involvement of complicated geometries and their interactions, make the simulations incredibly comprehensive. Therefore, it becomes difficult to establish confidence in these FE models through hand calculations or simple engineering judgements.

The answer for this is the validation of existing design by experimental testing prior to predicting the performance of new designs. If the overall strength and deflections predicted by FE and those observed during testing co-relate, FE procedure can be declared as foolproof [26].

However, validation challenge increases with completely new concept, such as “Sleep Seat” where no existing data or designs are in stock! One way is to build prototype of new design, test it, and validate FE model. However, the short timelines and tight budgets do not give this freedom. In addition, validation has its limits. If something goes wrong during testing e.g. malfunctioning of one of the data recorders, test results cannot be believed which can have detrimental effect on cost of NPD (New Product Development).

To overcome these issues, strategy used during this research is, verification of FE results by a combination of analytical calculations, guidance from authorities in this area and various checks using diagnostic tools provided by FE solvers. Checking the results in this manner is the most useful method for the earliest models in the sequence, when there are question marks on the appropriateness of the assumptions made and blunders are common e.g. use of incompatible system of units [27].

Normally, there are two types of checks to be performed on FEA results to ensure that results are consistent with real life behaviour of the component.

5.4.1 Computational Accuracy

While checking for computational accuracy for linear static analysis, analyst should look for reaction forces equilibrium and averaged and unaveraged stress difference.

Equilibrium Check means that the sum of reaction forces should be equal to the applied loads. If the model fails to show global force equilibrium, it means either loads were applied in local co-ordinate system when intended to apply in global co-ordinate system or some of the loads were applied to constrained nodes, which were ignored. So, in order to ensure the satisfactory solution, global equilibrium must be achieved. FEA results of preliminary model of “FWD beam and Leg V#1”, subjected to “Forward 9g” load with support conditions as explained in Section 5.2.1, satisfies force equilibrium check as shown in figure 5-6.

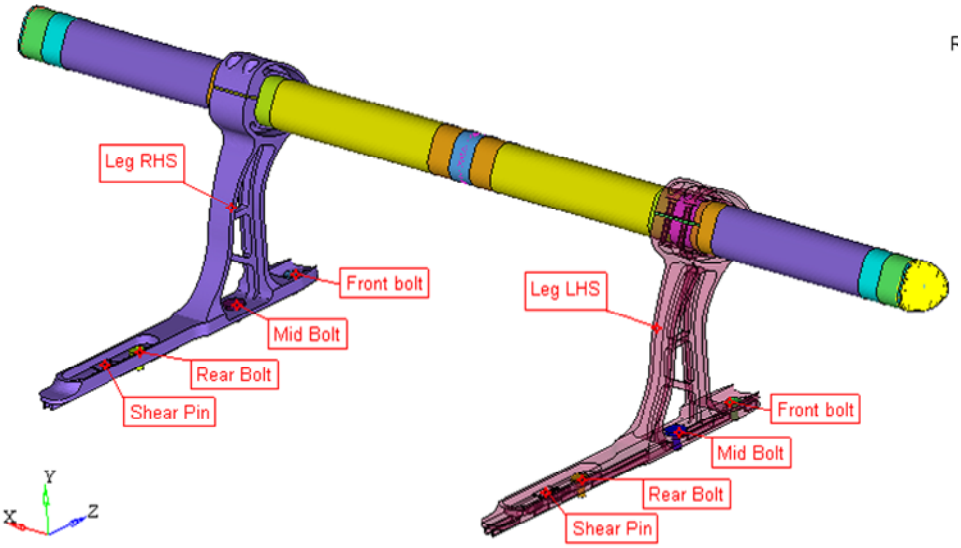

Load case CS25.561 , FWD 9g - Reaction Force summary						
Leg position / Bolt location	LHS			RHS		
	x , N	y , N	z , N	x , N	y , N	z , N
Front	-146.56	13296.52	0.00	146.32	13296.98	0.00
Mid	-32.53	1006.56	0.00	32.48	1006.55	0.00
Rear	-918.05	-17283.56	0.00	918.12	-17283.56	0.00
Shear pin	0.00	0.00	-6130.99	0.00	0.00	-6089.83
Track	1067.35	0.00	0.00	-1067.20	0.00	0.00
Sum	**-29.78**	**-2980.48**	**-6130.99**	**29.72**	**-2980.03**	**-6089.83**

	X	Y	Z	Remark
(LHS+RHS) Total Reactionforce , N	-0.06	-5960.50	-12220.82	As it can be seen that the reaction force configuration exactly matches the applied load scenario; force equilibrium conditions is satisfied.
Applied load (from SpreadSheet) , N		Qc	Pc	
	0.00	5960.40	12220.60	

Figure 5-6 Nomenclature for Reaction Force Extraction and demonstration of "Force Equilibrium Check" for the preliminary FE model of PLP

This check also provides an insight into, the magnitude and direction of applied load and co-ordinate system used. Sometimes, double of the load is applied or duplicate loads are present, which go un-noticed thereby under-estimating the design. Reverse case is application of less loads. When symmetric behaviour is expected, results can be un-symmetric due to inadvertently applied imbalanced loads. If this happens, in a non-linear FEA, analysts may take this as an error

due to incorrect interface definitions or incorrect friction model! So, though check for force equilibrium is a very basic and simple, it can be crucial and should not be ignored.

Averaged and unaveraged stress difference**,** One way to judge the adequacy of discretisation is, to look at the FEA results “with nodal averaging” and “without nodal averaging”. If stress contours line up from element to element i.e., there is no jump or discontinuity of stress between adjacent elements, convergence can be assumed. It is an important check as element type used for current analysis is of C^0 continuity (i.e. constant stress element). Since element shows only one value of stress (either compressive or tensile), two or more elements may be required through thickness to capture behaviour such as bending.

Figure 5-7 shows that there is a smooth variation between the stress contours and the difference between averaged and un-averaged results is not significant. It ensures that, a sufficient mesh refinement has been achieved.

Parameter	With Nodal Averaging	Without Nodal Averaging
Von – Mises Stress Plot	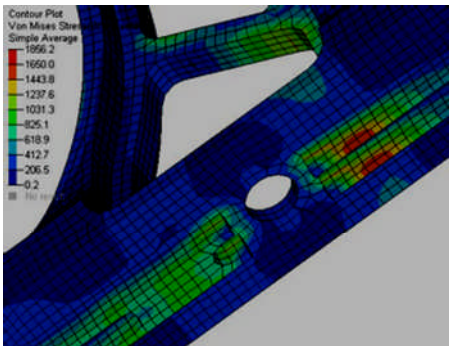	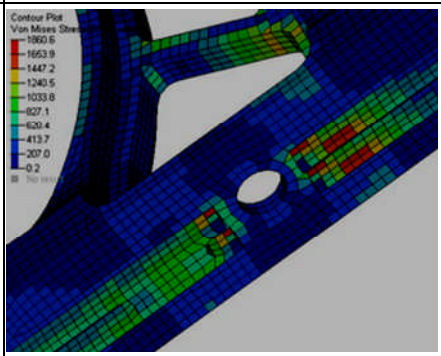
Maximum Value of the Von – Mises Stress (MPa)	**1630**	**1750**

Figure 5-7 Comparison between FEA results with and without nodal averaging. Leg V#1, Forward 9g

For non-linear FEA, checks such as residual force and moment, ratio of artificial damping energy to strain energy, distribution of contact pressure and forces transmitted across interfaces should be added to above checks.

5.4.2 Co-relation with expected physical behaviour

***Displacement continuity check*,** There are overall 12 components (2 legs, 1 FWD beam, 6 bolts and 3 inserts) involved in the FEA of preliminary model of "FWD beam and leg". If one or more components are not connected properly with rest of the structure, displacement plot will be discontinuous. Being unconnected, load will not be transferred to them. Hence, while rest of the structure undergoes deflection, unconnected components will not show any deflection. Therefore, first check that is performed on the model is by animating the deformed structure and it is observed that the model shows a continuous displacement pattern (Figure 5-8).

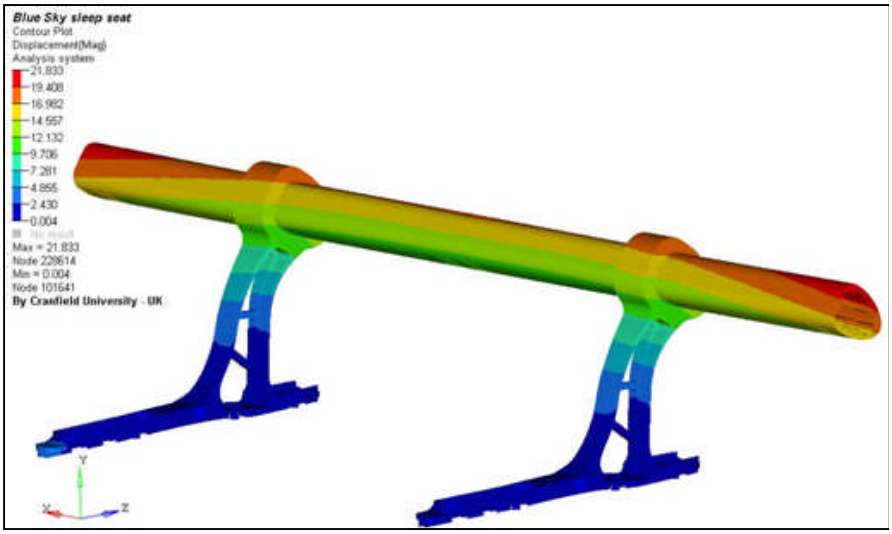

Figure 5-8 "FWD beam and leg assembly" satisfies Displacement continuity check.

This check also highlights mistakes made during load application. In one of the non-linear FEA of "FWD beam and leg" performed by author of this thesis, values of moment (1E6 N-mm) and force (3.4E3 N) were interchanged. The solution was not at all converging, due to a very large value of applied force (1E6 N). Efforts were focussed on modifying geometries, applying load in small

increments and trying all advanced solution techniques to avoid rigid body motion, in vain. Animation of the displacement contour (by mistake) showed the mistake! Therefore, before any deep interpretation of FEA results, animate the deformed shape (usually with a scale factor) and check for displacements at unexpected regions, in unexpected directions, surprisingly large or small magnitude.

Stress plot check**,** FEA results should show high stresses at sections where there are abrupt changes in cross-section or at parts where support conditions have been applied. Based on this logic, FWD beam and insert are expected to show lower stress values as compared to those seen in leg, when subjected to "Forward-9g" loads. Actual stress contour (Figure 5-9) corroborates the estimates. Hence, the FE procedure used satisfies expected stress response test.

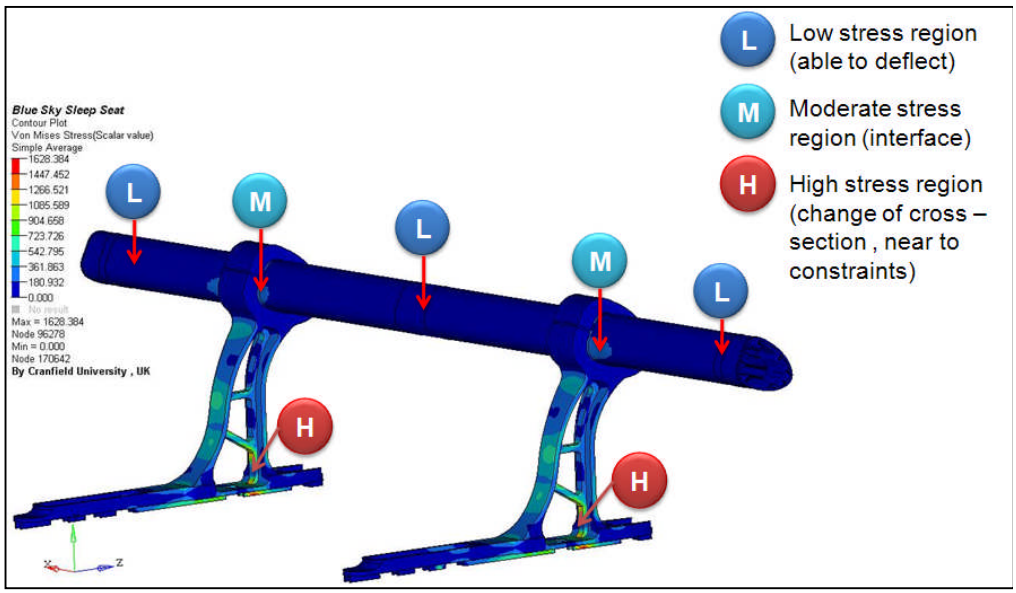

Figure 5-9 Expected Stress behaviour for "FWD beam and Leg assembly" when subjected to FWD 9g load

Conclusion from Chapter 5

In order to avoid investment of huge amount of time and efforts in developing detailed FE models right at the beginning, a “Sequential Modelling” approach was drafted. The logic behind this was stepwise refinement of FE input deck, based on previous FEA results, ultimately leading to a final model with all the necessary details. Thus, three stages in which a detailed FE model (with all non-linearities) of “Primary Load Path” would be achieved were defined.

In this chapter, preliminary (i.e. coincident nodes at the interface between FWD beam and leg) FE model of “FWD beam and leg” was developed. Mesh sensitivity study for leg, done using preliminary model, showed that tetrahedral elements with a global size of 4 millimetres, gives acceptable results at lower pre-processing and solutions costs. Ordered node-numbering scheme helps to reduce the time and disc-space required. FE models developed were rigorously checked for various quality checks from computational viewpoint as well as from closeness to expected real-life behaviour. The overall FE modelling procedure was found to be satisfactory.

Second point form the scope of the project (Section 1.3) was achieved in this chapter. i.e.

“This research will develop a practical modelling methodology that can be used to assist designers in assessing the suitability of a chosen seat configuration, through a sound understanding / application of the FE Method, together with demonstrating a critical assessment of the quality of the numerical results through appropriate verification methods”.

Next step was to develop an intermediate FE model of “FWD beam and leg assembly”.

6 Factors affecting leg design

So far, a sound and robust FEA methodology along with necessary checks has been developed for the preliminary model of “FWD beam and leg”. The next task would be to start the leg design. Immediate question is “How to represent the bolting of leg to the FWD beam in FEA?” Therefore, this chapter elaborates different studies conducted, to come up with a FE practice of attaching leg with the beam.

6.1 FE representation of connection between FWD beam and leg

In reality, leg would be clamped with the FWD beam with the help of two M5 studs of 12.9 class, as per the input from BlueSky (Figure 6-1).

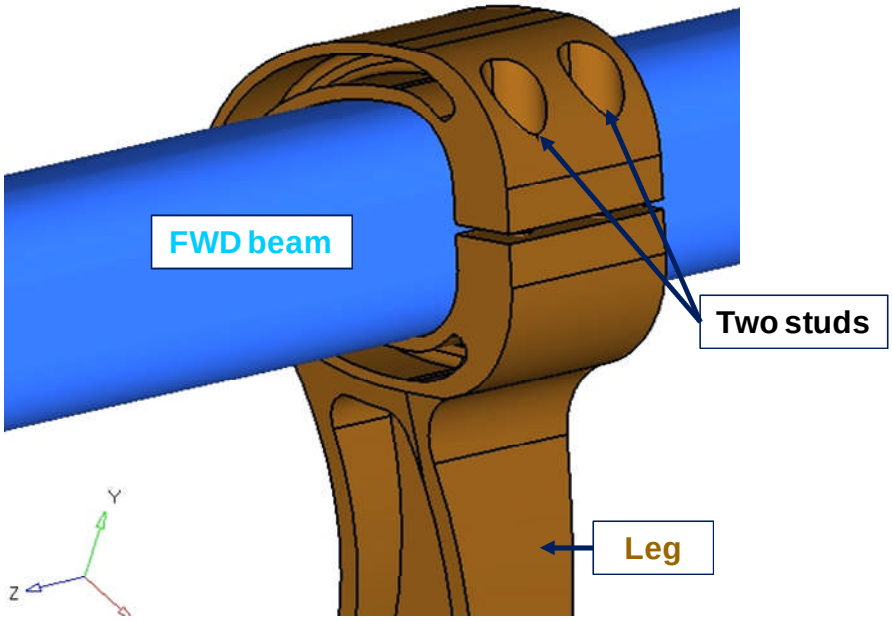

Figure 6-1 Leg is bolted to FWD beam

In FE model, the bolted joint between FWD beam and leg can be represented through,

- Use of coincident nodes in the contacting area. This technique was used in Section 5.2.1. As the project progresses, different design concepts of

leg and FWD beam would be required to model with FE. For each of such design iterations, it would be tedious and time consuming, to maintain coincident nodes between mating surfaces of FWD beam and leg. Therefore, this option was not suitable for future design work and was discarded.

Other two options were,

- Use of Tied contact at the overlapping surfaces of FWD beam and leg.
- Explicitly model bolt pre-load. This option requires detailed study of contact non-linearity as contact needs to be defined between leg and beam, stud heads and corresponding mating surfaces of leg. In addition, a methodology for FE modelling of bolt-preload must be developed.

Both of these options introduced contact non-linearity. Therefore, it was necessary at this stage, to upgrade the preliminary FE model of “FWD beam and leg” to first stage of “Detailed FE model”, by adding features such as contact at the beam and leg interface and simulation of bolt pre-load.

Naturally, this demanded a shift in solver too, from a linear to non-linear. Two non-linear programs identified were ANSYS and Abaqus/Standard. Coming sections discuss the advantages of choosing Abaqus / Standard for non-linear simulations and development of a procedure to model bolt pre-load.

6.2 Selection of Non-linear FE Solver

For years, analysts were confined to linear static stress analysis, so the choice of FEA software was limited. With the development in computer capacity, a range of FE packages is available with extended capabilities to perform different simulations including elastic and plastic transformations, buckling, fixed and sliding contacts, fatigue, creep large deflections and deformations, hyper elasticity, visco-elasticity and many others.

Typically, the type of output required, capability and compatibility with pre and post processors govern the choice of FE solver. In this research, three different

solvers i.e. Optistruct, Ansys and Abaqus were studied through their documentation available [24], [29], [30]. The parameters used for comparing different solvers were number of elements handling capability, degree of handling non-linear complexities, different types of elements available and tools to deal with contact non – convergence issues. Detailed comparison is given in “Appendix E”. Optistruct was chosen for linear static FEA as discussed in Section 4.5.

6.2.1 Abaqus/Standard for Non-linear Static Analysis

Consideration of detailed behaviour of the complex seat assembly will lead to non-linear analysis encompassing contact, material and geometric non-linearity. Abaqus/Standard provides accurate, robust and flexible solutions for these nonlinear problems [31]. It leverages advantages of high-performance parallel computing facilities which enables to include even minute details and can still reduces the turnaround time for high-fidelity results [31]. Capabilities of Abaqus/Standard can be listed as,

I. Bolt pre-load capability for detailed study of operating conditions.

II. Mature and advanced Element configurations

a) Incompatible mode elements for bending dominated problems

FEA of FWD Beam and leg assembly is mainly dominated by bending. In order to capture bending in a realistic manner, either high number of elements through thickness should be used (dense mesh) or elements with enhanced capabilities to capture bending (comparatively coarser mesh) should be used. In former case, solution time increases proportional to the square of dofs [27]. Abaqus allows to use fewer elements, without losing solution accuracy by providing “Incompatible mode elements” (This feature is demonstrated in Table 4-1, Section 4.6.3).

These lower-order quadrilateral continuum elements (C3D8I) are enhanced by incompatible modes to improve the bending behaviour [29]. There advantages are,

- In addition to the displacement dofs, incompatible deformation modes are added internal to the elements. The primary effect of these dofs is to eliminate the so-called parasitic shear stresses that are observed in regular displacement elements if they are loaded in bending.

- The incompatible mode elements perform almost as well as second-order elements in many situations if the elements have an approximately rectangular shape (Table 4-1, Section 4.6.3).

- Because of the internal dofs (13 for C3D8I), this element is somewhat more expensive than regular displacement element (C3D8). However, the additional dofs do not substantially increase the wavefront, since they can be eliminated immediately [29].

- In addition, it is not necessary to use selectively reduced integration, which partially offsets the cost of the additional degrees of freedom.

b) Modified quadratic elements for contact non-linear problems

The regular second order elements are not appropriate for contact problems with the default “hard” contact relationship [29]. The reason being, in uniform pressure situations, the contact forces are significantly different at the corner and midside nodes (they are zero at the corner nodes of a second-order tetrahedron), which may lead to convergence problems. However, Abaqus provides modified higher order elements (e.g. C3D8M) which alleviate this problem. They give rise to uniform contact pressures with the default “hard” contact relationship, exhibit minimal shear and volumetric locking, and are robust during finite deformation [29].

III. Stable and robust interface algorithm

Abaqus is known for its powerful, robust and highly efficient contact algorithm. Various contact algorithm types are available to model various interactions [31].

IV. Automatic damping of rigid body modes

Abaqus has inbuilt automatic stabilization algorithm with a damping factor, which typically works well to subside instabilities and to eliminate rigid body modes without having a major effect on the solution. Adaptive stabilisation schemes restricts the ever-increasing stabilization energy with reference to strain energy to ensure that solution is not dominated by viscous forces arising from undesirable large damping factors.

V. Contact diagnostic tool

This helps to review initial contact conditions such as over closer, openings, list of slave nodes and the master nodes to which slave nodes transfer the loads when in contact and a list of slave nodes that have failed to find an intersecting master surface [29]. It can track the status of interactions for all iterations. This helps to investigate causes of the terminated analysis. It also provides invaluable information on contact chattering, unrealistic and severe over closures and non-converging forces equilibrium conditions. The beauty of the tool is, it gives visual identification of the problematic region and numerically quantifies the severity of an error, which is a great help.

VI. Abaqus/Standard is compatible with Altair Hyperworks products such as Hypermesh and Hyperview [29].

Therefore, Abaqus/Standard was chosen to perform non-linear analysis of Sleep Seat when subjected to loads as per CS 25.561.

Next task was to determine how to use Abaqus / Standard to model bolt-preload.

6.3 Modelling of Bolt-Preload with Abaqus / Standard

Consideration of bolt-preload is important at the interface of FWD beam and leg as seen in Section 6.1. In Addition, seat will be attached to the track with the help of bolts, where effect of bolt pre-load may be required.

Even though the bolt itself is very well designed, this cannot make the joint more reliable [32]. Therefore, it is very important to study the influence of the bolted joints on the performance of the overall structure.

6.3.1 Background of bolt preloading

Advantages of bolt preloading can be stated as follows,

- Normally in a bolted joint, the joint is supposed to carry maximum of load. Without preloading, bolt is subjected to the entire applied load. Usually this leads to bolt failure through bending and shear forces acting on the bolt. With the help of pre-loading of bolt; bolt would not actually 'feel' any of the applied force until it exceeds clamp force of the bolt [32].
- Bolt preload reduces the cyclic loading from external load to such a level that the bolt can survive indefinitely. Therefore, it increases the fatigue resistance.
- Bolt preload increases the strength of the joint and closes the gap between the joints.

6.3.2 Method to calculate bolt preload

General formula used to calculate preload (F_i) is [33],

For reusable connections: $F_i = 0.75*A_t*S_p$

For permanent connections: $F_i = 0.9*A_t*S_p$

Where,

A_t is the tensile area of the bolt and
S_p is the proof strength of the bolt.

A free and reliable bolt-preload calculator is available on the Internet at, http://www.tribology-abc.com/calculators/e3_6a.htm [34] (General window for bolt – preload calculation is as shown in Appendix F).

This website takes into account, combination of size of bolt, class of bolt and frictional coefficients between bolt head and face, threads. It gives useful parameters such as tensile stress area of bolt, total tightening torque, and initial

preload. For present FEA analysis of sleep seat, bolt preload vales are calculated using this website with defaults values for initial tensile stress (60% of proof strength), and frictional coefficient (0.15).

For the M5 with 12.9 class studs in FWD beam, initial preload is around 9 KN. While for the mushroom-headed studs (M10 with 8.8 Class) in the track, it is around 22 KN. Please note, mushroom-headed studs in the seat track have been discussed in detail in Chapter 7.
Following section explains the procedure used to incorporate bolt pre – load in the present simulation.

6.3.3 Steps for bolt-preload modelling in Abaqus / Standard

In Abaqus/Standard, bolt preload can be specified by applying the load across the bolt cross- section [29]. This can be solved as a “General Step”. In lateral steps, the effect of bolt preloading step is propagated and any further external loading can be applied so that the bolt acts as a standard, deformable component responding to other loadings on the assembly, retaining the effect due to pre-loading [29].

Following steps have been used to apply a pre –load in present analysis,

I. Define the bolt cross- section surface. It must cut through the bolt geometry. It should be located on the internal faces of the elements across the cutting plane where the nut is tightened (Figure 6-2).

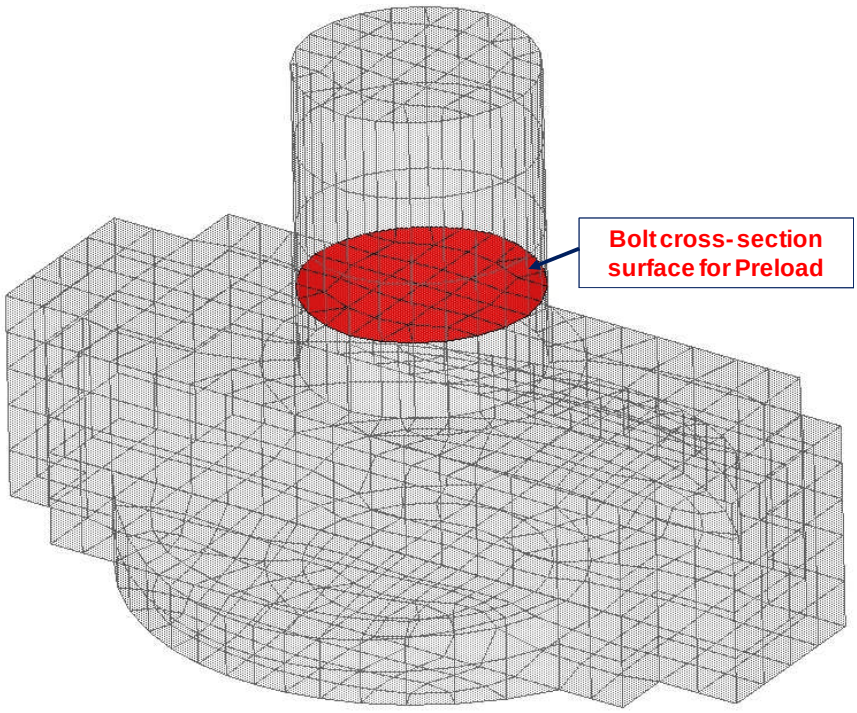

Figure 6-2 Internal Cross-Section over which Bolt-Preload would be applied [29]

Input file (*.inp) looks as,

Element set (_PRELOAD_S1 consisting of element numbers 99 and 102)

*Elset, elset=_PRELOAD_S1, internal, instance=PART-1-1, generate 99, 102,

Pre tension internal surface,

*Surface, type=ELEMENT, name=PRELOAD

_PRELOAD_S1, S1

II. Select the datum axis. One of axes of a co-ordinate system should be selected which indicates axis of the bolt (Local Y-axis in Figure 6-3).

III. Prescribe the value of pre-load calculated (Pre load of 9000 N is applied on pretension surface in Local Y direction (Figure 6-3),

While the Input file looks as,

** Pre-Tension Section for Bolt Load: Load-1
*Pre-tension Section, surface= PRELOAD, node=_Load-1_blrn_0., 1, 0.

** Name: Load-1 Type: Bolt load

*Cload

_Load-1_blrn_, 1, 9000.

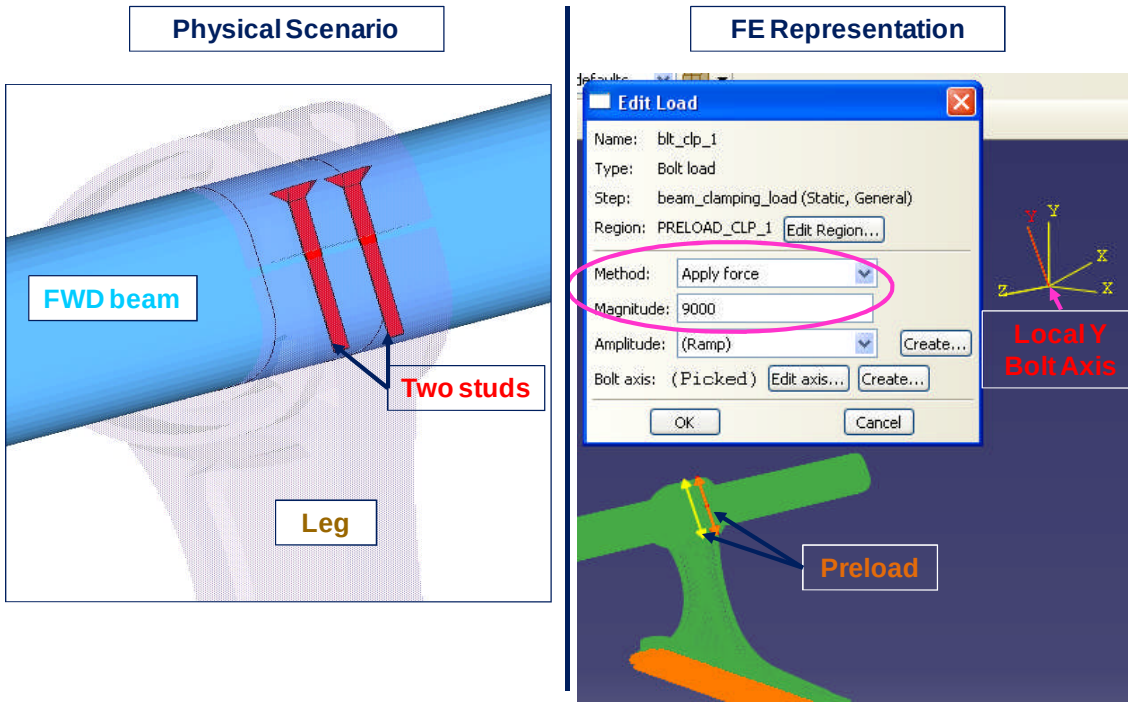

Figure 6-3 FE representation of Bolt Initial Tightening, Preload of 9000 N applied along the axis of the bolt in local co-ordinate system [29]

IV. Final step - Define interaction definitions between corresponding mating parts i.e. between FWD beam and leg, bolt head and its resting surface on leg.

** INTERACTIONS

** Interaction: INT_1-1

*Contact Pair, interaction=INT_1, small sliding, type=SURFACE TO SURFACE

HEAD_CON, UPPER_PLT_MAS

** Interaction: INT_1-2

*Contact Pair, interaction=INT_1

UPPER_PLT_CON, BOT_PLT_MAS

This established the procedure for modelling bolt-preload in Abaqus / Standard. In the next step, bolt pre-load in the FWD beam studs was actually simulated and stress levels induced in corresponding components (for “Forward 9g” loads) were compared with those obtained from the “tied contact” (between FWD beam and leg) model, which was the one of the main objectives of this chapter as discussed in Section 6.1.

6.4 Comparison between Tied Contact and Bolt-Preload for Interface of FWD beam and Leg

In Case I, tied interface was defined between the mating surfaces of leg and FWD beam (Table 6-1, Cross-sectional cut under “With Tied Contact” heading).

In Case II, each stud (bolt) was explicitly modelled. A contact interface was defined between head of the stud and corresponding mating surface of leg between contacting surfaces of FWD beam and leg and between initial openings of the leg (Figure 6-4).

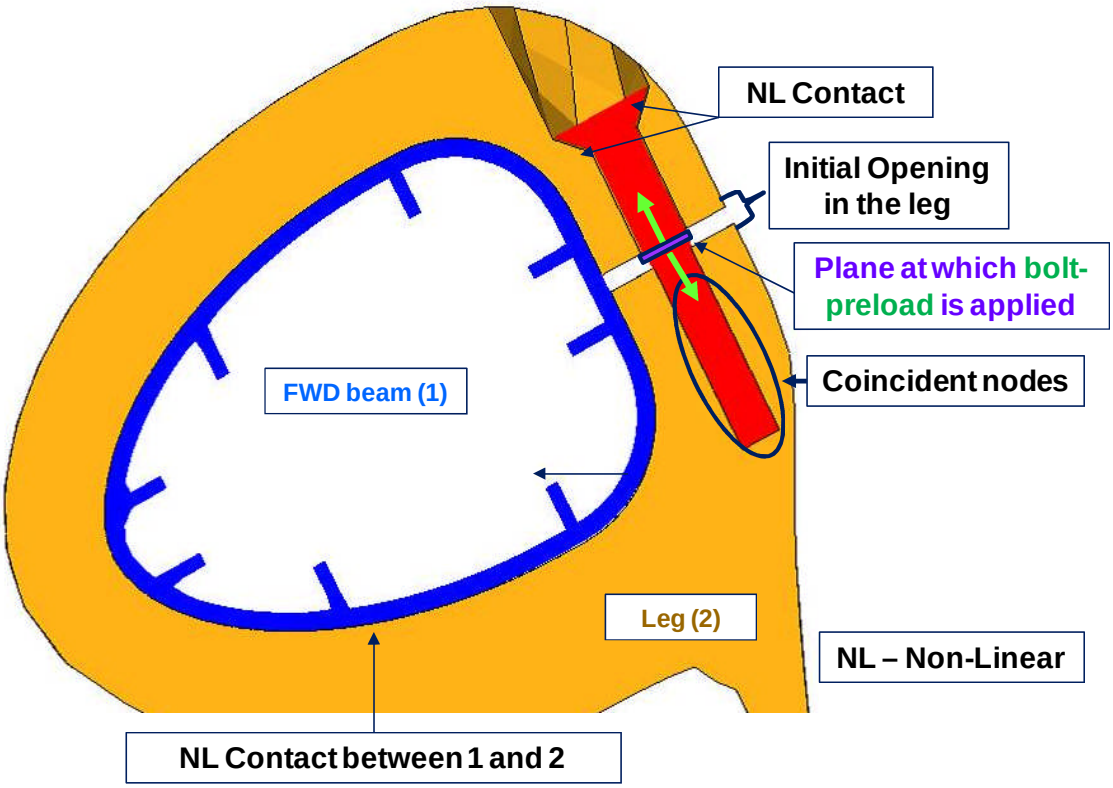

Figure 6-4 Non -Linear Contact definitions and plane at which bolt-preload is applied

To represent the threaded connection between stud and leg, coincident nodes were used between engaging depth. A bolt preload of 9KN was applied at the midway between initial openings of the leg (Figure 6-4).

A due care was taken such that there were no initial penetrations between contacting surfaces.

For Case I, simulation was run in one load step. For case II, two load steps were defined. In Step I, bolt preload was simulated. Starting point for the Step II (in which “Forward 9g” load was applied) was, the final stage of Step I, so that the effect of bolt pre-load was retained. The two cases were compared mainly considering the stress levels induced in the FWD beam and leg, pre-processing time and the solution time (Table 6-1).

Parameters		With Tied Contact	With Bolt Preload
Solution Time		2 Hours 12 min.	4 Hours 36 min.
Size of Result file (*.ODB) , mb		290	400
Pre - Processing time required, Hour		1	5
Cross-Sectional Cut		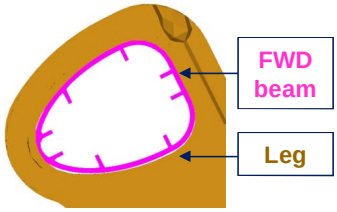	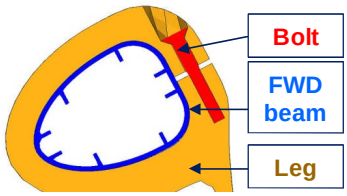
von Mises stress, MPa	FWD beam	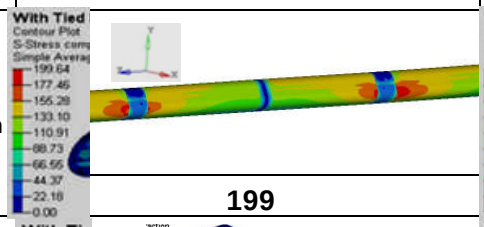 199	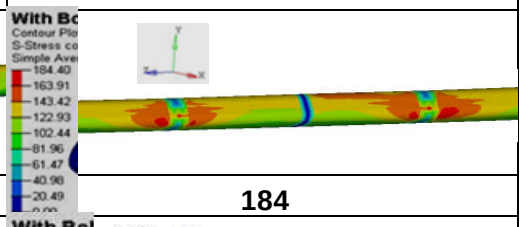 184
	Leg	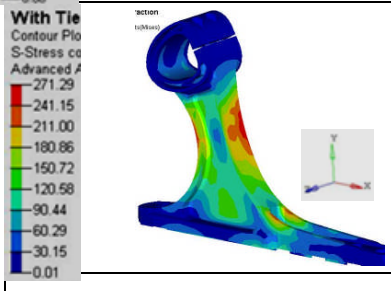 271	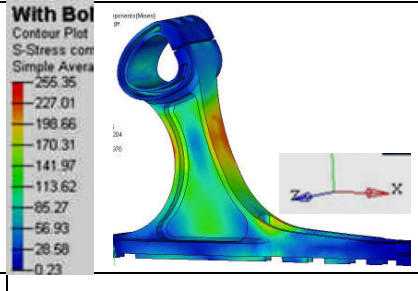 255

Table 6-1 Comparison between FEA results obtained with Tied interface (LHS) and with bolt pre-load (RHS) for "Forward 9g"

It can be inferred from Table 6-1 that,

- The variation in the maximum von Mises stress observed in the FWD beam in two cases is not significant (0.08 %). Higher stresses (increase of 0.06%) are observed in the leg in “Tied Contact” simulation, as the interface of leg, FWD beam acts as a single entity. However, the location of the high stress is same. Therefore, from FEA viewpoint there are no major differences (<1%) in the stress values.
- An interesting observation can be made when pre-processing time is compared. The time required for preparing the input deck with bolt-preload is almost five times that with tied interface. Solution time with tied contact is almost half of the time required with bolt-preload.
- Another parameter of tied contact is that even though initial penetrations are present in the contacting surfaces, those are not treated as interference fits that need to be resolved [29]. This is an extremely useful characteristic as, it imparts flexibility for FE modelling of parts in contact and dramatically reduces the efforts required to achieve zero initial penetration.

As almost same results were obtained with 80% reduction in pre-processing effort and 50% in solution time, it was decided to use “Tied Contact” definition between leg and the FWD beam. It was deployed for the bolted connection between boomerang and FWD beam.

Conclusion from Chapter 6

This chapter was all about finding, a computationally economical FE representation of a bolted joint between “FWD beam and leg” that can give acceptable results. This introduced contact non-linearity and hence Abaqus / Standard was chosen as a solver. Three different cases for accounting a bolted joint studied in this research are: coincident nodes for mating surfaces (studied under Preliminary model – Chapter 5), tied contact between mating surfaces and actual FE modelling of bolts. For the last case, a stepwise procedure to simulate “bolt-preload” using Abaqus / Standard was developed. Two separate

FE models were built considering “tied contact” and “bolt-preload” between “FWD beam and leg”.

FEA showed that the results obtained using tied interfaces are in close tolerances (+/- 1%) to those from bolt preload. Considering simplicity (80% less efforts) and flexibility (unaffected solution due to initial penetrations) of definition and less solution time required (50% reduction) for analysis, it was decided to use tied interface definition between FWD beam and leg.

Thus, the third point from the scope of the project (Section 1.3) was fulfilled, i.e.

“FE Models developed will be piecewise, as design of leg is critical for static 9g load case. This task will involve mesh sensitivity studies, prudent choice of element formulation, techniques for modelling bolt behaviour / preload and non-linear contact”

7 Seat Interface loads

According to the aircraft manufacturer's requirements, seat structure should be designed in such a way that, static loads applied by the seat to the floor should not exceed floor structural capability [35]. The task for designer is to arrange location and number of studs used to fasten the seat assembly with the track , in such a way that the maximum tension induced in the studs is below the allowable limit provided by the aircraft manufacturer. The static loads developed at the seat and track interface are called as "Seat track Interface loads" and they depend on the length of the leg (separation between front and aft connections of leg with track).

Thus, design of the seat leg is governed by its strength to carry the loads as specified in CS 25.561 as well as by the interface loads. Therefore, aim of this chapter is to develop a methodology to estimate "Seat Interface Loads".

Interface loads are calculated for all the static load conditions as per CS 25.561. In present research, initially interface loads have been calculated for "Forward 9g" load case being the most critical one. It generates maximum vertical loads in aft tension studs than any other load case specified by CS 25.561 (as discussed in Section 4.1.2).

Seat track interface loads should be calculated for all the occupant-loading scenarios i.e. all seats occupied, one seat unoccupied, two seats unoccupied etc [35]. Since the seat structure under consideration for the present analysis is a dual symmetric configuration, only three different combinations are possible,

- Case I: all the (two) seats occupied,
- Case II: two cases with either of seats unoccupied.

For present design of "Sleep Seat", Case I would induce maximum vertical loads in the studs. Hence, only this case has been considered for interface load calculations. The weight used for interface load estimation is the "Total Seat weight" along with the weight of the occupants (explained in Section 4.1.1) i.e. 87.48 kg.

7.1 Description of Seat Track Assembly

In “Sleep Seat”, three mushroom-headed studs are used to fasten the leg to seat track. Locator pin, which seats in the rearward position, also acts as a shear pin. Figure 7-1 shows the assembly of seat track with studs and shear pin.

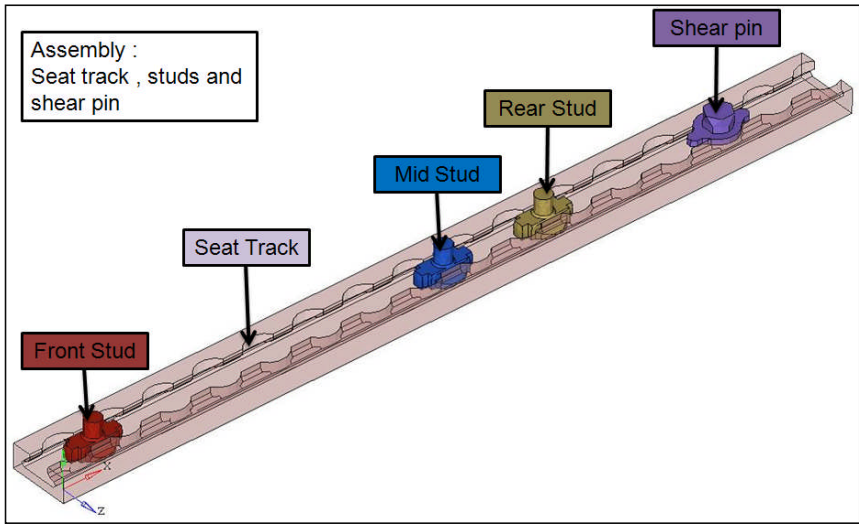

Figure 7-1 Assembly of Seat track, Mushroom-headed studs and Shear Pin

It would be interesting to estimate the contribution of each of the studs in carrying the applied loads. Since, “Sleep Seat” under consideration, is not being developed eyeing for a particular airline, a specific guideline limiting the seat interface loads is not available (at present).

A traditional approach for Interface load calculation is through hand calculations using force and moment equilibrium equations [35]. However, for “Sleep Seat”, this method was not useful and FEA was strongly required (explained in Detail in Appendix G).

Integration of track, studs and shear pin with preliminary FE model of “FWD beam and leg” increased complexity, in term of contact non-linearity. Therefore, a study to understand “How contact works in FEA?” was undertaken during this research. Findings of this study are discussed in coming section.

7.1.1 Consideration of Contact Compatibility in Abaqus / Standard

In a real world, when the two separate surfaces touch each other such that they become mutually tangent, they are said to be in “contact”. Since the stiffness of the parts touching each other, depends upon the contact status, “open or closed”, contact is a changing-status non-linearity [36]. The challenge to simulate contact interaction between two bodies is due to the following characteristics of contacting bodies,

- They do not inter-penetrate.
- They transmit compressive normal forces and tangential frictional forces.
- Often they do not transmit tensile forces (open contact).Therefore they are free to separate.

In FEA, if two independent parts are present without any stiffness relationship between them, then the resulting stiffness matrix will be uncoupled [27], [36]. The consequence of this is that parts may pass through each other during the course of simulation. Contact definition between these parts helps to prevent such unrealistic behaviour.

Penalty method form Abaqus / Standard was used to enforce this interpretability condition (known as “Contact Compatibility”) [29]. Following three parameters play a very important role in successful simulation and meaningful results during contact non-linear FEA.

7.1.2 Discretisation of contacting surfaces

In contact formulation, the location and conditional constrains applied on each surface to simulate the contact, depend on contact discretisation. Abaqus/Standard offers two contact discretisation options: a traditional “Node-to-Surface (NSD)” and “Surface-to-Surface (SSD)” discretisation [29]. In order to define interactions between various components in “Sleep seat”, SSD scheme has been used. The key characteristics of SSD are,

SSD considers the shape of both the slave and master surfaces in the region of contact constraints.

In general, contact conditions are established for slave side such that, they cannot penetrate into the master surface; however, the master side can penetrate into slave surface. For NSD, these conditions are strictly enforced at slave nodes (discrete points). Therefore, NSD simply resists the penetrations of slave nodes into master surfaces resulting in highly concentrated contact forces at slave nodes [29]. This leads to spikes and valleys in distribution of “Contact Pressure (CPRESS)” across the surface. In addition, since constraints are present only at discrete points, a possibility of large, undetected penetration of master surface into slave side can not be denied.

In SSD, contact conditions are enforced in an average sense over the slave surface rather than at slave nodes. Therefore, some penetrations may occur at individual nodes; but deep and undetected penetrations of master surface can not occur [29]. As SSD resists penetrations in an average sense over finite region of slave surface, smoothening of contact forces naturally happens thereby improving the contact pressure accuracy.

Refinement of mesh at the contact pair lessens the discrepancies between the SSD and NSD, but for a given mesh refinement, SSD tends to provide more accurate and sensible results [29].

SSD involves more number of nodes per contact constraint and therefore, increases the solution cost. The use of SSD for “Sleep Seat” can be justified as “High Performance Computing (HPC)” facility is used which increases the solution speed and accurate transfer of loads across the interfaces is important.

7.1.3 Contact Tracking approach

It determines the relative motion between two contacting surfaces. Abaqus/Standard provides two options: Small-Sliding Tracking (SST) approach and Finite-Sliding Tracking (FST) approach [29].

The FST approach was selected because of following advantages,

- FST allows for arbitrary relative separation, rotation and sliding of the contacting surfaces.
- Contact area and the contact pressure distribution are calculated according to the current orientations and deformed shape of the model, which is a more realistic representation of physical behaviour [29].
- As seen in Section 7.1.2, “SSD scheme was chosen. Contact conditions for FST algorithm converge in fewer iterations with SSD than with NSD [29]. The reason being; upon sliding between contacting bodies; STS shows more continuous behaviour.

However, FST approach is computationally expensive, as the position of slave, needs to be monitored during each iteration for its possible contact along with the entire master surface.

7.1.4 Assignment of “master” and “slave” roles

This is an important parameter, which governs penetration of contacting surfaces, solution time and convergence rate. Since for “Sleep Seat”, SSD procedure is used, the effect of incorrect choice of master and slave surface on solution is less detrimental than NSD procedure [29]. However, if the slave surface is much coarser than the master surface, the solution time increases considerably. Therefore, guidelines used for assigning master and slave surfaces are summarised as follows,

- A surface with coarse mesh should be a master surface.
- Master surface should be stiffer than slave surface. Combination of stiffness of the structure and material should be used to decide stiffer surface.
- Master surface definition should extend enough to account for all expected motions of slave surface and deformation of contacting bodies. In case, this condition is not followed; a slave node that “Falls Off” its master surface in one iteration may contact it in the next iteration. This

phenomenon is called as “Contact Chattering”. This is of particular importance in case of “Sleep Seat” as, the FST approach that allows large relative motion between contact pairs is used. In case of SST, “falling off” of the slave node is not an issue since; slave node does not travel on the actual surface of the model.

7.2 FE Modelling of Remaining Parts

Seat track and Mushroom headed studs, “Seat Interface Loads” are calculated at the interface of mushroom head and corresponding mating surface of track. Hence, proper representation of the stiffness and sufficient number of nodes at the interface, determine the technique used for FE modelling of these studs and track. Design of the track is fixed by airliners to suit their fuselage structure and hence is constant. Mushroom-headed stud is a standard “Aerospace Certified” part and variable is only its location and number of studs used, which can be accommodated through multiple copies of same mesh. So, during entire seat designing process, track and studs need to be modelled only once and therefore hexahedral elements are used as shown in Figure 7-2,

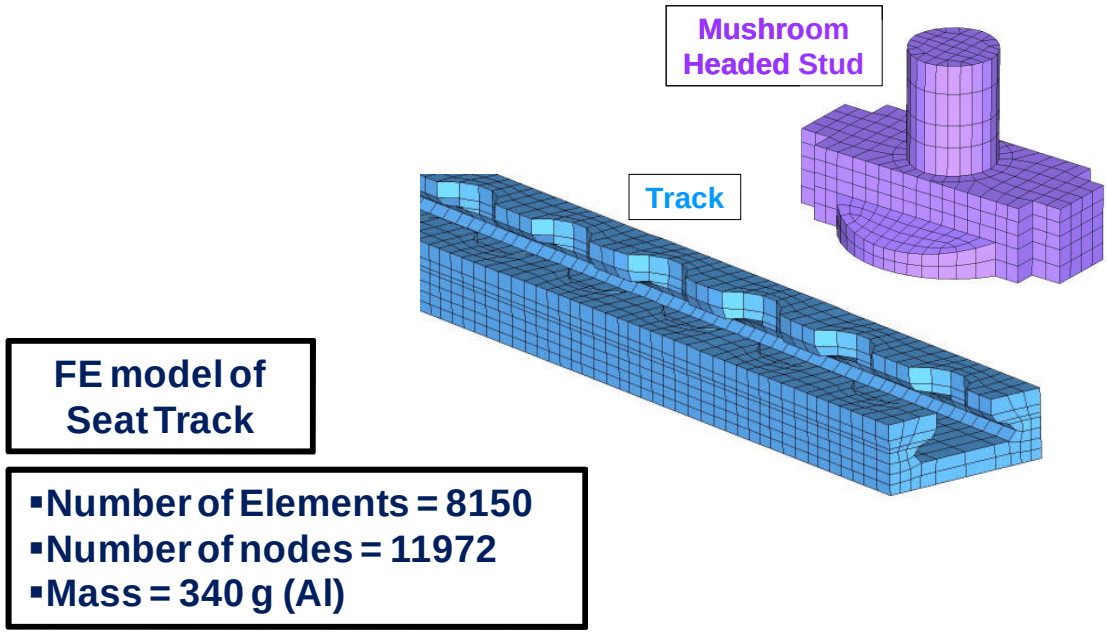

Figure 7-2 FE model of track and mushroom headed stud

Sufficient care has been taken to provide a dense mesh on the mushroom surface where the stud will have interface with track. This modelling technique ensures, proper distribution of contact constraints and forces on a considerable area thereby avoiding highly localised contact stresses as well as convergence issues due to modelling.

7.3 Definition of contact at various mating parts

Figure 7-3 shows the cross-section of the leg and track, giving the details of parts considered and interactions defined. Contact pairs can be summarised as follows,

- Seat track and foot-section of the leg,
- Shear pin and leg, Shear pin and track.
- Each of the mushroom-headed studs and corresponding mating surfaces of track and leg.
- Each of the nuts and corresponding mating surface of leg.
- Leg faces in beam clamping area, each of FWD beam clamping stud and its resting surface on leg and FWD beam and leg(When stud in FWD beam was explicitly modelled).Without stud, tied contact was defined.

Coincident nodes were used between FWD beam and corresponding reinforcing inserts. In addition, threaded extension of the FWD beam clamping stud, had coincident nodes with corresponding hole in the leg.

Thus, thirty contact pairs were involved (when stud in the FWD beams were modelled. Without them, twenty-four), in the intermediate FE model of "FWD beam and Leg Version 8” assembly. Loads and load application point remained same as discussed in Section 5.2.1.

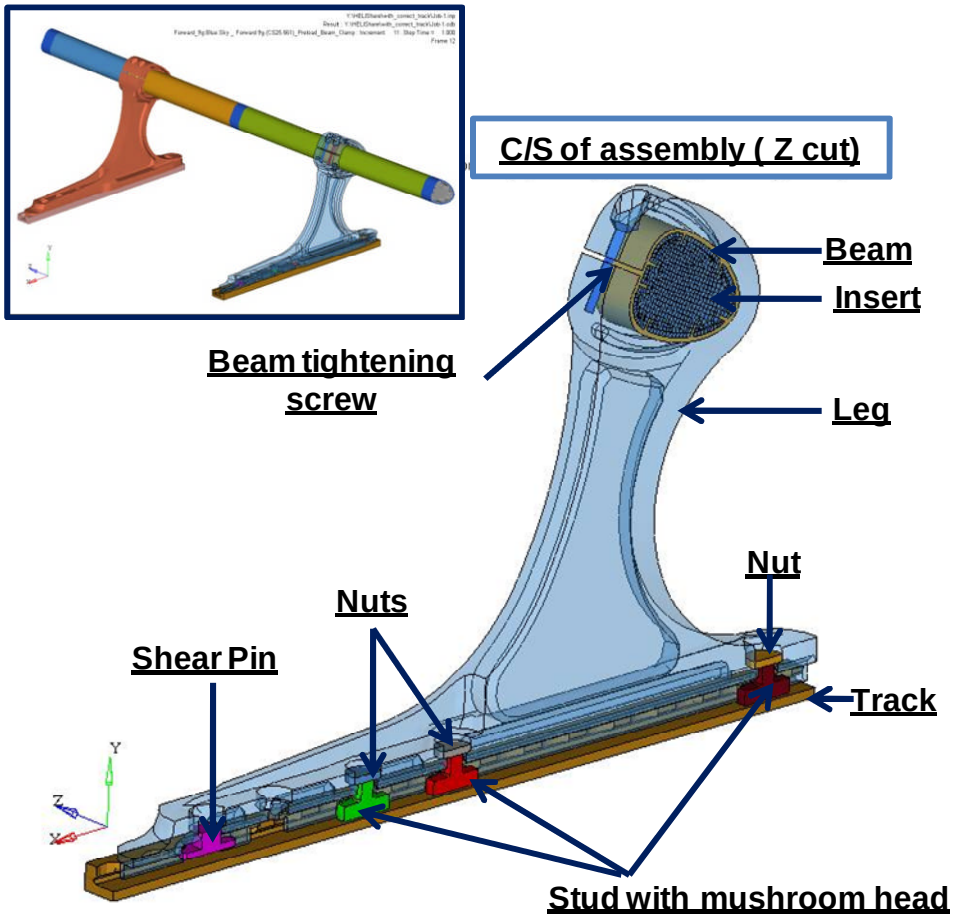

Figure 7-3 Intermediate FE model of "FWD beam and Leg" with Seat track, Mushroom-headed studs and Shear pin

7.4 Technique to extract Interface Loads from Contact pairs

The interaction between seat and track was divided into three separate contact pairs i.e. contact between each of the stud and track (1, Figure 7-4), shear pin and track (3, Figure 7-4) and bottom of leg and track (2, Figure 7-4), with track as master surface in each definition. Figure 7-4 shows three different contact pairs. Nodes in the Circled region are used for extracting contact forces i.e. interface loads.

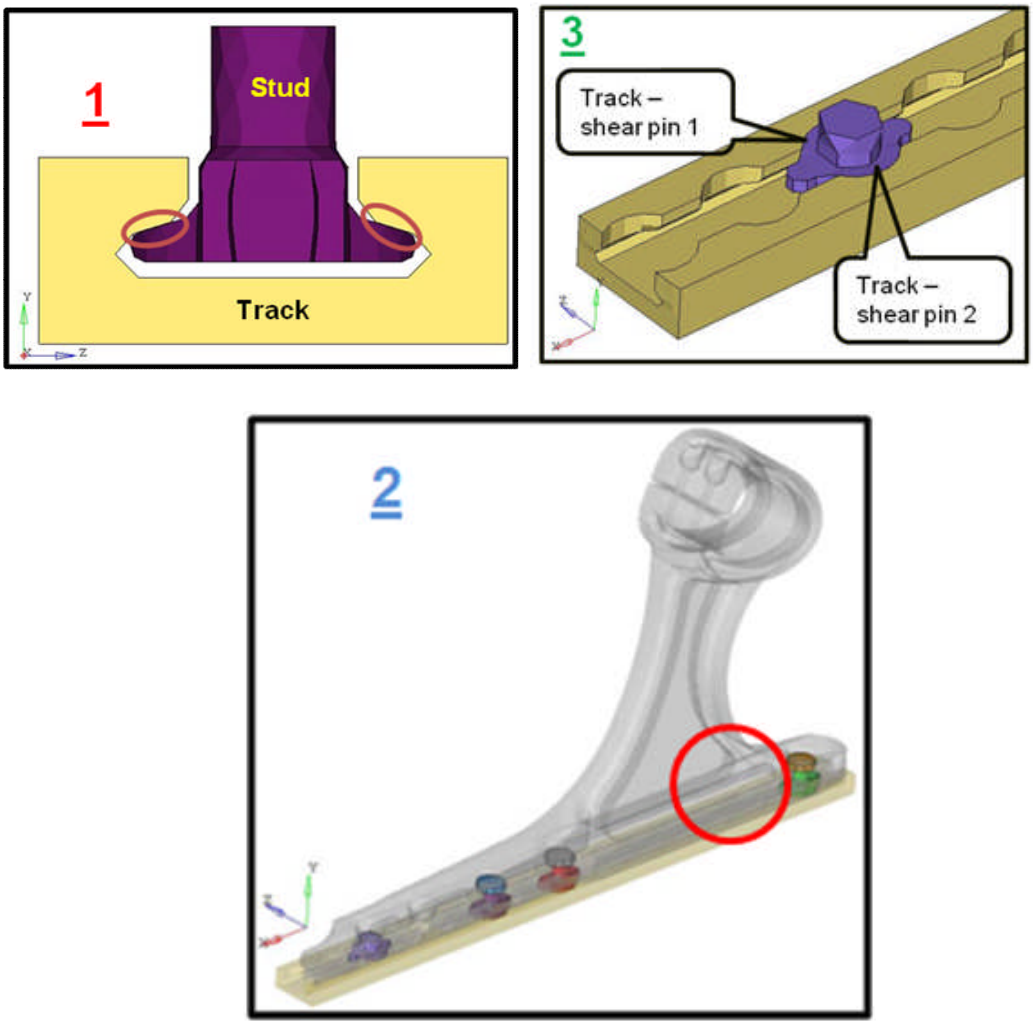

Figure 7-4 Interaction definitions used to extract Interface loads

The history output providing contact force in each Cartesian axes was requested in Abaqus / Standard Step-definition which looks like,

*Output, history

*Contact Output, master=LHS_REAR, slave=LHS_TRACK

CFN1, CFN2, CFN3, CFNM

Where, LHS_REAR and LHS_TRACK are the names of master and slave surfaces respectively.

CFNn is the normal contact force in n= 1, 2 3 and M is X, Y, Z direction and total resultant respectively.

Thus, this section discusses the importance of “Seat Interface Loads” during seat designing and develops a stepwise logical approach for their estimation using FEA.

During design of leg V#8, interface loads were one of the main driving factors along with the strength to sustain applied “Forward 9g” loads. Three different configurations were studied based on stud arrangements and vertical loads induced in them. A brief description of this exercise is given in Appendix H.3.

With this, all the preliminary studies required for designing (for CS 25.561 loads) of a “Seat leg” are completed. Before going for the next chapter, which takes an overview of actual design activities, it is worth to take a note of some good FE practises developed in this journey.

7.5 Important features during FE modelling

7.5.1 Structural Idealisation to achieve good mesh quality

“…. analysts spend around 75% of their time cleaning up the geometry imported from CAD software. This ritual is a MUST to get a regular and good quality FE model [37]…”

Many times, quality of the mesh generated is affected by the topological details. Surface fillets and edge radii given for the aesthetic purposes, fall in this category. Often small pinholes are difficult to capture with the desired element size. Nodes get stuck at the edge of the hole giving an irregular and poor quality mesh. If small element size is used to capture such pinholes then the model size becomes bigger, costing valuable computer memory and runtime! Influence of these features on the strength of the component is also negligible. Hence, they can be removed without much concern; to get a better mesh quality. This exercise is known as “Structural Idealisation”.

During “Structural Idealisation”, a due care must be taken so that removal does not lead to, initial penetrations or clearances after meshing (explained in Section 7.5.2). Figure 7-5 shows how “Structural Idealisation” helped to achieve a regular and good quality hexahedral mesh pattern in case of a mushroom headed stud. Without it, only tetrahedral mesh pattern was achievable. This mesh pattern suffered from, high aspect ratio and poor element quality as, smaller elements were required to capture details like surface fillet. It made the transition from dense mesh to coarse mesh difficult.

Importance of Geometry "Clean-Up"	**Original Geometry**	**Unwanted (for FEA) details**
	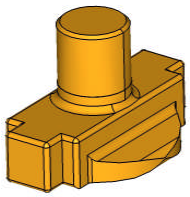	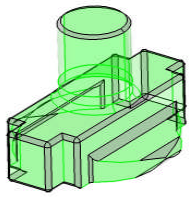
FE model	**Geometry as "It Is"**	**With Geometry "Clean-Up"**
	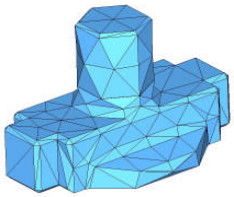	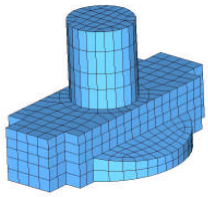

Element Quality Matrix		
Parameter	**Actual value (Target Value)**	
Aspect ratio	133.56 (<5)	3.2(<5)
Skew	90(<60)	40(<60)
Minimum angle (deg)	0.43(>20)	53(>45)
Maximum angle (deg)	136(<120)	125(<135)
Number of nodes	16418	1426
Tetra Collapse	0.01(>0.2)	Not applicable

Figure 7-5 Effect of Structural Idealisation on improving Element Quality of FE model of Mushroom-headed stud

Whilst it is possible to defeature a CAD model, most FE processors are limited in their functionality (as they are designed to develop an FE input deck and are not intended as a CAD package). Stress engineer can assemble the parts using an FE pre-processor, difficulties will be encountered due to a lack in knowledge of,

- correct orientations of individual components,
- Engagement depths.
- Position and number of fasteners
- Position and number of spot-welds
- Relative distances between sub-assemblies.
- Tolerances for tied contact

Therefore, a practice should be made such that, input from CAD is without unrequired features and parts are at correct locations.

7.5.2 Effect of Initial Penetrations and Clearances

Generally, strategy used for FE modelling of assembly is to build the models of individual parts first and then assemble based on CAD references to form the complete model. CAD models of the assembly are provided with close manufacturing tolerances and exact mating surfaces. “Structural Idealisation” leads to an interesting situation of initial penetrations or initial clearances when FE model of assembly is built.

Initial Penetration, Abaqus/standard interprets as interference fit (even though unintentional) and tries to resolve it during first increment [29]. In many cases, strain increment in first step itself (before load application) becomes 50 times higher than the yield strength of the material (considering non-linear material model); then solution stops. If linear material model is used, solution progresses. However, very high and unrealistic stresses occurred during the initial time step corrupt final results. This was observed for the interaction between “FWD beam and leg”, which occurs along the elliptical counter. These highly curved regions caused initial penetrations due to different discretisation strategies used. Figure 7-6 shows the initial penetrations between contacting surfaces of FWD beam (Slave Surface) and leg (Master surface).

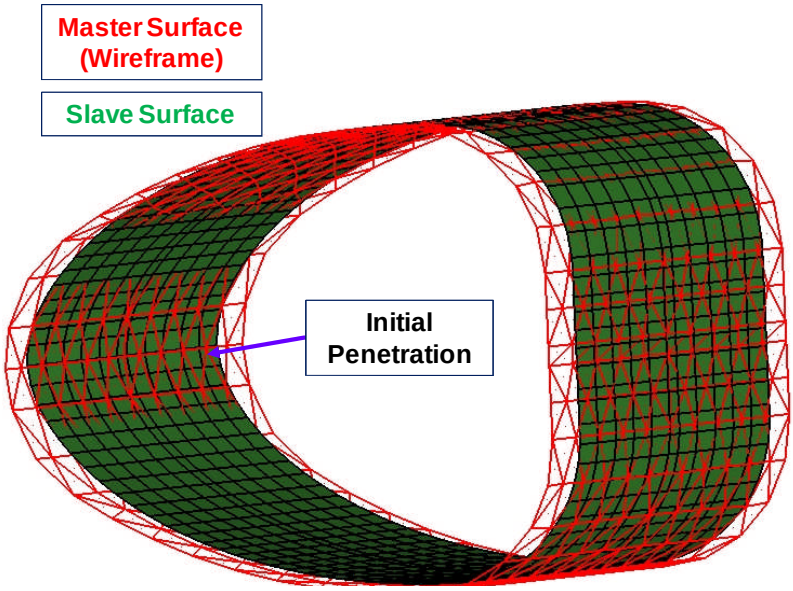

Figure 7-6 Initial Penetration due to discretisation

"Forward 9g" loadcase with bolt-preload was simulated with these penetrations. FEA stress results were compared to those obtained from the same model (Table 7-1) but this time, without initial penetrations achieved using "Standard R Tri" as explained on Page 93 of this report.

	With Initial Penetration	Without Initial Penetration
State before load application	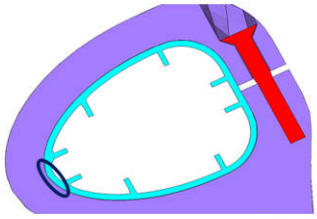	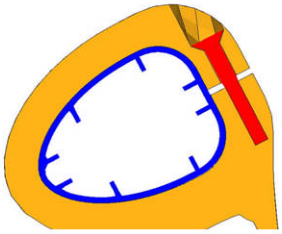
von Mises stress plot at first time increment (0.05% of total load)	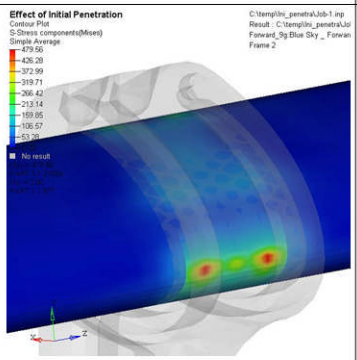	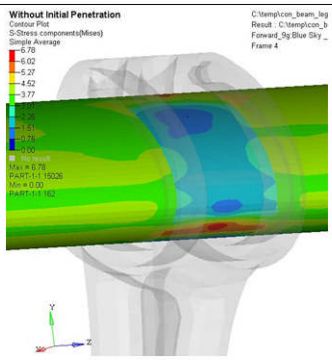
	480 MPa	6.7 MPa
Solution Time	9 Hours 10 min.	4 Hours 36 min.

Table 7-1 Initial Penetration results in unrealistic high contact stresses

As seen from Table 7-1, very high stress of 480 MPa is observed during initial increment of load (0.05% of total load) when initial penetrations were present in the model. If compared with the yield strength of a general Aluminium alloy (375 MPa), this indicates the FWD beam is undergoing plastic deformation during bolt tightening, which is misleading. With zero initial penetrations, a reasonable and realistic stress value of 6.7 MPa was obtained. The total solution time including bolt preload step and “Forward 9g” load step was 9 hours and 10 minutes for the model with initial penetrations, since Abaqus / Standard tried to resolve this inadvertent “Interference fit” in several iterations before finding an equilibrium solution. The simulation time reduced by 50% when, there were no initial penetrations.

In case of initial clearances (Figure 7-7), FEA algorithms undergo severe discontinuities in the initial stages and fail to detect the contact. When many bodies are held together, only through contact, frictional sticking is effectively used to constrain the rigid body motion. However, to generate friction, contact pressure has to develop which is not possible due to initial clearances! Therefore, for initial conditions, friction is not an effective tool. Unfruitful attempts are made to cut back the time step and to stabilise the solution. In most of the cases, this strategy does not help and solution fails due to unrestrained motion flagging an error message as “One or more bodies are experiencing very large translation or rotation, magnitude of which exceeds the solver limit” [29], [30].

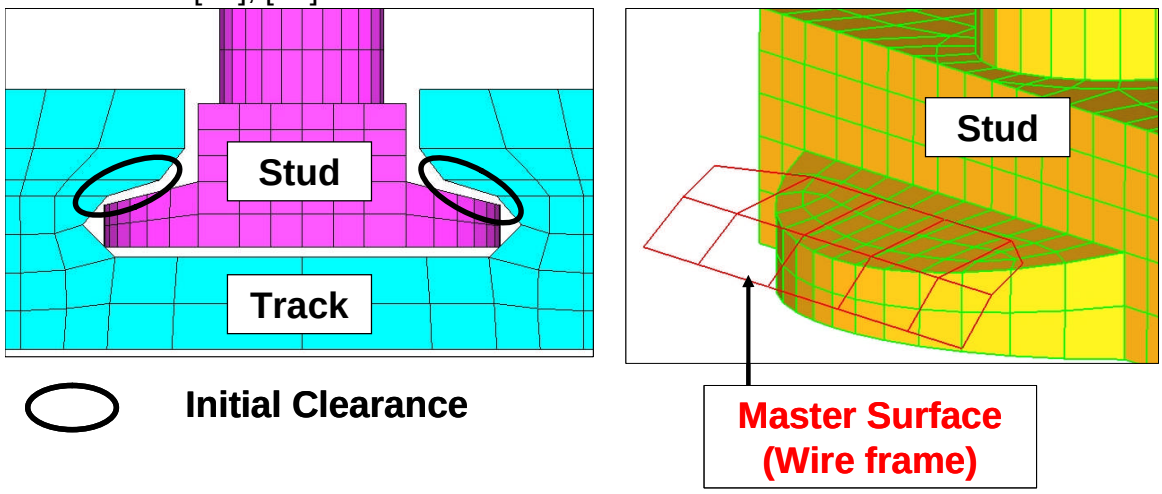

Figure 7-7 Initial clearances between contact pairs and mismatching element densities at interface hampering progress of solution

7.5.3 Remedy to successfully deal with initial penetrations and clearances

Some solvers can remove the initial penetrations or initial gaps without necessarily straining the structure. However, this distorts the mesh considerably. In addition, tolerance used for such corrections is very small and same value is used for all contact pairs by default. For “Sleep Seat” where large number of contact pairs are involved, it becomes time consuming to update such tolerances for each and every interface definition for each design modification.

Use same element faces in mating area, when two individual FE models built with solid elements are assembled, outer faces of one of the components should be generated and a visual check should be made for penetrations or unrealistic clearances. Wherever possible outer element faces (in the region of mating surfaces) of one component should be used to build the FE model of its mating component and later on two components should be detached from each other to model contact. This will ensure that there are no initial penetrations or clearances in the model since exactly matching elements on same plane are used and will be beneficial to avoid rigid body motions since the bodies would be just touching each other at the onset of solution (Figure 7-8).

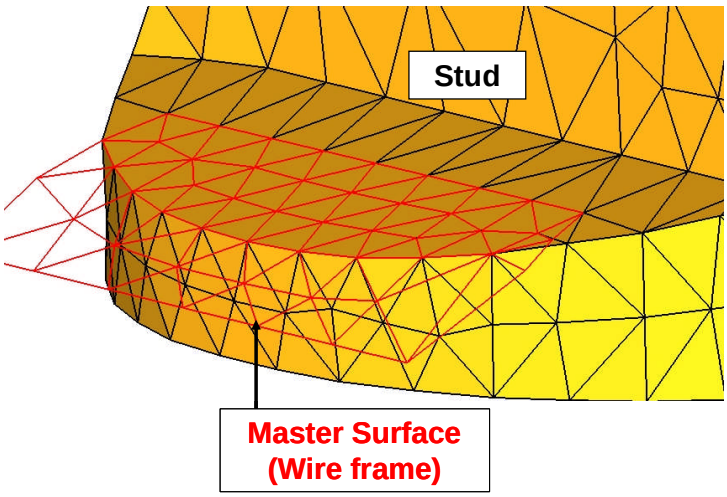

Figure 7-8 Modified discretisation at the interface to avoid initial penetrations and clearances

Due to mathematical approximations and discretisations, modelling of “Zero Gap” in geometry does not ensure that it is “Zero in FEA”. Hence, automatic adjusting should be used, but with care.

Visual Check, If shell elements are used then that part should be rendered with corresponding shell thickness and a visual check should be made.

Clever use of Mesh algorithm, Figure 7-9 shows, “Standard R-tri” mesh pattern has been used instead of “Union Jack R-tri” to avoid initial penetration when two surfaces with dissimilar element types are defined in an interface. Due to complex geometry, tetrahedral elements are used for leg (Section 5.2.3) while FWD beam has been modelled with hexahedral elements (Section 4.6.3). When “Union Jack R-tri” elements were used there was a considerable twisting of the elements down the width of the leg and elements protruded out of the plane introducing initial penetrations. With the use of “Standard R-tri”, this problem was eliminated as a perfect straight mesh down the length without twisting was obtained. This points out that, just with the change of meshing algorithm, problems of penetrations or unrealistic clearances can be avoided.

Union Jack R Tria	**Standard R Tria**
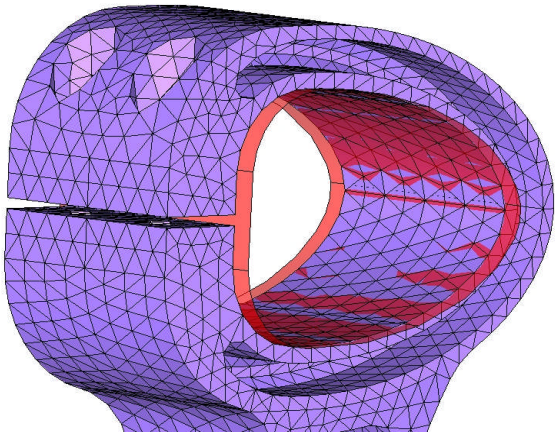	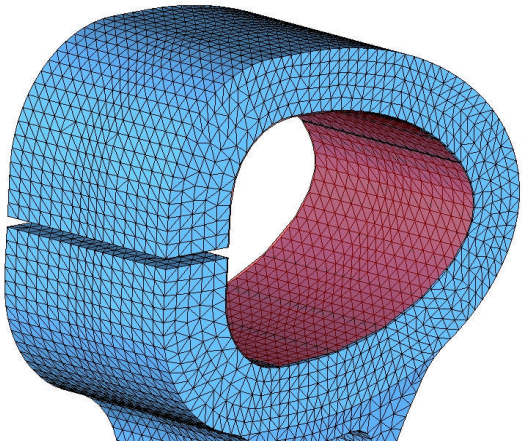
Elements protruding out of the mating surface (transparent red surface) causing Initial Penetrations	Elements following exact planer offset of the mating surface (transparent red surface). No Initial Penetrations. Better initial condition for contact establishment.

Figure 7-9 Change in element pattern to avoid initial penetration/clearance.

Bolt Pre-load was successfully used to deal with “Rigid Body Motion”. A nominal pre-load of 1KN – 2KN was used in mushroom-headed studs in first load step. It helped to close initial gaps and to establish contact. In second load step, main load e.g. “Forward 9g” was applied. This was one of the major innovative findings during this research.

7.6 Element Quality Check-list

During building of FE model, it is very important to minimise discretization errors. They are introduced in the solution due to distorted elements. So better the element quality less is the “Discretization noise”! These errors are called as “Controlled Errors” as, if the FE quality is controlled then their effect can be minimised.

Once the FE modelling of the parts is done, visual check should be made by plotting the mesh and geometry. Model should be thoroughly examined to see if appropriate representation of geometry is done, if mesh seeds seem adequate and if element shapes are poor. Visual checks expose badly shaped elements easily. One trick to rectify poorly shaped FE model is to remesh the local region surrounding problematic elements instead of remeshing the entire surface. This technique has been found to be very powerful during this study [24], [27].

Shrink plot, immediately shows missing element. Sections cuts in different directions yield extremely important information as initial penetrations or unphysical gaps between components. Edge display is another powerful tool to identify unconnected elements in case of a shell mesh. Similarly, selective scaling and local enlargements can be used to scrutinise minute details [27]. Hypermesh has “Element Check” panel, which gives an indication of distorted elements [24].

Pre-processors create a summary of material properties used, section properties assigned and cross-sectional properties used for all the components. Documentation of this data should be encouraged. Before submitting the full-blown analysis, a check run should be done. This gives valuable information as,

- List of unconnected nodes and elements
- Elements sharing a common node but with different dofs assigned at that node commonly known as overconstrains
- New nodal positions of contact surfaces to remove over closures (if automatic adjustment option is activates)
- List of slave nodes that are not able to intersect with defined master surface in case of tied contact. This is of utmost important as, slave nodes that are not tied to their master surface, remain unconnected thought the simulation.
- Amount of memory and disc space required.

Conclusion from Chapter 7

FE model of “FWD beam and leg” developed so far, was providing stress levels experienced by leg when subjected to CS 25.561 loads. However, design of leg is equally governed by “Seat Interface Loads”. Due to unconventional design concept of leg in “Sleep Seat”, procedure used by “Boeing Specifications”, was not applicable to calculate interface loads and it was decided to use FEA for it. Therefore, it was essential to integrate seat track, mushroom-headed studs and shear pin with the preliminary FE model of “FWD beam and leg” increasing the complexity and challenge to deal with contact non-convergence.

Using Abaqus / Standard documentation, penalty method was used to enforce contact compatibility between mating parts. Surface-to-Surface descritisation with “Finite-Sliding Tracking” approach was used and a technique to extract interface loads using FEA was developed. Therefore, in this chapter “Intermediate FE model of “FWD beam and leg” which could provide stress response and interface loads and involved contact non-linearity was accomplished (Figure 5.1, Second stage). Based on this model, design iterations for leg (V#1 – V#8) were studied as explained in Appendix H.

Good FEA practices such as “Structural Idealisation”, pre-cautionary steps to avoid initial penetrations and “Rigid Body Motion”, and thorough assessment of input file were developed and discussed at length in this chapter. Use of bolt pre-load to control unrestrained motion of parts during contact non-linear FEA was a major achievement.

Please note, FE modelling practices discussed here should be considered more as concepts rather than die-hard rules for seat modelling. The precise list of rules can not be presented as each of the rules may have an exception that can be twisted to an advantage in a typical situation.

Once robust FE models are developed, next phase is the actual design phase. Chapter 8 discusses the evolution of FWD beam and leg design.

8 Design Phase

In Chapter 6 and 7, FEA results for the beam and leg assembly are discussed from FE procedural point of view. This chapter takes the overview of development of design of components in “Primary Load Path” using FEA results a baseline and concludes a detailed FE model of “FWD beam and leg” by adding material non-linearity.

8.1 Design of FWD beam

Cross–section and its thickness are the main design variables for the design of FWD beam. Section 4.6.3 corroborated the confidence in using spreadsheet for preliminary sizing of FWD beam. Therefore, using spreadsheet, elliptical cross-section with two millimetres wall thickness was chosen and this tentative design was held constant for future simulations (with different designs of leg). Please note that, this was accomplished by CISM prior to this research [21].

8.2 Design of Reinforcing Insert for FWD beam

During FEA of intermediate model of “FWD beam and leg assembly”, von Mises stress of 413 MPa was observed in the FWD beam near its attachment with leg (Figure 8-1). As this is above the yield limit of a general Aluminium alloy (375 MPa), FWD beam will experience permanent deformation when subjected to “Forward 9g” load. Spreadsheet could not predict this, as it accounts only for bending stresses.

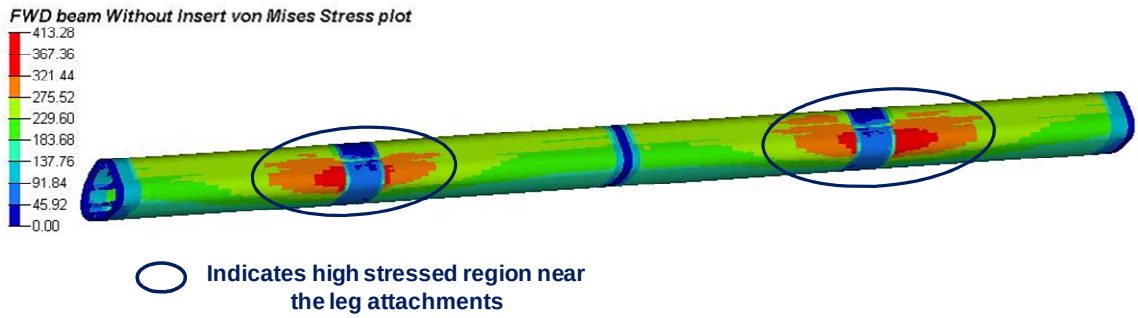

Figure 8-1 von Mises stress of 413 MPa for FWD beam without insert (Forward 9g load)

Hence, local reinforcement for the FWD beam was necessary where leg is attached to the beam. In addition, to prevent distortion of FWD beam due to clamping of boomerang, such an insert would be required at the boomerang and beam connection. Hence, insert with two millimetres thickness was placed inside the FWD beam at five locations as shown in Figure 8-2. These inserts were modified with a solid-web at the mid section due to following thoughts,

- FWD beam will experience large forces due to clamping of boomerang and leg, which will deform (partial collapse) elliptical cross-section of beam locally.

- Beam design is dominated by bending due to applied ‘Forward 9g” and “Downward 6g” loads. Addition of solid web in the mid position will increase the second moment of area in the loading directions and will reduce the stress levels in insert as well as in FWD beam.

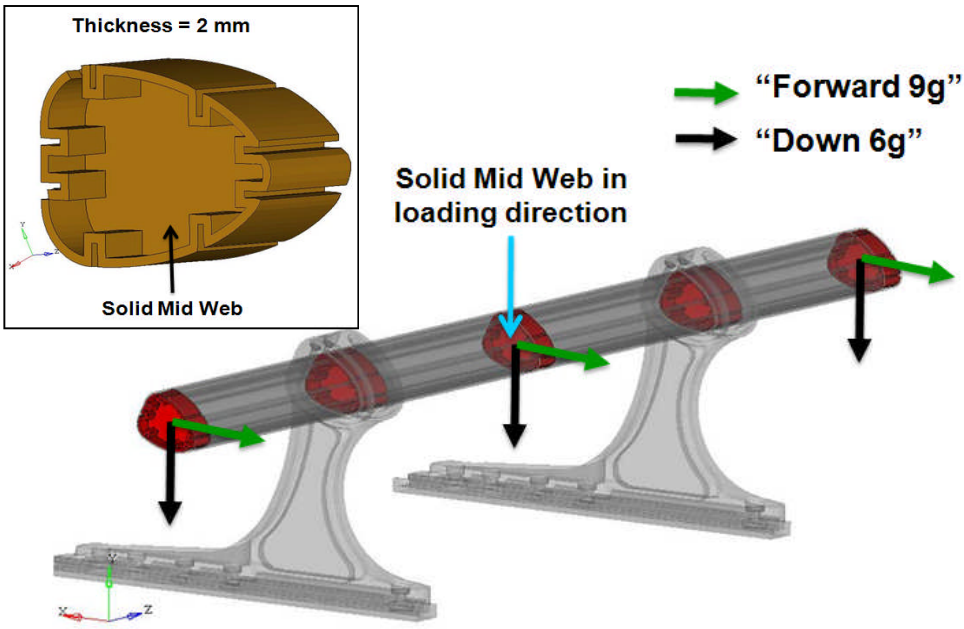

Figure 8-2 Location and Design of Reinforcing Insert in FWD beam

Figure 8-3 confirmed that reinforcing inserts in the FWD beam have brought down the stresses in the FWD beam (Forward 9g) from 413 MPa to 229 MPa. Thus the stress levels are within the elastic limit (375 MPa), which is a significant achievement.

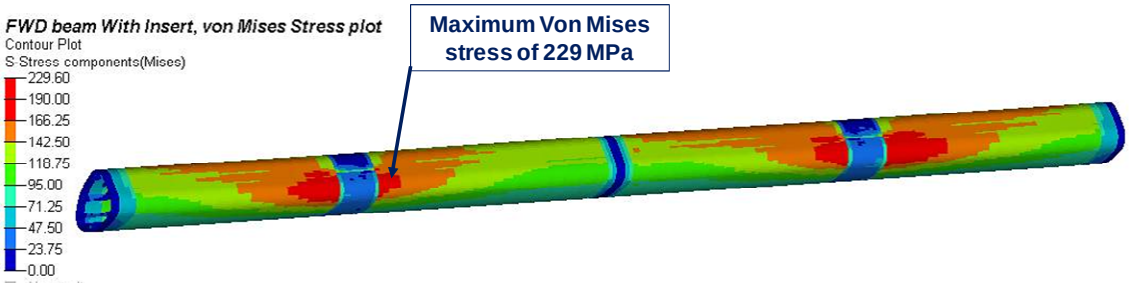

Figure 8-3 von Mises stress plot for FWD beam with insert (Forward 9g load). 44% improvement over results without insert.

If design of FWD beam would have been modified, increase in its overall thickness (as FWD beam is made by extrusion process) would have made it bulkier and heavier (50% increase in mass). In addition, stronger dies, plungers and powerful driving motor required for extruding such a thick FWD beam, would have increased manufacturing and handling cost. Interestingly, inserts offered deign improvement with minimal increase in mass (12% increase in mass) and little alteration in the manufacturing set up that would be used for FWD beam (as the thickness of FWD beam and inserts is same -2 mm). Please note, actual dimensions and mass of FWD beam and insert can not be provided in this report due to “Non-Disclosure Agreement” signed between Cranfield and BlueSky.

Next stage in insert design would be its optimisation (e.g. thickness). However, for present research, only static loads (CS 25.561) are considered. In case of dynamic loads, (CS 25.562) situation may change. Hence, it was decided to move on with further design activities of leg, by tentatively freezing current design of insert.

8.3 Design of Leg

The objective behind leg design was to come up with a design of that is “safe” against the applied “Forward 9g (CS 25.561)” loads. The interpretation of word “Safe” in the current analysis is taken as, maximum von Mises stress value observed in the leg should be below the yield point of a general Aluminium alloy (considered as 375 MPa).

From design viewpoint, different regions in the leg are classified as shown in Figure 8.4.

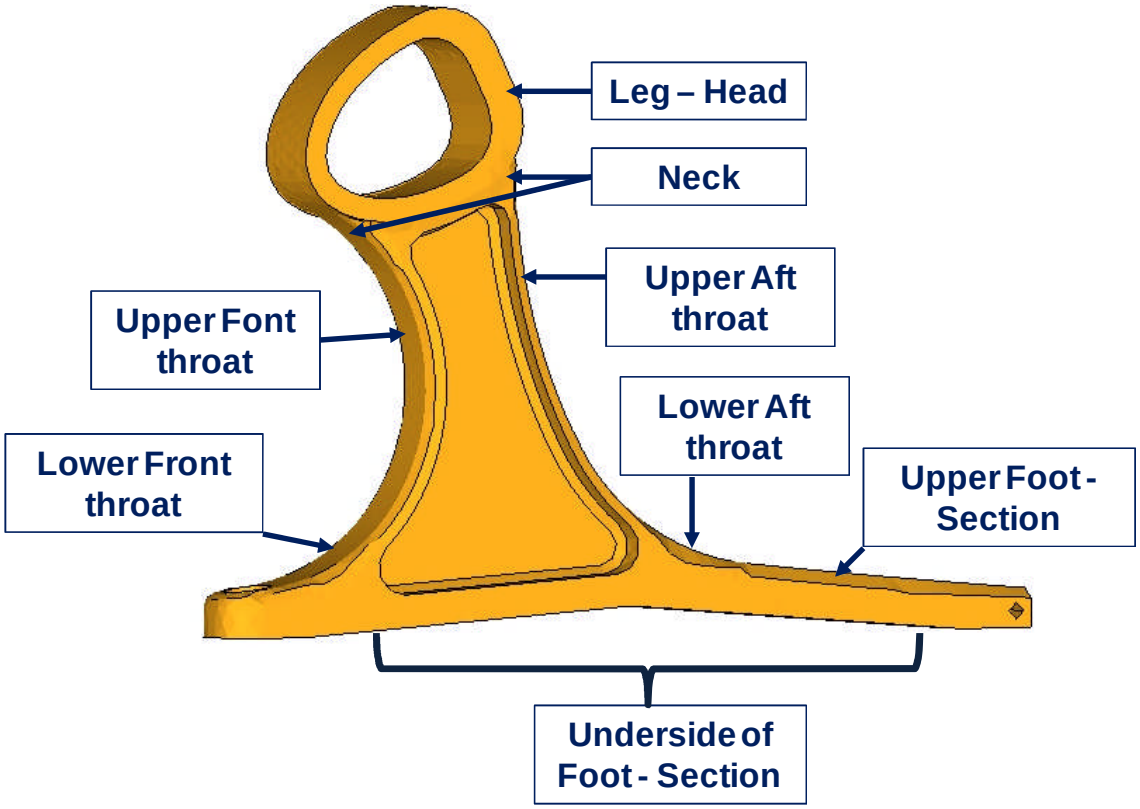

Figure 8-4 Nomenclature of leg from "Design Viewpoint"

Design of the leg was the most time consuming activity during this research. Overall nine different leg variants were analysed as the different inputs were received from Blue-Sky regarding variations in the design philosophies, anchor connection and continuous upgrade of support conditions with added details.

In First eight leg variants, the leg was directly attached to the seat track through mushroom-headed studs and shear pin. However, in the later stage of the project (after seven months from the start date), Boeing Specifications (BS) were received. BS changed the manner in which the seat structure would be attached to the seat track via leg. According to BS, leg should not be in direct contact with the track and additional component should be used to connect leg with the track.

This was a paradigm shift in the project as all earlier leg design (leg variant V#1 till V#8) were no longer useful. However, the detailed FE models developed for these variants (sequential approach), methodologies developed for extracting seat interface loads, simulating bolt pre-load and stress levels estimated were extremely useful for FEA of “FWD beam and leg (as per BS)”. To restrict the volume of present report, leg variants V#1 to V#8, have been briefly explained in Appendix H.

Coming section discusses leg designing as per BS and demonstrates the application of all earlier findings for the leg designing. The word “earlier” in this section means the FEA of leg variants V#1 till V#8 for “Forward 9g” loadcase.

8.3.1 Design of Leg V#9 inline with Boeing Specifications

“Stay-out Zone” should be incorporated in seat leg to eliminate direct loading of leg during floor deformation [35]. “Stay-out Zone” is the minimum vertical clearance between top of the seat track and foot section of the leg in the span from front connection to aft pivot. At mid span the clearance should be 0.5 inches with a gradual decrease to 0.1 inch towards either end (Figure 8-5).

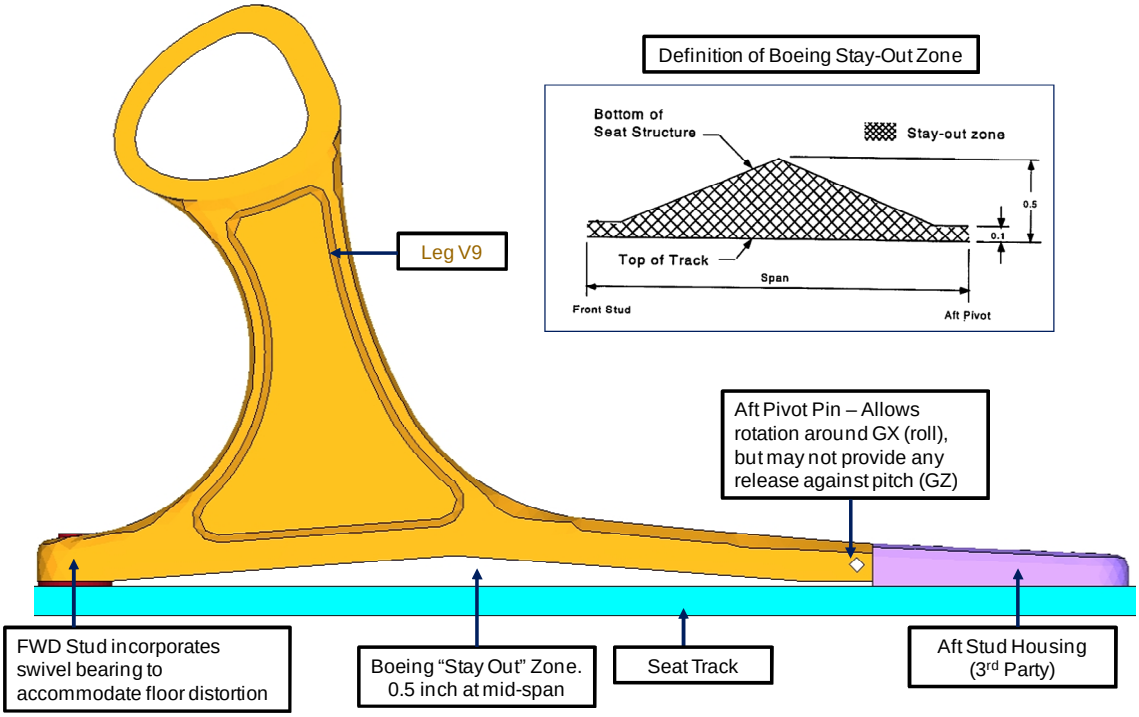

Figure 8-5 Leg Design V#9 to accommodate "Stay-Out Zone" as per "Boeing Specifications" [35]

In order to avoid direct anchoring of leg to the track, "Aft Stud Housing (ASH) was used to house the mushroom-headed studs and a shear pin as shown in figure 8-6 [35].

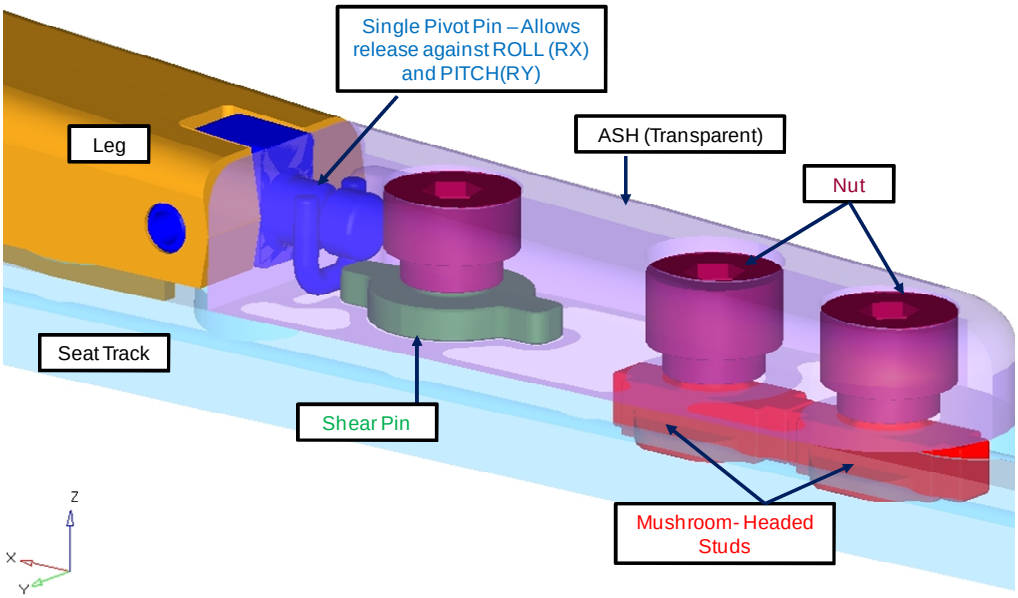

Figure 8-6 Aft Stud Housing (ASH) attached with leg through "Single Pivot Pin" and with track through mushroom-headed studs and shear pin

ASH has two tension studs (maximum limit of three) which are separated by three inches. Shear plunger mounted between ASH and track has engagement depth of 0.16 inches (minimum 0.15 inches) with track and a nominal diameter of 0.7 inches (maximum 0.708 inches).

In order to avoid secondary loads being applied to the seat structure, ASH has been attached to the seat leg with a “Single pivot pin” (Figure 8-6) which allows free relative Pitch +/- 10 degrees and Roll +/- 5, between leg and the track [35]. Swivel bearing in the front ensures that leg will have same relative movements during seat pre-deformation (Figure 8-7).

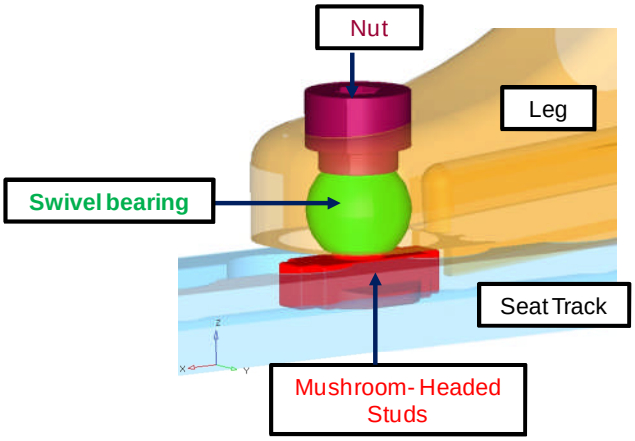

Figure 8-7 Swivel bearing in the front leg fitting

Another major decision was to reduce the overall width of leg from 50 mm (earlier leg variants) to 30 mm due to following reasons,

- From earlier FEA results, it was seen that the lower throat and foot section of the leg is not subjected to high stress levels.
- In addition, the von Mises stress observed in the upper throat region are within the yield limit (Leg V#8, Appendix H.3).

In order to avoid localised stresses at leg and FWD beam interface, C-clamp of 10mm width was designed and was placed at either end of leg (Figure 8-8). Reduction in the width of the leg and addition of “C-Clamp” resulted in reducing the weight of leg from 1100g (earlier versions) to 760g still providing the local reinforcement in the high stress region.

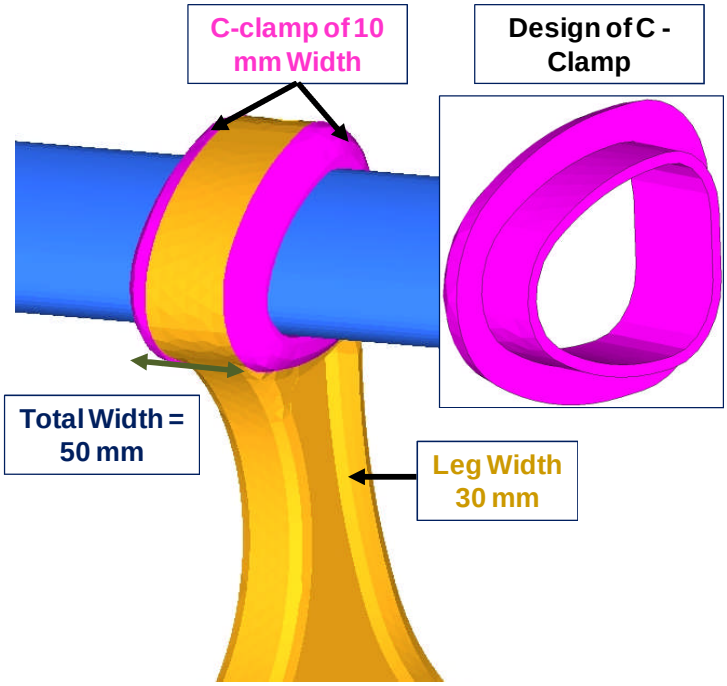

Figure 8-8 Design of C-clamp, which provides local stiffening at FWD beam and leg interface

8.4 Accomplishment of "Detailed" FE model of "FWD beam and leg"

Front and Rear Seat fittings are "Aero-Space Certified" parts and are safe against applied loads as per CS 25.561 (Input from BlueSky). Therefore, it is not in the leeway of the designing team to alter their designs. Their stiffness has been accounted though tetrahedral FE models (quicker way) (Figure 8-9).

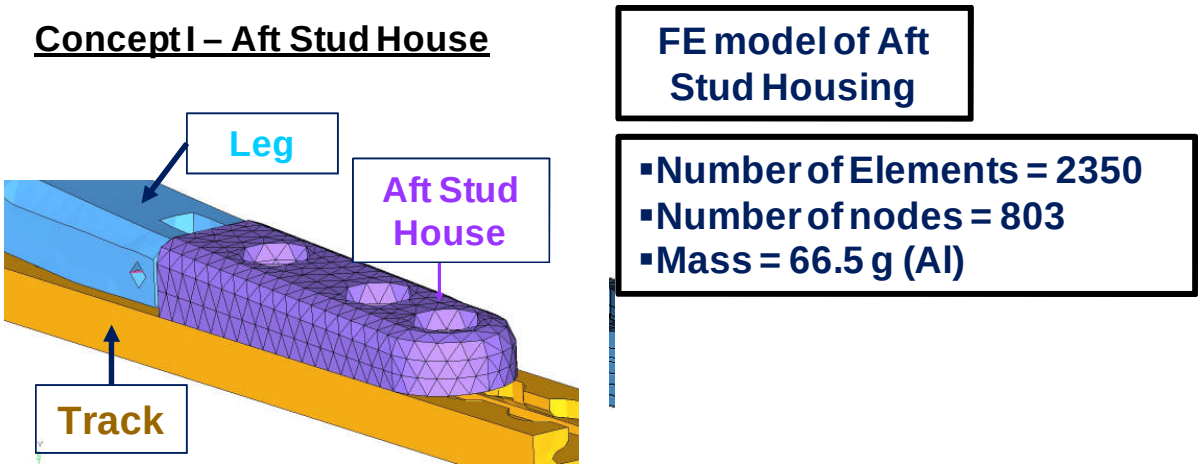

Figure 8-9 FE model of the Aft Stud Housing

Connection between different parts, “Single Pivot Pin” between leg and ASH can be accounted by two ways in FE modelling. One is to use special elements called “Connector elements” which apply “Kinematic Constraints” enforced with Lagrange multipliers [29]. They provide outputs as forces and moments transmitted across the joint, that is a useful tool to study the strength of the joint. However, Lagrange multipliers are additional solution variables. This increases the problem size and in turn the solution time [29].

Second way, to account for connections is to use “Multi-Point Constraints (MPC) with “release” [27], [29]. MPC eliminate dof at one of the coupling nodes involved in the connection thereby reducing the problem size. They do not produce any output as force and moment transferred across the joint. Combination of selected rotational dofs results in a behaviour identical to special purpose “Connector elements” without any output.

- Selection of three-displacement dof along with three rotational dof acts as a rigid region following the motion of reference node [29].
- Selection of three-displacement dof along with two rotational dof acts as a revolute or pin joint.
- Selection of three-displacement dof along with one rotational dof acts as a universal type joint.

As far as the scope of present study is concerned, appropriate transfer of load across the joint is required and not the detailed output at the joint. Hence, approach of MPC with a release of “Pitch” and “Roll” is adopted to model the connection between leg and ASH (Figure 8-10). This makes problem size smaller and hence gives faster results.

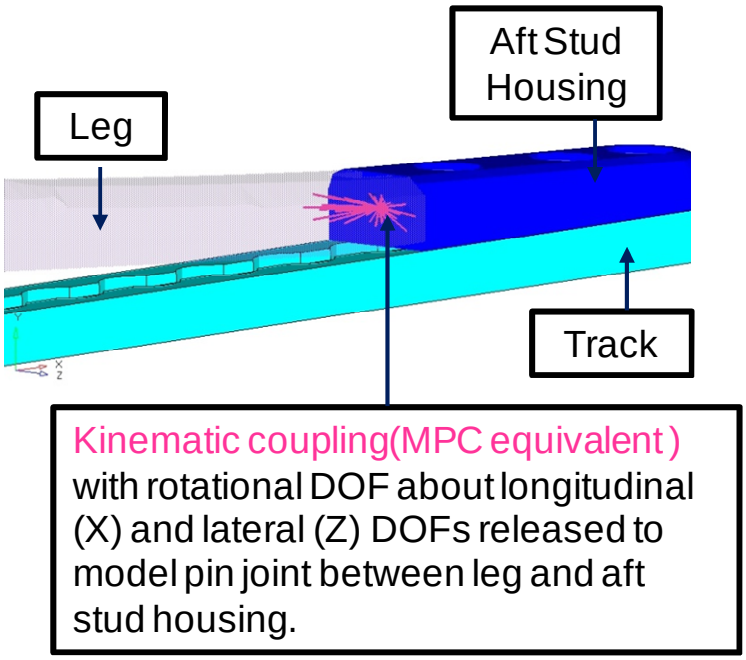

Figure 8-10 FE representation (using MPC with "End Release") of the Pivot pin between leg and Aft Stud Housing

In order to study the detailed behaviour of “Swivel Block” in the front leg fitting, it was decided to explicitly model the sphere and other parts involved and contact definitions were defined between them. Thus, a very detailed FE model was developed as shown in Figure 8-11

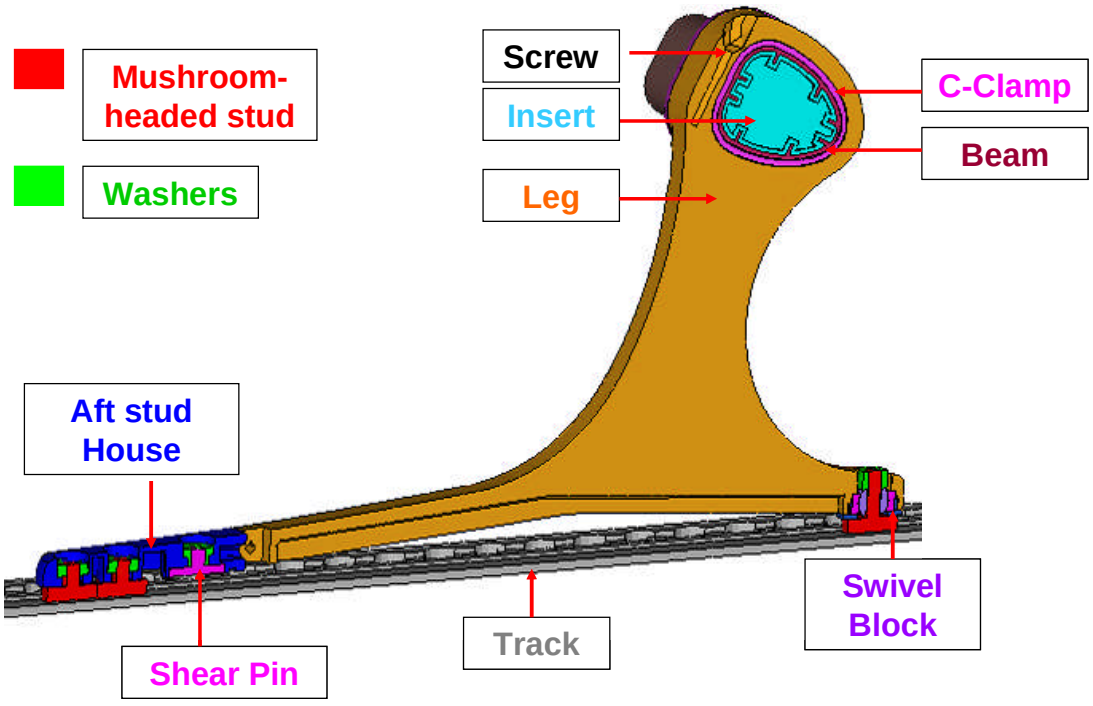

Figure 8-11 Cross-section of the detailed FE model of FWD beam and leg V#9 showing parts considered for FEA

Contact pairs defined can be summarised as follows,

- Seat track and ASH,
- Each of the nut and corresponding mating surface of ASH.
- Shear pin and ASH, Shear pin and track.
- Each of the mushroom-headed stud and corresponding mating surface of track and ASH
- Mating surfaces in the front swivel bearing.
- Leg faces in beam clamping area, each of FWD beam clamping stud and corresponding resting surface of leg and FWD beam and leg(When stud was explicitly modelled at the FWD beam and leg interface).Without stud, tied contact was defined.

Coincident nodes were used between FWD beam and corresponding reinforcing inserts. In addition, threaded extension of the FWD beam clamping stud had coincident nodes with corresponding hole in the leg.

Thus, forty-six contact pairs were involved (when studs in the FWD beams are modelled, without them, forty), in this FE model of "FWD beam and Leg Version #9" assembly. Loads and load application point remained same as discussed in Section 5.2.1.

Non-linear material properties were used for FWD beam and leg to account for permanent deformation if any (Appendix I). In addition, solution scheme with non-linear geometry option was activated in Abaqus / Standard [29]. Thus, a detailed FE model of "Primary Load Path" involving all the three types of non-linearities (contact, material and geometry), all parts (FWD beam, reinforcing inserts, C-clamp, leg, aft stud housing, track, mushroom-headed studs, front swivel block and shear pin – Figure 8-11), which could estimate stress and interface loads when subjected to loads as per CS 25.561, was developed.

8.5 Discussion Of Results for Leg Variant #V9 – Forward 9g

Maximum von Mises stress of 375MPa is observed at the underside of foot section near lower throat area due to high bending moment (Figure 8-12).

Permanent deformation of 0.5% is observed at the same location. Therefore, Leg V9 is “Unsafe” against “Forward 9g” loads (“Safe” leg design means maximum stress < Yield limit as given in Section 8-3).

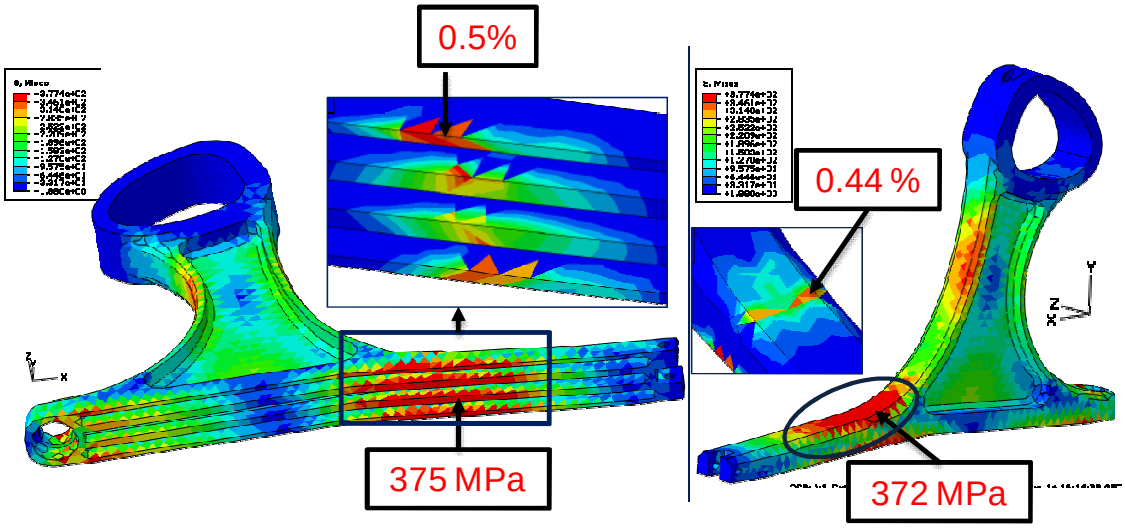

Figure 8-12 von Mises stress plot for leg V#9 without nodal averaging (Forward 9g)

Design improvement for Leg V#9 was required. The regions of leg to be improved were decided by studying principle stress components and normal stress components.

Figure 8-13 gives the maximum principle stress plot for Leg V#9 (Forward 9g). It can be readily seen, upper and lower aft throat and upper foot section, experience tensile stresses above yield. Therefore, second moment of area of this region needs to be improved to reduce the stress levels. Same region was defined to be a “Design Region” for Free-Shape Optimisation technique used to design the leg (Figure 9-1, Chapter 9).

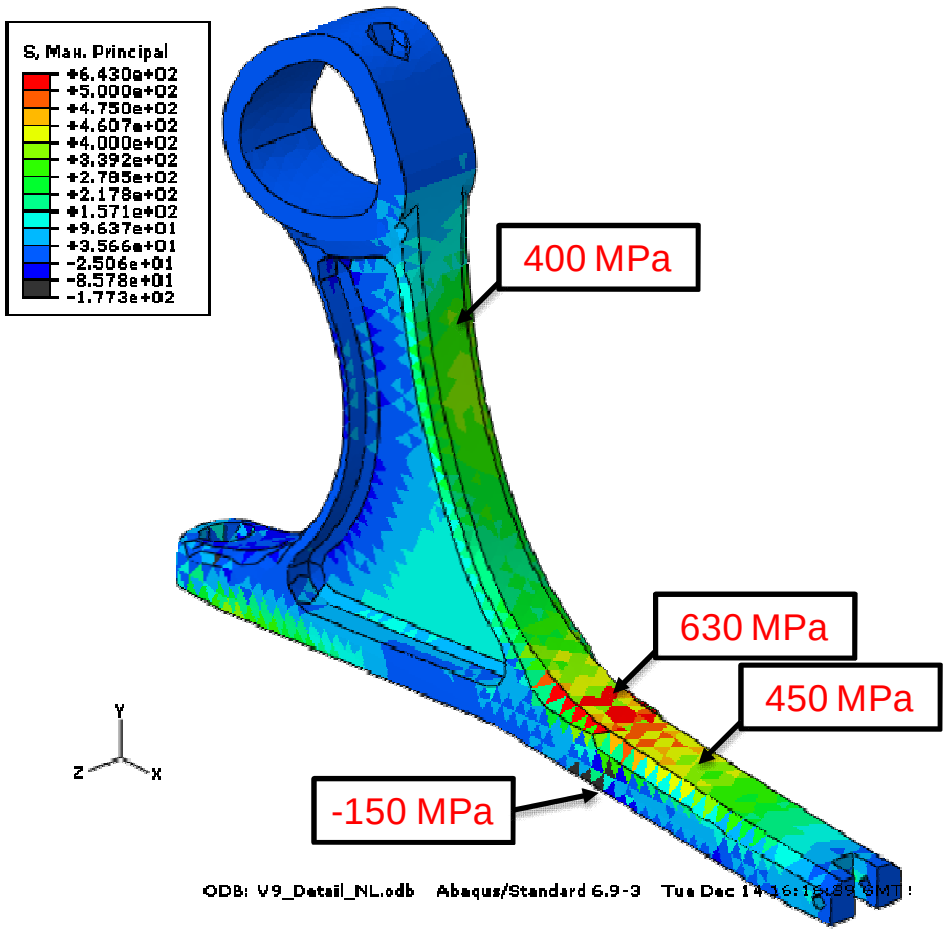

Figure 8-13 Maximum Principle stress plot for the leg V#9 (Forward 9g) - An indicator of design improvement

Conclusion from Chapter 8

How the designs FWD beam, reinforcing inserts and leg C-clamp were derived from FEA results was explained in this chapter.

Using spreadsheet, elliptical cross-section with two-millimetre thickness was chosen for FWD beam. Addition of reinforcing inserts in the FWD beam was a cost-effective solution, which brought down the von Mise stress observed in the beam from 413 MPa (above Yield limit of 375 MPa) to 229 MPa. The most dynamic and challenging part was “Design of leg”. Leg V#8 was found to be safe against critical load cases of “Forward 9g” and “Downward 6g” (Appendix H-3). However, later on “Boeing Specification” emphasised use of additional

block (Aft Stud Housing - ASH) to assemble leg with the track. This was a major change in the project as earlier leg designs (V#1-V#8), were directly mounted on seat-track. Joints used to attach ASH with leg and track, ensured a free relative movement (“Roll” and “Pitch” of 10 degrees) between seat-track and the seat structure avoiding secondary loading of the leg during seat pre-deformation. Using “Boeing Specifications”, Leg V#9” was constructed, which was declared as “Unsafe” against “Forward 9g” loads, by FEA results.

A major outcome of this chapter is the detailed FE model of “FWD beam and leg” (Primary Load Path). Fourth point from scope of the project was reached in this Chapter i.e.

“Analysis led design of leg/seat track interface to investigate reaction loads generated and integrity of seat track. Develop detailed non-linear FE Model(s) that represent the load path of the seat for 9g load cases”

It was decided to use commercial optimisation tools to achieve the design of leg, which can sustain the applied CS 25.561 loads without yielding.

9 Free Shape Optimisation of Leg

Design of the seat leg is driven by multidisciplinary measures such as leg should [6], [16],

A. Have sufficient strength to resist loads as specified in CS 25.561

B. Have mass less than 1 kg,

C. Be easy for machining,

D. Have sufficient room for usage of hoppers and

E. Be elegant.

The shape of the leg is strongly driven by D and E from the above list and BlueSky was keen to keep the basic shape as that of leg V#9. Based upon these inputs following optimization strategy was defined,

I. “Free-Shape Optimization (FSO)” of the baseline design (Leg V#9) would be done to estimate the maximum design envelop of the leg (subjected to mass constraint) that satisfies the strength requirements. This ensures that parameters A, B, D, and E are covered.

II. Output of the FSO would be converted into intermittent leg design.

III. Design concept given by FSO would be then converted into realistic design with the help of DFM (Design For Manufacturability) techniques, which covers requirement “C”.

IV. If the mass of the exceeds 1kg barrier, topology optimisation would be done next.

Therefore, optimization strategy will consider all the major aspects, which contribute towards leg design.

9.1 Free Shape Optimisation - Background

FSO technique is inbuilt in Optistruct (linear static solver used earlier) [24]. Hence, preliminary FE model of “FWD beam and leg (variant used V#9)” could be easily modified to suit the format of input-deck required for FSO. Therefore, the thought with which Optistruct was selected initially (Section 4.5) proved to be really beneficial and directly applicable for FSO.

In FSO, the periphery of a structural component is changed to satisfy the objectives and constraints that are pre-defined. Free-shape design regions are defined through the DHAPE bulk data entry in Hypermesh panel [24]. The grids on the periphery of the structure form the “Design region” and during design iterations, these grids move along the updated normal to the surface.

Parts considered for free-shape optimisation

Half-symmetric preliminary FE model of the “FWD beam and leg V#9 assembly” is considered for the optimization study, which includes following parts,

Leg, FWD beam, C- Clamp between FWD beam and leg, Reinforcing insert in FWD beam, Aft Stud Housing, front, mid and rear mushroom-headed studs.

The reason to choose “Preliminary FE model of “FWD beam and Leg V#9” (Preliminary means coincident nodes at FWD beam and leg interface) can be explained as follows,

- Interaction definition at contacting surfaces of FWD beam and leg or involvement of seat track introduces “Contact non-linearity”.
- However, optimization techniques used for the present study, estimate some important responses (e.g. compliance) based on linear static loadcases only.
- Hence, track and shear pin is not considered and their representative boundary conditions are applied to the model and coincident nodes have

been used at FWD beam and leg interface, thereby keeping the process under “Linear Static” spectrum.

9.2 Definition of parameters for Free Shape Optimisation

Ideally, free-shape design region is selected where the local shape of the structure is most sensitive to the expected responses. In present case, grids in the high stress region are selected (Section 8.5), as the main concern is to reduce the stress levels experienced by the leg.

Two different locations have been selected on the structure where shape can vary independently i.e. A – Front, and C- Rear (Figure 9-1).

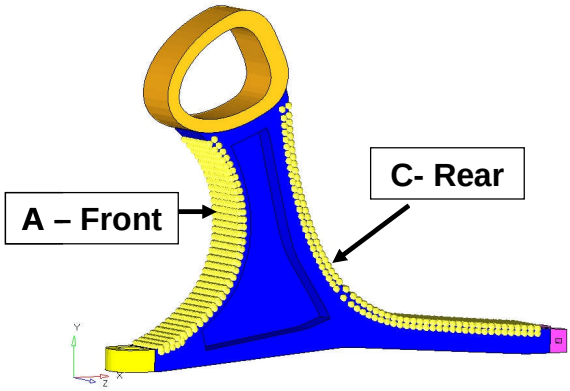

Figure 9-1 Design region for free-shape optimisation of Leg V#9

9.2.1 Parameters for Free Shape Design Region

Direction Type, This directs the movement of grids in design region. In case of leg, grids are unconstrained which means that they can move inside as well as outside the initial part boundary.

Move Factor (MF), maximum allowable movement of the grid during an iteration is equal to (MF*average mesh size of the design region) [24]. MF of 0.3 is considered in the present analysis, which makes simulation more stable at the same time slower!

Mesh smoothing layers (NSMOOTH), As FSO progresses, grids in the design region move in order to satisfy the constraints. Hence, six layers of internal grids adjacent to these grids are defined via NSMOOTH in order to avoid excessive mesh distortion.

Symmetry constraint, Since the symmetric designs are always preferred due to their ease during manufacturing, 1 – plane (XY plane as shown in Figure 9-2) symmetry constraint has been defined on the leg.

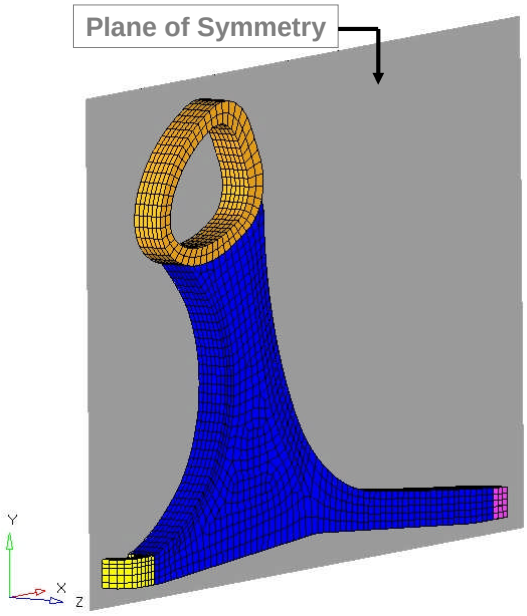

Figure 9-2 XY Plane of symmetry for the leg V#9

Additional Constraints, The width of the leg is fixed and is 30 mm. It is desirable not to exceed this limit (Input from BlueSky). Hence, grids in the front and rear design regions are restricted from moving in lateral (Z) direction (Figure 9.2).

Objective Function, Inertia loads considered for the FSO are all the loads specified in CS 25.561 b-3 (Appendix A.1) as show in Figure 9-3. Spreadsheet was used to convert these loads (CS 25.561) from their loading point (discussed in Section 4.3, Appendix J) to equivalent forces and moments to be applied in local co-ordinate system of FWD beam.

In order to consider the effect of these five different loadcases; “Weighted Compliance” response has been defined.

Weighted Compliance $C_w = \Sigma W_i * C_i$, [24]

Where,

W_i is the weight factor of each load case which is considered unity.

C_i is compliance of each individual loadcase.

i = 1, 2… 5 (i.e. five loadcases)

Thus, the objective of this FSO is minimization of “Total Weighted Compliance”.

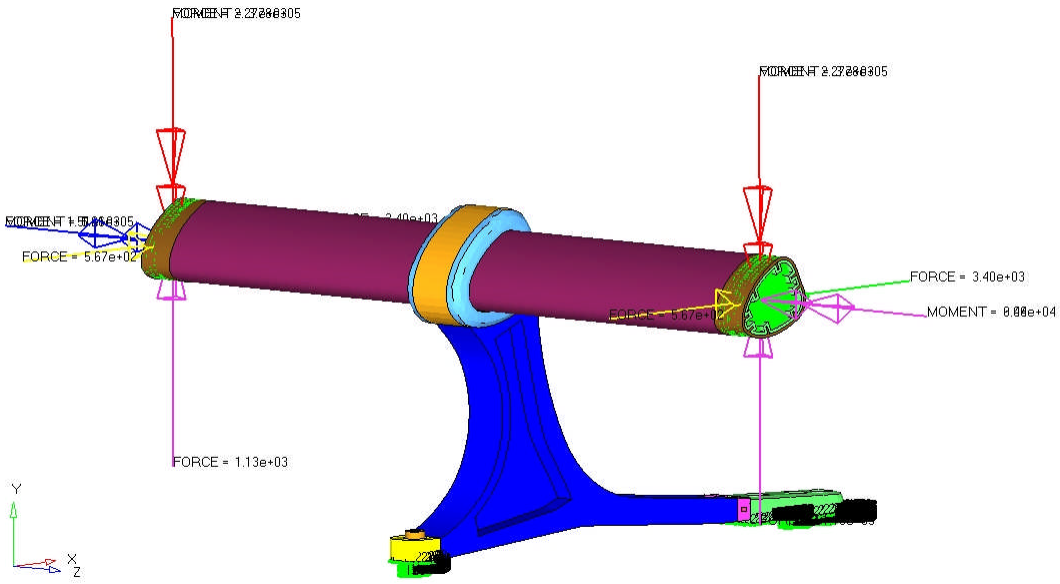

Figure 9-3 All inertia loads specified in CS 25.561 are considered for FSO of Leg V#9

Design constraint, Apart from constraints such as symmetry (manufacturing constraint), controlled movement of grids (FE constraint) and perturbation and direction constraints (simulation stability factors); it is essential to define design constraints.

Previous FEA results of FWD beam and Leg assembly show that leg is subjected to high stress levels (375 MPa with 0.5% plastic strain – Section 8.5). Hence, upper bound of 250 MPa (von Mises stress) has been applied as a design constraint on the peripheral elements (Figure 9-4). The limit of 250 MPa has been chosen (though the yield is at 375 MPa), in order to keep some margin for dynamic loads (CS 25.562 – not accounted in present research).

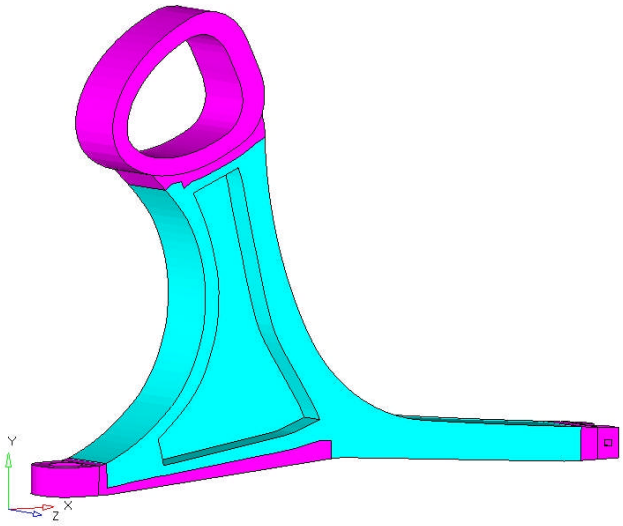

Figure 9-4 Design constraint of 250 MPa(von Mises stress) is applied on peripheral elements shown in Cyan colour

Boundary Conditions, Nodes on faces S1 (front bottom surface of the leg) and S2 (bottom surface of aft stud housing) are constrained for vertical direction to represent resistance offered by the track in –Y direction (Figure 9-5). (Note: non-linear spring element can be used to model contact and separation behaviour with respect to track. Nevertheless, this needs determination of stiffness of corresponding components, which demands more time and adds complexity to the model. Hence, appropriate representative constraints are applied on S1 and S2).

Nodes in the bottom portion of the studs are constrained for vertical movement and shear pin for lateral and longitudinal.

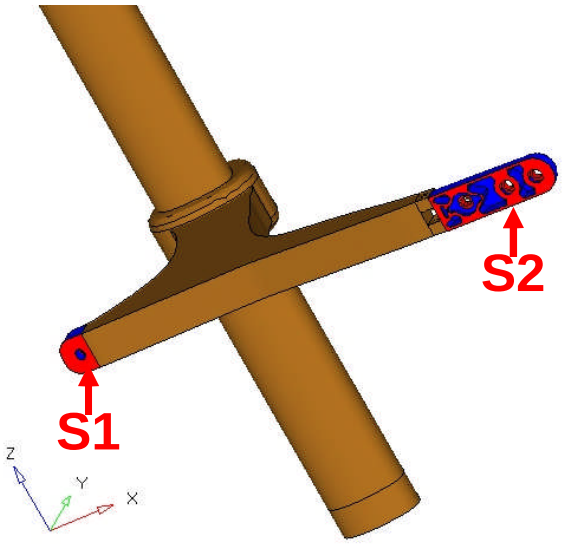

Figure 9-5 Definition of S1 and S2

9.3 Discussion of Results of FSO of Leg V#9

Simulation stopped after 20 design iterations as some elements in the rear design region were too much distorted. However, a careful interpretation of results gave lot of useful and sufficient inputs to carry out further design work.

The objective of this FSO was to minimize total weighted compliance for all the inertia loads as specified in CS 25.561 b (3). 52.4% reduction in total weighted compliance has been achieved (Figure 9-6).

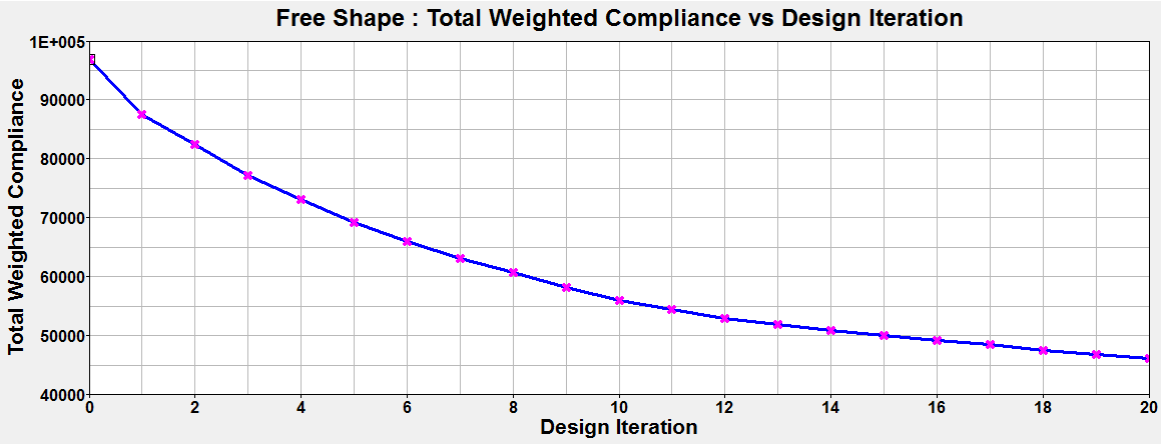

Figure 9-6 52.4% reduction in "Total Weighted Compliance" achieved by FSO of Leg V#9

9.3.1 Variation in the Design Constraint (von Mises stress)

The important design aspect was reduction in von Mises stress levels experienced by leg V#9 during non-linear FEA of detailed assembly model of "FWD beam and leg" (Section 8.5). Considering FEA results from earlier simulations, six different high stress locations have been identified for different loading scenarios. Figure 9-7 shows these zones and their identification mark. One or two high stress elements (which are representative of trend of von Mises stress in localized area) have been taken from each of these six zones and variation in von Mises stress in those has been monitored for each design iteration. Following sections discuss the results for Forward_9g, Downward_6g, and Sideward_4g loadcases being the most critical (as seen in Section 4.1.2).

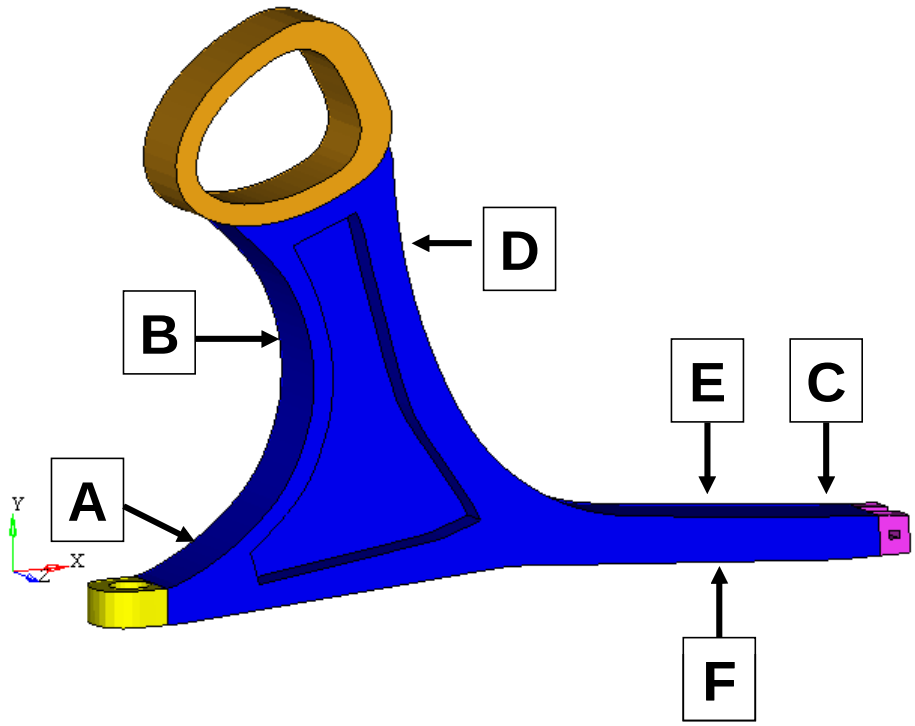

Figure 9-7 Nomenclature of High Stress zones in the leg

Forward 9g, High stress locations in leg when subjected to Forward 9g loads are B, D, E, and F.

Figure 9-8 shows variation in von Mises stress levels for each of the design iterations at these locations. It can be inferred from the figure that stress values have dropped down in iteration 20 from their reference values in iteration 1.

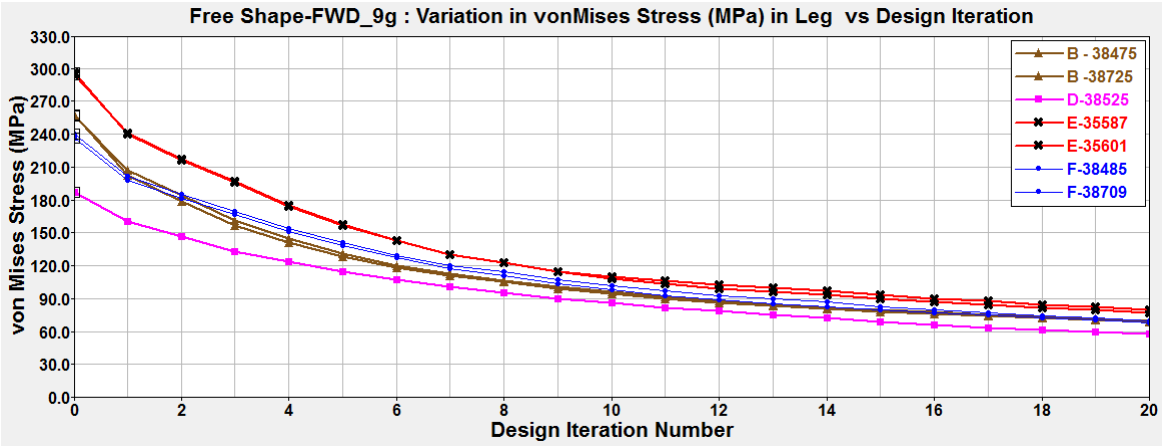

Figure 9-8 Variation in the maximum von Mises stress observed in B, D, E, and F Vs. Design iterations during FSO of Leg V#9 (Forward 9g)

Table 9-1 gives von Mises stress observed at these locations at iteration number 1 and 20 and corresponding percentage drop. On an average about 70% drop in stress can be seen and hence significant reduction in stress has been achieved.

Design Iteration	1	20	
High Stress Location	von Mises Stress (MPa)		% Drop
B	257.8	69.2	73.2
D	186.6	57.5	69.2
E	294.3	79.5	73.0
F	240.2	69.5	71.1

Table 9-1 70% reduction in the maximum von Mises stress in Leg V#9 (Forward 9g) achieved by FSO

Side_4g, High stress locations in leg when subjected to Side 4g loads are A, B and D. It can be seen from Table 9-2 that at location "A", von Mises stress of 426.8 MPa has been observed with initial design configuration (i.e. at iteration 1) which is above the yield limit of general Aluminium alloy. After free-shape optimization, it drops down to 130.8 MPa i.e. almost 69.4% and is well below the yield limit.

Design Iteration	1	20	% Drop
High Stress Location	von Mises Stress (MPa)		
A	426.8	130.8	69.4
B	317.1	68.4	78.4
D	369.3	92.9	74.8

Table 9-2 Percentage reduction in the maximum von Mises stress in Leg V#9 (Side 4g) from Iteration 1 to 20, achieved by

In other loadcases von Mises stress levels observed in the leg with initial configuration (iteration 1) are not critical from strength point of view. Table 9-3 summarizes the results for inertia loads applied in Down, Up and rear directions.

Loadcase	Design Iteration	1	20	% Drop
	High Stress Location	von Mises Stress (MPa)		
Downward_6g	B	70	19	72.9
Up_3g	B	34.9	9.5	72.8
Rear_1.5g	E	50	15	70.0

Table 9-3 % reduction in the maximum von Mises stress in Leg V#9 for Down 6g, Up 3g and Rear 1.5g loadcases, achieved by FSO

9.3.2 Design modifications suggested for Leg V#9 by FSO

The basic idea behind FSO is that the shape of the design region is altered in order to bring down the stress levels. Therefore, a designer is interested in the final “Shape Change”. Figure 9-9 shows the overall shape change in the leg at design iteration 20. Original design of leg is shown in magenta wireframe. Plots for grid movement in individual Cartesian axis have been shared with BlueSky through internal delivery.

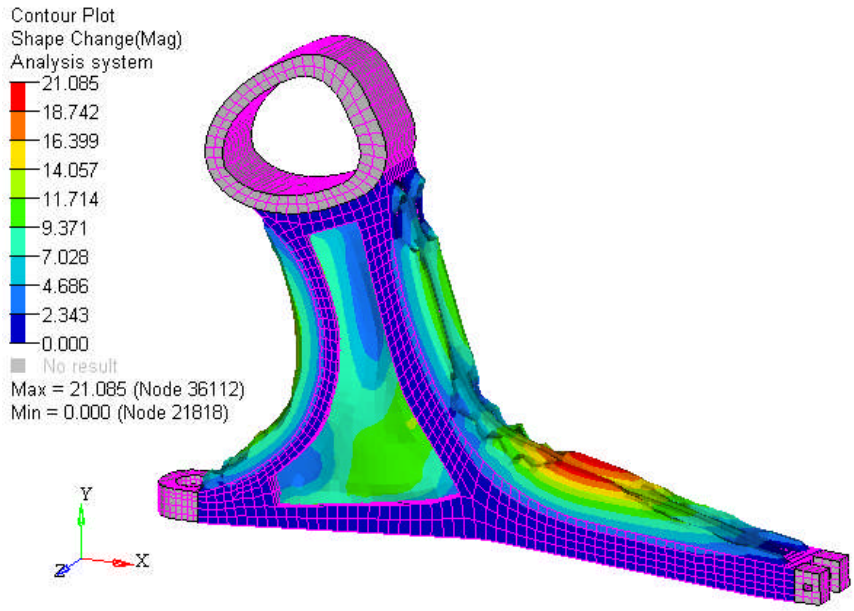

Figure 9-9 Magnitude of shape change for Leg V#9 after the FSO

Mass of the leg before FSO was 0.76 kg, which became 1.1kg after optimisation. Thus, recording an increase of 44.7%.

9.3.3 Exporting final design in CAD format

Next step after FSO is the recovery of modified geometry for the further use. The requirement during this export is to create smoothed surfaces applying optimization results to the design region. OSSmooth, which is semi-automated design interpretation software, facilitates such a recovery [24]. Using OSSmooth command from Hypermesh panel following CAD data was generated in “igs” format (Figure 9-10).

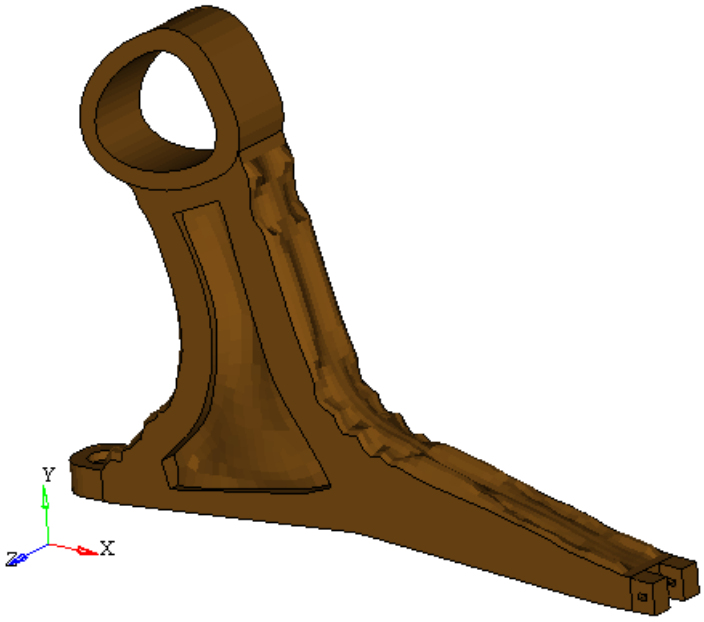

Figure 9-10 Output form free-shape optimisation in "igs" format using "OSSmooth"

9.4 Summary - Free-shape Optimization

- Grids on front and rear faces of the leg were selected as design regions since high stress points were observed from previous FEA of "Forward beam and leg assembly" (observed in Section 8.5).

- All inertial loads as per CS 25.561 b (3) were considered. Optimization problem definition was to minimize total weighted compliance from all these loadcases subjected to a cap of 250 MPa on von Mises stress. Other constraints such as symmetry, maximum movement in one design iteration and restriction on movement of grids in particular directions were applied from practical as well as from simulation stabilization angle.

- Though the simulation stopped after 20 design iterations, useful and sensible information was interpreted from the results at 20^{th} iteration. Total weighted compliance was reduced by 52.4 %. In "Forward 9g" loadcase maximum von Mises stress was reduced by 73%. In "Side 4g"

loadcase, von Mises stress of 426.8 MPa, which was above yield limit, was reduced to 130.8 MPa (well below the yield limit). In other loadcases, on an average 70% drop in von Mises stress levels was achieved.

- The mass of the leg increased from 0.76 (original Leg V#9) kg to 1.1 kg resulting in increment of 44.7%. Though the design of the leg became stronger after FSO, mass of the leg can be brought down further. “Topology Optimisation” can be done to put a cap on mass. However, it was decided to tentatively freeze this design.

- OSSmooth panel from the Hypermesh was quite handy and useful in recovering the geometry after FSO with minimum and smoothed surfaces in “igs” format. This output was given to BlueSky designers to render the final design concept for leg.

- Thus, Free-shape Optimisation feature of Altair Engineering was found to be quite efficient and useful in not only getting the shape of the outer boundary when subjected to various constraints but also in recovering the geometry useful for next design stages.

Thus, the fifth point defined in the scope of the project (Section 1.3) was satisfied in the section i.e.

“Additional design work may be required if poor performance is demonstrated, which may be through manual design modifications, or the use of commercial optimisation tools”

Next task was to perform non-linear FEA of the complete seat with this leg design to,

- Check the strength of the overall design when subjected to CS 25.561 loads,

- Check the robustness of detailed FE assembly of “FWD beam and leg (new concept as per FSO)” when coupled with rest of the structure,

- Estimate “Seat Interface loads” for “Forward 9g” loads.

9.5 Non-linear FEA of Complete Seat

As seen from previous sections, a detailed FE model of “FWD beam and leg” involved all types of non-linearities i.e. material, contact and geometric. It could also predict “Seat Interface Loads”. In addition, solutions for non-convergence issues like rigid body motion, initial penetrations were found out. Methodologies to define interaction between mating parts and to represent various joints between sub-assemblies were studied in detail and documented. In summary, principles and procedures required to carry a non-linear FEA of complete seat were well established and executed by this time. Therefore, remaining task in front of the author was to build FE model of remaining seat structure and assemble it with detailed model of “FWD beam and leg”.

9.5.1 FE modelling strategy for remaining parts

Boomerang, is a connecting member between seat sub-structure and superstructure. It is directly attached to the seat belt attachment bracket, backrest tube and FWD beam. It will experience out-of-plane bending when subjected to “Side 4g” loads and hence high stresses will be induced especially near belt anchorage. Therefore, it was decided to use brick elements (two elements through thickness) for FE modelling of boomerang (Figure 9-11). A dense and regular mesh was achieved in the area near the belt attachment point (Figure 9-11, Insight) to capture the stresses in a better way.

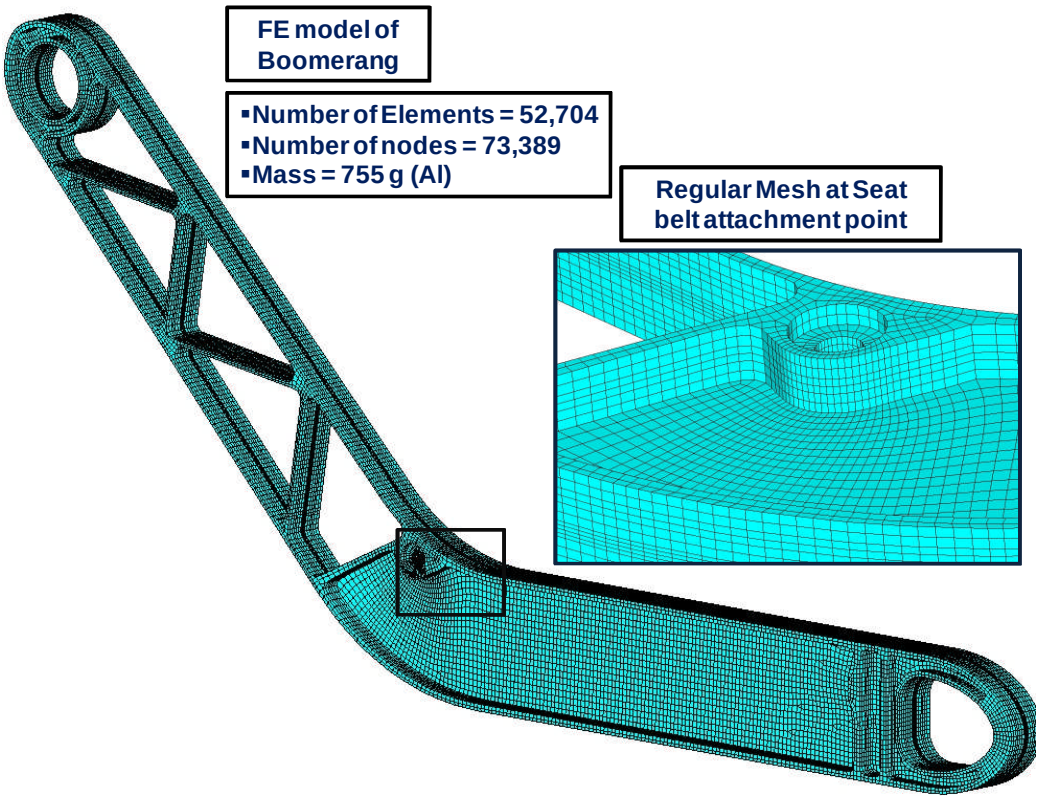

Figure 9-11 FE model of Boomerang

Seat pan thickness (1mm to 2mm) is very less as compared to other two dimensions. Hence, shell elements have been used for its FE modelling. Midsurface representation has been used. Vertical planar symmetry has been considered to reduce the modelling effort. In order to reduce the number of elements and hence the solution time, elements with high aspect ratio have been used in the midspan of the pan where less stress levels are expected. In the area of high stresses, dense mesh with aspect ratio less than 3:1 has been used. In order to avoid, abrupt changes of mesh pattern around the holes (where nodes get stuck on the edge of hole) washer surfaces have been created and regular evenly sized mesh is achieved as shown in Figure 9-12,

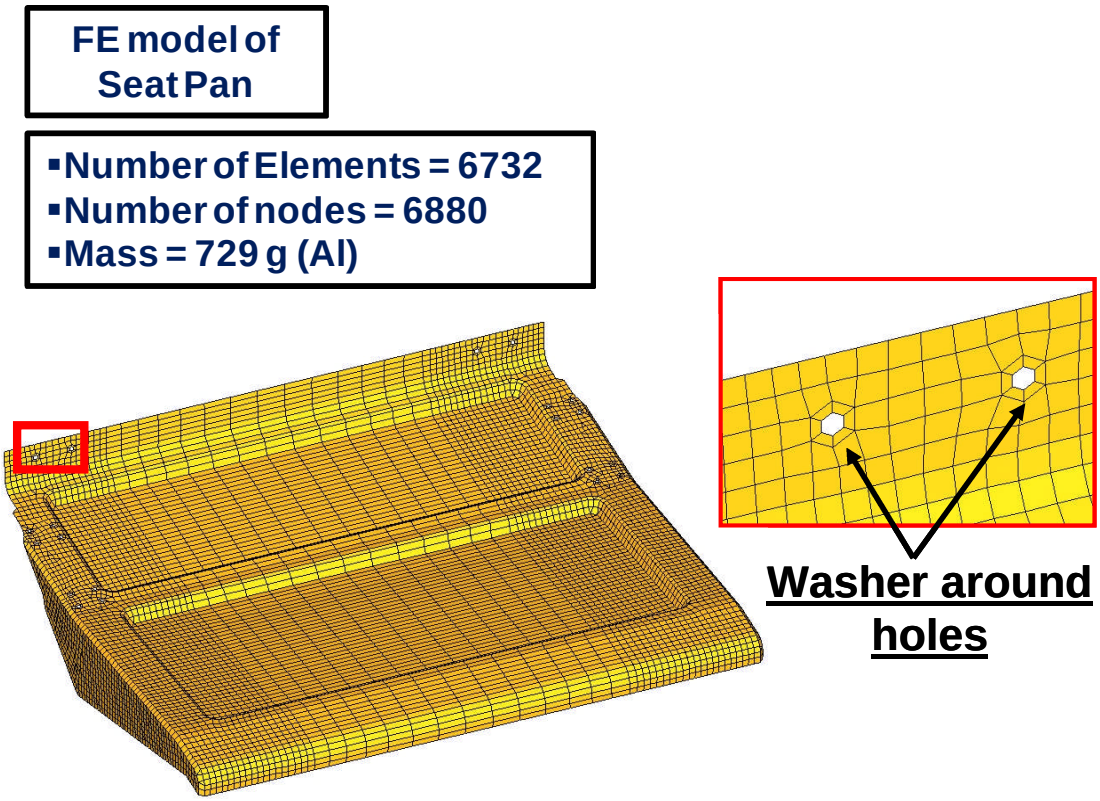

Figure 9-12 FE model of Seat pan

9.5.2 Interaction Definitions for Complete Seat model

Contact pairs defined can be summarised as follows,

- Seat track and Aft Stud Housing (ASH), Butting surfaces of leg and ASH
- Each of the nuts and corresponding mating surfaces of ASH.
- Shear pin and ASH, Shear pin and track.
- Each of the mushroom-headed stud and corresponding mating surface of track and ASH
- Contacting surfaces in the front swivel bearing.
- Seat pan and boomerang, Seat pan and connectors, Boomerang and Connectors
- Tied contact between,

  C-clamp and leg, C-clamp and FWD beam, Interface of boomerang and FWD beam, Connection between boomerang and backrest tube.

- MPC connections at attachment points between,

  Seat pan and Connectors (shown in Figure 9-13), Boomerang and Connectors

- MPC with release in “Pitch” and “Roll” connecting leg and ASH

Thus, complete seat model includes total 62 contact pairs with penalty algorithm, 11 tied contacts, 32 MPC connections (rigid) and 2 MPC connectors with “End Release” (Figure for reference 8-10). Total number of nodes and elements are 354862 and 285679 respectively. Total mass of this seat structure is around 7 kg.

Bottom surfaces of track were constrained for all dofs during simulation and loads (as per CS 25.561, applied separately) were applied at the point discussed in Figure 4-5, Section 4.3 (Figure 9-14). Only “Forward 9g”, “Side 4g” and “Downward 6g” loadcases were solved(as per the request from BlueSky) and detailed reports were delivered to BlueSky. Same FE assembly used for these loadcases can be used for “Rear 1.5g” and “Up 3g” loads, with a change in direction of load.

On an average, it takes about sixteen hours with four processors to simulate one loadcase for High Performance Computing facility available at Cranfield University.

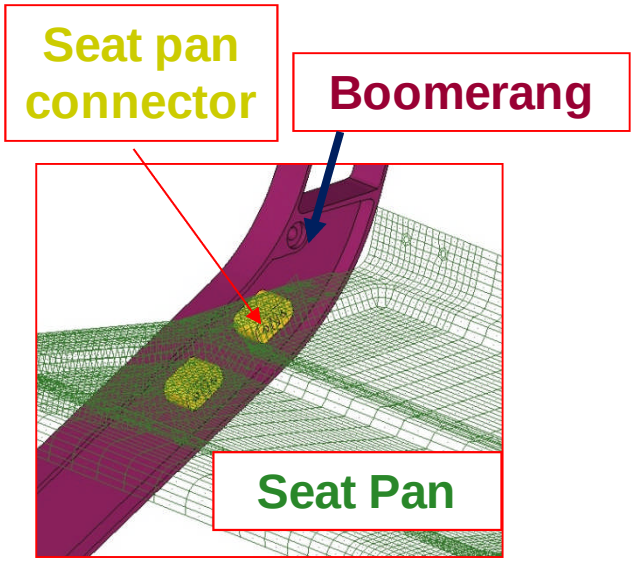

Figure 9-13 Location of Seat Pan Connector

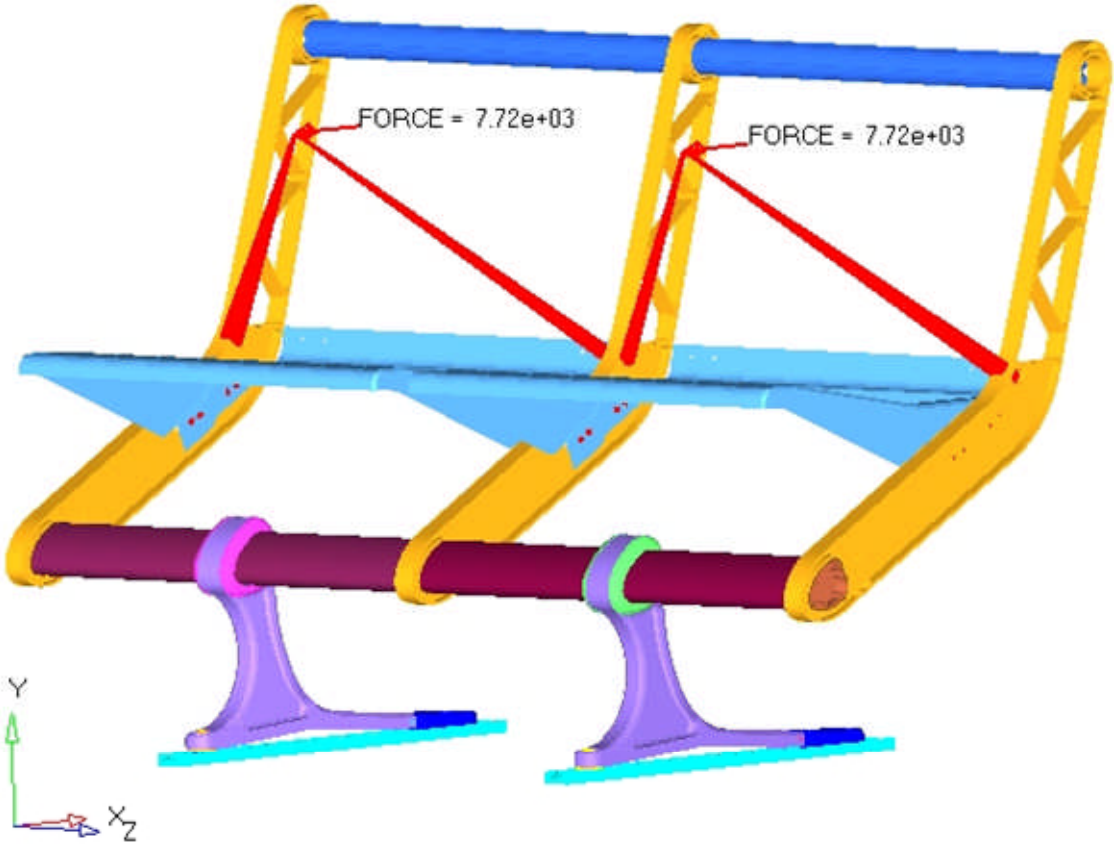

Figure 9-14 FE model of the Complete Seat Subjected to "Forward 9g"

9.6 Discussion of FEA Results of Complete Seat

Before interpretation of results, it was ensured that the FE model satisfies all the quality checks as specified in “Verification Framework” (Section 5.4). As used earlier, maximum von Mises stress criteria is used to check against yield limit of general Aluminium alloy (375 MPa) for each component. In coming sections, stress plots are given only for FWD beam and leg (Forward 9g load) and boomerang (Side 4g load), being the critical components and loads. Stress contours for all the components for each of the loadcases simulated are present in internal deliverables and have been communicated with BlueSky.

9.6.1 Von Mises stress plot for Leg (V#9 modified) – Forward 9g

As seen from Figure 9-15, maximum von Mises stress observed at the upper foot-section is 140 MPa. Therefore, present design of leg is “Safe” against “Forward 9g” loads applied as per CS 25.561.

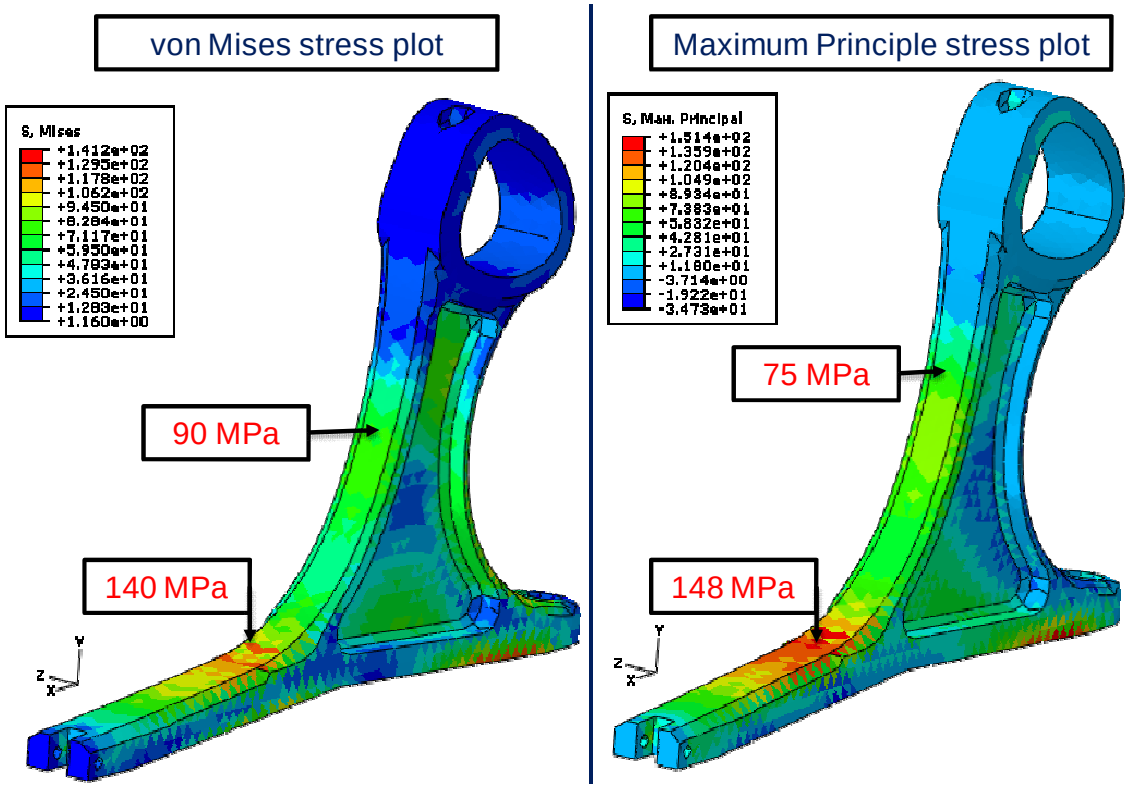

Figure 9-15 von Mises stress for Leg (V#9 modified) < Yield limit. Design is Safe for Forward 9g.

9.6.2 Von Mises stress plot for FWD beam – Forward 9g

As seen from Figure 9-16, maximum von Mises stress observed in the FWD beam near its connection with leg is 145 MPa. Therefore, present design of FWD beam is “Safe” against “Forward 9g” loads applied as per CS 25.561.

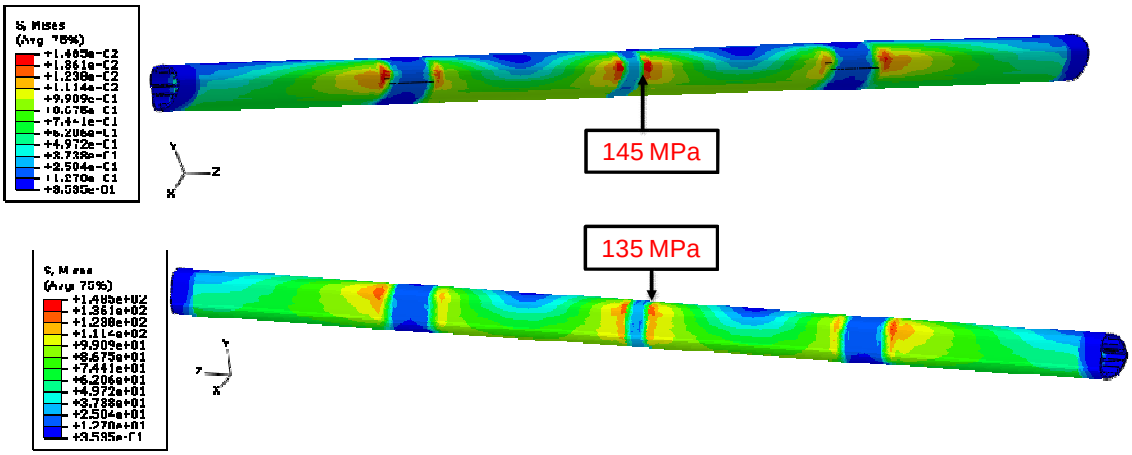

Figure 9-16 von Mises stress for FWD beam, Front and rear views. Design is Safe for Forward 9g.

9.6.3 Von Mises stress plot for boomerang – Side 4g

As seen from Figure 9-17, maximum von Mises stress observed in the boomerang near its attached with FWD beam is 420 MPa with a plastic strain of 0.2% for Side 4g load. This occurs due to abrupt change in the cross-section. In addition, a von Mises stress of 385 MPa with a plastic strain of 0.15% is observed at the side wall near seat belt attachment point (Figure 9-16). This region is subjected to out-of-plane bending due to applied Side 4g load. Therefore, present design of boomerang is “Unsafe” against “Side 4g” loads and needs design improvement.

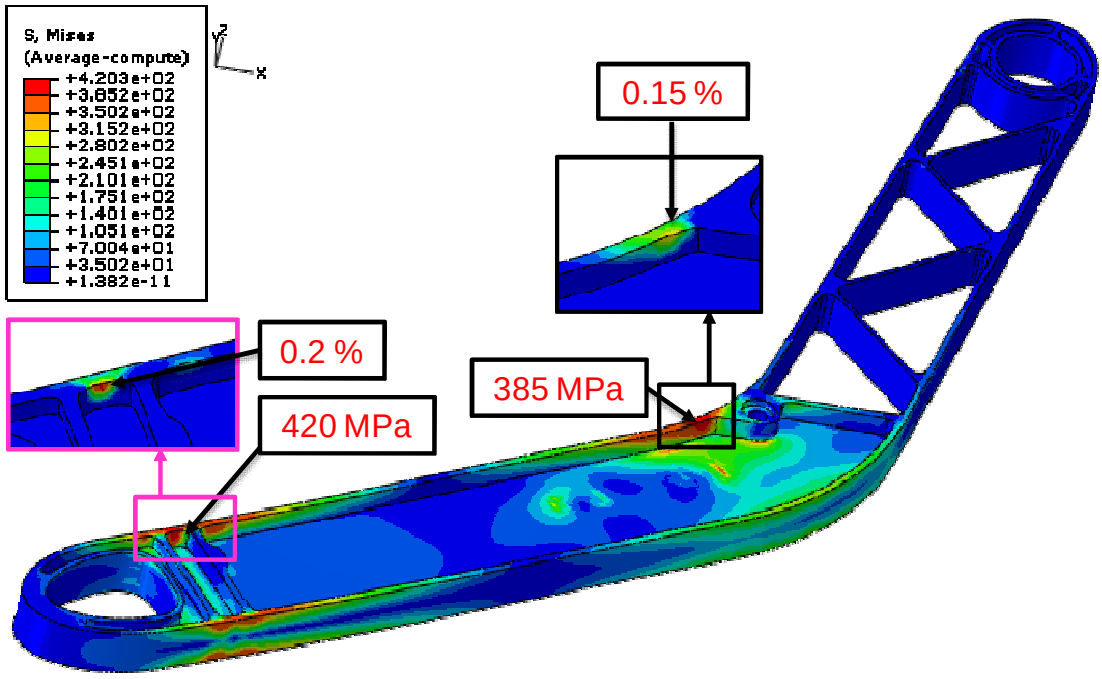

Figure 9-17 von Mises stress of 420 MPa in boomerang (Plastic strain of 0.2%). Design is Unsafe for Side 4g.

All other components except seat pan (for Downward 6g loadcase) are found to be safe for all the loads as specified in CS 25.561. A detailed description of stress contours and their interpretation is available in internal reports and has been delivered to BlueSky.

“Downward 6g” loads are uniformly distributed on the Seat pan [23]. Hence, seat pan experiences very high deformation. As a “Dummy Design” of seat pan is used for present research, stresses induced in pan due to applied “Down 6g” can not be considered and hence not produced here. “Dummy Design” means, seat pan dimensions and its attachment with connector are approximated to suit other seat dimensions. In the next phase, when the actual design of seat pan would be available, current “Dummy Design” would be replaced by actual design and “Downward 6g” loadcase would be simulated once again to estimate the stresses developed in the seat structure.

Due to non-disclosure agreement signed with BlueSky, dimensions of components involved in seat structure and their exact masses can not be given in this report.

9.6.4 Seat Interface Loads for “Forward 9g” loadcase

Maximum vertical load (F_Y) generated in the tension studs (i.e. Mushroom-headed studs) is required by Airliners [35]. Hence, for the complete seat structure (Leg V#9 with ASH) subjected to “Forward 9g” load, seat interface loads were estimated using the methodology developed in Chapter 7. Stud nomenclature used and the values of F_Y are given in Figure 9-18.

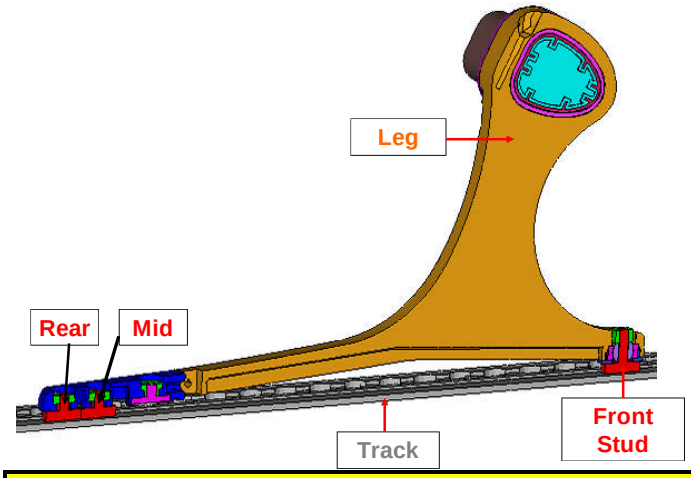

"Seat Interface Loads" in Mushroom-headed studs due to "Forward 9g" load (only Vertical component)	
Stud position	**F_Y , N**
Front	6281.88
Mid	13014.70
Rear	3007.78

Figure 9-18 "Seat Interface Loads" estimated by the non-linear FEA complete seat structure (Forward 9g)

It can be observed from Figure 9-18 that, the maximum vertical load of around 13 KN is induced in the mid stud. As “Sleep Seat” is not developed for a particular airline, limit value for F_Y is not available (at present). Since the structure and loading (Forward 9g) is symmetric, F_Y has been given only for one side.

A methodology should be developed to verify the interface loads calculated (Figure 9-18). Condition of force equilibrium (Section 5.4.1 – Computational accuracy) is achieved (details present in internal delivery).

Thus, the sixth and final requirement of the scope of present research (Section 1.3) was met in this chapter, which is “Develop a full-scale FE Model of the complete seat and demonstrate compliance for static load case”.

In next chapter, conclusion drawn from this entire project is drawn and activities that can be undertaken for further studies have been briefly discussed.

10 Conclusion

The challenge for the author in the research undertaken was, to develop a complete FE model of “Sleep Seat” involving necessary details as non-linearities and different joints. The requirement of this FE model thus developed was that it should be computationally economical and should provide the outputs such as stresses induced in each component and interface loads. Using these results, design modifications were supposed to be carried out so that the new seat design is: compatible with safety regulations, easy to manufacture and with lower weight than the present designs.

As a starting point, historical developments in this area and business potential of this research were studied (Section 2.2) and it was found that design of an aircraft seat is one of the most happening fields in today’s commercial air carries. Certification Specifications (CS); being applicable to Europe as well as to USA (with little modifications); were chosen as a guideline for safety . Considering time available for research (one year) and the requirement posed by BlueSky, it was decided to consider only static compliance (known as “9g Compliance”) i.e. loads as per CS 25.561. Further literature review was done to study crashworthiness principles to be incorporated during seat designing (Section 2.4). Generic Requirements (GR2) were chosen as a guideline for comfort of a seat (Section 2.5).

BlueSky provided initial seat design and it was found to be compatible with GR2 requirements (Section 3.1.2). Next task was to evaluate strength of this design when subjected to loads as per CS 25.561, using virtual simulation tools as prototype building and their physical testing would have resulted in huge amount of money and time.

Literature review and previous experience concluded that straightway use of simulation packages to perform non-linear FEA of complete seat is not advisable. Therefore, it was decided to focus on “Primary Load Path (FWD beam and leg), PLP” and on “Forward 9g” loadcase, being a critical for overall success of the project. Analytical model for the FWD beam was

developed(Spreadsheet), which could estimate bending stress induced in it (for Forward 9g and Downward 6g loads) with design variables such as its cross-section and thickness. As a start up in FEA, “Mesh Sensitivity Study (MSS)”, which helps to select appropriate element type and their density, was performed for FWD beam. Results obtained from, FWD beam built with, two brick elements through thickness (with aspect ratio of 3:1); were compared with those from spreadsheet and excellent co-relation was observed.

Next component in PLP is “Seat leg”. Based on MSS, tetrahedral element with a global size of four millimetres was finalised for FE modelling of leg. It was decided to adopt “Sequential Model Development Approach” to arrive at a final detailed FE model of PLP required for leg designing (Figure 5-1). In this regard, following critical areas were studied thoroughly and documented for further reference,

Ordered node numbering scheme should be used to get optimum solution time (Section 5.3).

Procedures to verify computational accuracy and co-relation with physical behaviour of FEA results; of “FWD beam and leg” for loads according to CS 25.561; was drafted. It was found that, results satisfy all the checks (Section 5.4).

FWD beam is attached to the leg with the help of two M5 bolts. Three different ways to represent this bolted joint in FEA were studied: coincident nodes at FWD beam and leg interface (Case I- preliminary model), tied contact (Case II) and actual modelling of studs and corresponding contacts (Case III). Flexibility (to absorb initial penetrations), less pre-processing time required (80% lesser than that in Case III) and acceptable results; favoured the used of “Tied contact” definition at “FWD beam and leg” interface, for all further simulations (Section 6.4).

During study of bolted joint between “FWD beam and leg”, a stepwise procedure for FE modelling of “Bolt-preload” and its integration with inertia loads

(CS 25.561); was developed and implemented (Section 6.3). This feature was not only useful for estimating the stress levels encountered in FWD beam during its assembly with leg, but it also proved to be a very power technique in preventing “Rigid body motion” in contact non-linear simulations.

Leg designing depends on its strength as well as “Seat Interface loads (SIL)”. Being innovative design, it was not possible to use a traditional procedure given in “Boeing Specifications” for calculating SIL. Hence, use of FEA for extracting SIL was inevitable. Activities such as understanding nature of contact non-linear problems, special needs of contact descritisation, assigning “master” and “slave” definitions and classification of contact pairs in suitable groups for evaluating SIL were accomplished through pilot studies, and a systematic approach for SIL using FEA was developed (Chapter 7). With this study, an “Intermediate” FE model of PLP was completed.

In the design phase, an elliptical cross-section with two millimetres thickness was chosen for FWD beam using spreadsheet (Section 8.1). Von Mises stress levels induced in the FWD beam due to “Forward 9g” loads showed that its design should be improved for strength. An economical solution for this was achieved through the design of local reinforcing inserts, which reduced the potential high cost of manufacturing, handling and Quality control of FWD beam with increased thickness (Section 8.2).

Leg variants V#1 to V#8, were based on principle of “direct attachment of seat structure with the seat track” and were analysed for “Forward 9g” using intermediate FE model of PLP. However, “Boeing Specification”, which were received in the second phase of present research (after seven months from initial start in February 2010), stressed that leg should not be directly attached to the track (to avoid excessive damage of the seat structure during seat pre-deformation). Therefore, a separate block called, “Aft Stud Housing” was involved (in modified leg V#9), which was connected with track through mushroom-headed studs and a shear pin and with the leg through a single pivot pin (ensuring free relative movement – pitch and roll, between track and rest of the seat structure, thereby avoiding secondary loading of leg). All these minute

details were incorporated in intermediate FE model of PLP. In addition, this model was updated for material and geometric non-linearity. Thus a detailed FE model of PLP(comprising of FWD beam, inserts, leg, seat track, mushroom-headed studs, shear pin, leg clamps and swivel bearing), which could give outputs such as stress and interface loads when subjected to loads as specified in CS 25.561 (converted in local co-ordinate system of FWD beam using spreadsheet) was accomplished. Results of “Forward 9g” loadcase showed that the new leg design is “Unsafe” against applied “Forward 9g” loads (Section 8.5).

It was decided to make use of “Free-Shape Optimisation (FSO)” package built-in Optistruct, to arrive at a final design of leg. A methodology of optimisation; considering manufacturing constraints, strength requirements for all the static loads (CS 25.561), and functional needs; was developed and successfully utilised in leg designing (Section 9.4). Using “OSSmooth” design modifications suggested by FSO were incorporated in Leg V#9.

A non-linear FEA of complete seat structure (PLP, Boomerang, Seat pan and backrest tube) with new leg design (suggested by FSO), showed that the seat structure is “Safe” against the critical loads (Forward 9g, Side 4g and Downward 6g) as specified in CS 25.561, except the boomerang when subjected to “Side 4g” loads. Since, approximate design of seat pan was used, high von Mises stress observed in it for “Downward 6g” load were ignored.

Therefore, all the milestones defined in the “Objective and Scope of Research undertaken” (Section 1.3) were achieved and project was concluded at this stage.

In Summary, methodologies for following features in FEA were developed using pilot studies and were successfully used during the design of “Sleep Seat”, which is a “Real time” project.

- FE modelling strategy for individual components of “Sleep seat”, through “Mesh Sensitivity Study”,
- Framework to critically assess the FEA results,

- Solutions to deal with “Rigid Body Motion” and “Initial Penetration”, which hamper the progress of the simulation,
- Modelling of “Bolt Pre-load” using Abaqus / Standard,
- Extraction of “Seat Interface loads”,
- To obtain the converged solution for the complete seat subjected to static loads (CS 25.561) including all types of non-linearities i.e. contact, material and geometry; using Abaqus / Standard.
- Use of Free-Shape Optimisation software to arrive at a final design (e.g. critical component like leg) considering manufacturing, design, functional and aesthetic aspects.

10.1 Future Scope

Prototyping of the seat structure (at least PLP) should be done (based on designs suggested through outcome of current research) and physical testing should be performed for the loads as per CS 25.561. A comparative study, between the results obtained by experimental testing and those by FEA of present research, would yield the “Closeness” between two; indicating improvements required in FE models or in boundary conditions. This would be a major topic; successful co-relation between FEA and reality will increase confidence in FEA thereby avoiding the need of any future testing.

Present FE model of complete seat can be improved by replacing “MPC elements with release” by actual “Connector elements” to account for the forces transferred across the joints e.g. between Seat leg and Aft stud housing

Contact pairs modelled in this research include a default coefficient of friction of 2%. Influence of change in the value of coefficient of friction on FEA results of corresponding components can be studied.

In present FEA, MPC elements have been used for load application. Improvement can be made by incorporating a anthropometric dummy or the body blocks, seat belts and a detailed attachment between two.

Current design of leg weighs 1.02kg. Topology optimisation can be used to bring down its weight without sacrificing strength.

Present design of boomerang can not sustain “Side 4g” loads. Its design can be improved at the seat belt attachment point and at front end (near FWD beam – Figure 10-1). Boomerang can be modelled using shell-solid combination (Figure 10-1), which will reduce input file size and solution time. It is a typical combination of solid, bulk portion in area where it is supposed to be assembled with FWD beam (solid elements) and thin portion in the upper part where it is not subjected to carry any major load(shell elements). An experimental study focussing on stress and strain at the interface of shell-solid can be undertaken.

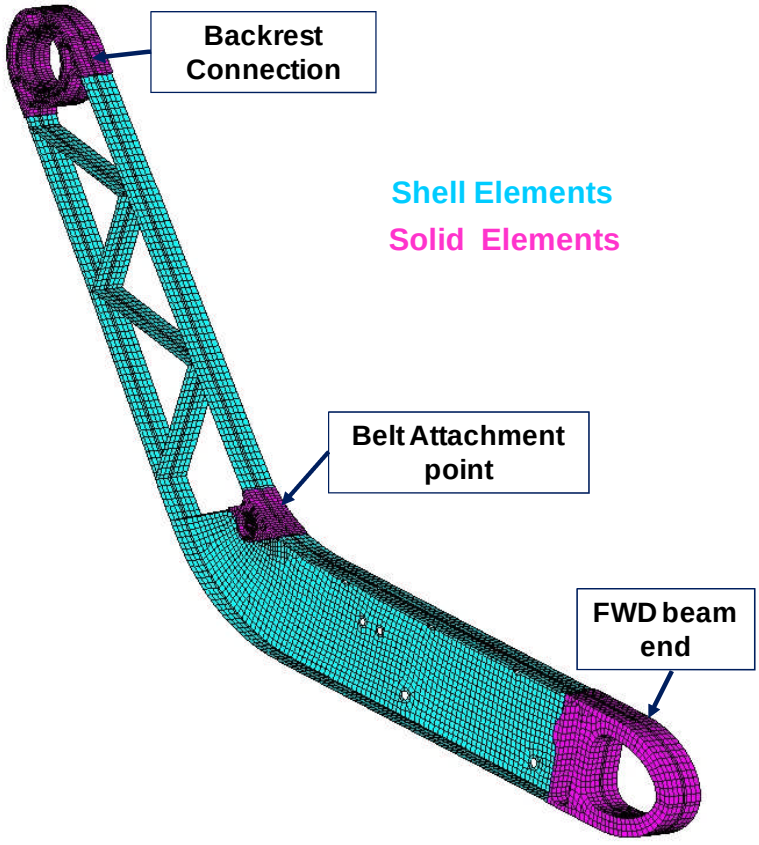

Figure 10-1 Proposed FE model of Boomerang (Shell-Solid Combination)

Tentative design of “Seat Pan” was used to build the complete seat structure. A project can be undertaken to design “Seat Pan” that sustains the “Downward 6g” loads.

Use of different grades of Aluminium or advanced materials like composite panels, stretched fabric (for seat pan) can be studied in order to further bring down the weight or manufacturing costs.

A methodology to verify the “Seat Interface loads” calculated by FEA can be developed.

Author of this report thinks that, present FE model of complete seat can be tuned (without enormous efforts) to perform seat pre-deformation; a state of seat structure before application of dynamic loads CS 25.562. In the second phase of the project, a FEA methodology can be developed to perform non-linear dynamic analysis of complete seat subjected to dynamic loads as per CS 25.562.

REFERENCES

1. Andy Shankland, VP Marketing Airbus (20 May 2010.) '*Developing the Airbus A380 and A350XWB',* RAeS/CCAAA Handley Page lecture.
2. Flight International Magazine 4-10 May 2010
3. "European Vehicle Passive Safety Network 2" Report Task 5.6 on Aircraft Safety released on 25 February 2004.
4. Flight Global Magazine, Air transport Intelligence News 10th February 2010, an Article by Ghim-Lay Yeo http://www.flightglobal.com/articles/2010/02/10/338228/thais-new-a330s-delayed-due-to-seat-problems.html
5. Roy Turvaville, Certification & Structures Engineer, '*MSc Software Success Stories for B/E Aerospace'* http://www.mscsoftware.com/success/details.cfm?Q=286&sid=278(a)
6. Robinson D, "BlueSky Designers Ltd." 57, Surrey Technology Centre, "Surrey Research Park", GuildfordGU27YG. http://www.blueskydesigners.com/
7. A&D Supplier Innovation Challenge, November 2-3, 2010, Phoenix AZ , http://www.aviationweek.com/events/current/sic/
8. 'Definition of Aircraft', http://en.wikipedia.org/wiki/Aircraft
9. 'Types of fixed-wing aircrafts' http://en.wikipedia.org/wiki/Aircraft#Fixed-wing
10. EASA , Annual Safety Review 2006, http://www.easa.europa.eu/ws_prod/g/doc/COMMS/Annual%20Safety%20Review%202006.pdf
11. EASA , Annual Safety Review 2007 , report ISSN 1831-1636 http://www.easa.eu.int/ws_prod/g/doc/COMMS/Annual%20Safety%20Review%202007_EN.pdf
12. National Transportation Safety Board, Annual Review OF Aircraft Accident Data U.S. General Aviation, Calendar Year 2005 NTSB/ARG-09/01 http://www.ntsb.gov/publictn/2009/ARG0901.pdf
13. Barth T (2009) '*AIRCRAFT CRASH SURVIVABILITY FROM VISCOUS INJURY IN VERTICAL IMPACTS'* , PhD thesis, SAS – Cranfield University

https://dspace.lib.cranfield.ac.uk/bitstream/1826/4002/1/T_Barth_Thesis_2009.pdf

14. 'European Aviation Safety Agency Homepage' http://www.easa.europa.eu/home.php
15. Olschinka C, Schumacher A (UIM 2006) *'Dynamic Simulation of Flight Passenger Seats',* LS-Dyna Anwenderforum, Hamburg University of Applied Sciences. http://www.dynamore.de/documents/papers/forum2006/passive-safety/dynamic-simulation-of-flight-passenger-seats
16. European Aviation Safety Agency, Certification Specifications (CS) for Large Aeroplanes CS25; Amendment 8, 18 December 2009. http://www.easa.eu.int/agency-measures/docs/certification-specifications/CS-25%20Amendment%209.pdf
17. FAA, '*A Summary of Crashworthiness Information of Small Airplanes',*Report- No. FS-70-592-120A http://www.dtic.mil/cgi-bin/GetTRDoc?Location=U2&doc=GetTRDoc.pdf&AD=AD0756811
18. Federal Aviation Administration, Technical Report ADS – 24 , Sept. 1964
19. Civil Aviation Authority, CAP (Civil Aviation Publications). CAP 747, Section 2 Part 3 GR number 2. http://www.caa.co.uk/docs/33/CAP747.pdf
20. Hirlam M (April 2002) '*Human Factors Case Study AIRCRAFT SEATS',* University of Sheffield Department of Mechanical Engineering.
21. Brown J and Hughes K (January 2010), "SleepSeat_PRELIM_BEAM_ANALYSIS_UPDATEDLOADS.xls", Crashworthiness, Impact and Structural Mechanics Group, Cranfield University, UK.
22. Brown J and Hughes K (18th December 2009) '*SLEEPSEAT Analysis PROGRESS REPORT'*.
23. TSO-C39a, AIRCRAFT SEATS AND BERTHS (24 February 1972), Department of Transportation, Federal Aviation Administration Aircraft Certification Service Washington, DC http://rgl.faa.gov/Regulatory_and_Guidance_Library/rgtso.nsf/0/0FAEF96A8A3C339C86256E8C005C62A6?OpenDocument

24. Altair Hyperworks 10.0 Documentation , http://www.altairhyperworks.com/ClientCenterHWLoginForm.aspx?from_page=ClientCenterHWTutorialDownload.aspx
25. 'Altair Hyperworks 10.0 Documentation , Section – Aero-space Modelling' www.altairhyperworks.com/html/en-us/rl/ivws_aero_modelling.aspx
26. mechanical engineering , the magazine of ASME vol. 132/no.5 may 2010
27. Cook, Malkus, Plesha, Witt (Fourth Edition) Concepts and applications of Finite Element Analysis, John Wiley and Sons Publication. ISBN 9814-12-683-7
28. P. Seshu (August 2010) Textbook of Finite Element Analysis, Eighth Printing, ISBN 978-81-203-2315-5
29. Abaqus 6.9 Online Documentation , http://abaqus.civil.uwa.edu.au:2080/v6.9/books/usb/default.htm
30. Ansys Inc. Theory Reference (Release 9.0) November 2004 http://www1.ansys.com/customer/content/documentation/90/ansys/a_thry90.pdf
31. Abaqus 10.0 Online Documentation , http://www.simulia.com/solutions/automotive_crashworthiness.html
32. A report on 'Why Bolt Preload is Important' by Bolt Science Limited, Victoria House, 16 Rotherwick Avenue Chorley, Lancashire, UK PR7 2PY http://www.boltscience.com/pages/basics2.htm
33. Shigley, Mischke, Standard Handbook of Machine Design, McGraw-Hill Publication, Second Edition, ISBN 0-07-056958-4
34. A. Van Beek, '*Advanced engineering design -Lifetime performance and reliability'* ISBN-10: 90-810406-1-8 http://www.tribology-abc.com/calculators/e3_6a.htm
35. Boeing Specifications (1993) '*D6 36238 Passenger Seat Structural Design and Interface Criteria Rev C'*
36. A report on 'Nonlinear Contact Analysis Techniques Using ANSYS' by Mechanics Development Group Ansys http://ansys.net/ansys/papers/nonlinear/contact_tech.pdf
37. Wu Li (2007), Automatic Conversion of Conceptual Geometry to CFD Geometry for Aircraft Design.

http://ntrs.nasa.gov/archive/nasa/casi.ntrs.nasa.gov/20070032918_20070033081.pdf

38. Bhonge P(December 2008) ‘ A methodology for aircraft seat certification by dynamic finite element analysis’ PhD thesis, Wichita State University

APPENDICES

Appendix A Certification Specifications

EASA (European Aviation Safety Agency) is an agency of EU (European Union) which looks after the safety analysis and research of civil aviation [14]. EASA owns the responsibility for airworthiness certification of all aeronautical products and parts developed and used under the EU member States [14]. Amendment 8, published on December 18th, 2009 (Annex to ED Decision 2009/01/R) gives the CS (Certification Specifications) for Large Aeroplanes (CS-25). CS 25.561 and CS25.562 from “Subpart C–Structures”; provides the structural requirements of a seat under emergency landing conditions [16]. Please note CS 25.561 and CS 25.562 reproduced from Amendment 8 (Annex to ED Decision 2009/01/R) as it.

A.1 CS 25.561 - General Emergency Landing Conditions [16]

a) The aeroplane, although it may be damaged emergency landing conditions on land or water, must be designed as prescribed in this paragraph to protect each occupant under those conditions [16].

b) The structure must be designed to give each occupant every reasonable chance of escaping serious injury in a minor crash landing when — proper use is made of seats, belts, and all other safety design provisions [16].

g – Acceleration due to gravity,
Loads have to be applied separately and not as a combination of loads.

CS25.561 General, clause B	Direction of loading	Ultimate Inertia forces, in terms of g	Safety requirement
3.i	Upward	3.0	Seats and items of mass (and their supporting structure) must not deform under any loads up to those specified in any manner that would impede subsequent rapid evacuation of occupants [5].
3.ii	Forward	9.0	
3.iii	Sideward , on the seats and their attachments	4.0	
3.iv	Downward,	6.0	
3.v	Rearward	1.5	

Figure 10-2 CS 25.561 General Requirements (Static) [16]

A.2 CS 25.562 Emergency Landing (Dynamic) [16]

a) Each seat type design approved for passenger occupancy must successfully complete dynamic tests or be demonstrated by rational analysis based on dynamic tests of a similar type seat, in accordance with each of the following emergency landing conditions [16].

b) Dummy to be used: a 170-pound (77.11 kg) anthropomorphic, test dummy sitting in the normal upright position.

Case description	Position	Requirement
Clause Number : 25.562 b(1) A change in downward vertical velocity, (Δv) of not less than 35 feet per second (10.7 m/s).	Aeroplane's longitudinal axis canted downward 30 degrees with respect to the horizontal plane and with the wings level [5].	Peak floor deceleration must occur in not more than 0.08 seconds after impact and must reach a Minimum of 14g.
Clause Number : 25.562 b(2) A change in forward longitudinal velocity (Δv) of not less than 44 feet per second (13.4 m/s).	I). Aeroplane's longitudinal axis horizontal and yawed 10 degrees either right or left, whichever would cause the greatest likelihood of the upper torso restraint system (where installed) moving off the occupant's shoulder, and with the wings level [5]. ii). Where floor rails or floor fittings are used to attach the seating devices to the test fixture, the rails or fittings must be misaligned with respect to the adjacent set of rails or fittings by at least 10 degrees vertically (i.e. out of parallel) with one rolled 10 degrees [5].	Peak floor deceleration must occur in not more than 0.09 seconds after impact and must reach a minimum of 16g.

Figure 10-3 CS 25.562 General Requirements (Dynamic) [16]

A.3 Common requirements for CS 25.562 tests [16]

I. Where upper torso straps are used, tension loads in individual straps must not exceed 1750 pounds (794 kg). If dual straps are used for restraining the upper torso, the total strap tension loads must not exceed 2000 pounds (907 kg).

II. The maximum compressive load measured between the pelvis and the lumbar column of the anthropomorphic dummy must not exceed 1500 pounds (680 kg).

III. The upper torso restraint straps (where installed) must remain on the occupant's shoulder during the impact.

IV. The lap safety belt must remain on the occupant's pelvis during the impact.

Each occupant must be protected from serious head injury. Where head contact with seats or other structure can occur, protection must be provided so that the head impact does not exceed a Head Injury Criterion (HIC) of 1000 units [5]. The level of HIC is defined by the equation

$$\mathbf{HIC} = \left\{ (t_2 - t_1) \left[\frac{1}{(t_2 - t_1)} \int_{t_1}^{t_2} a(t)dt \right]^{2.5} \right\}_{max}$$

Where —

t 1 is the initial integration time,

t 2 is the final integration time, and a(t) is the total acceleration vs. time curve for the head strike, and where (t) is in seconds, and (a) is in units of gravity (g).

V. Where leg injuries may result from contact with seats or other structure, protection must be provided to prevent axially compressive loads exceeding 2250 pounds (1021 kg) in each femur.

VI. The seat must remain attached at all points of attachment, although the structure may have yield.

VII. Seats must not yield under the tests specified to the extent they would impede rapid evacuation of the airplane occupants.

Appendix B Sleep seat satisfies GR2

Dimension B –

B_A ➡ At Arm Rest Level

B_C ➡ At Seat Cushion Level

All dimensions are in inch.

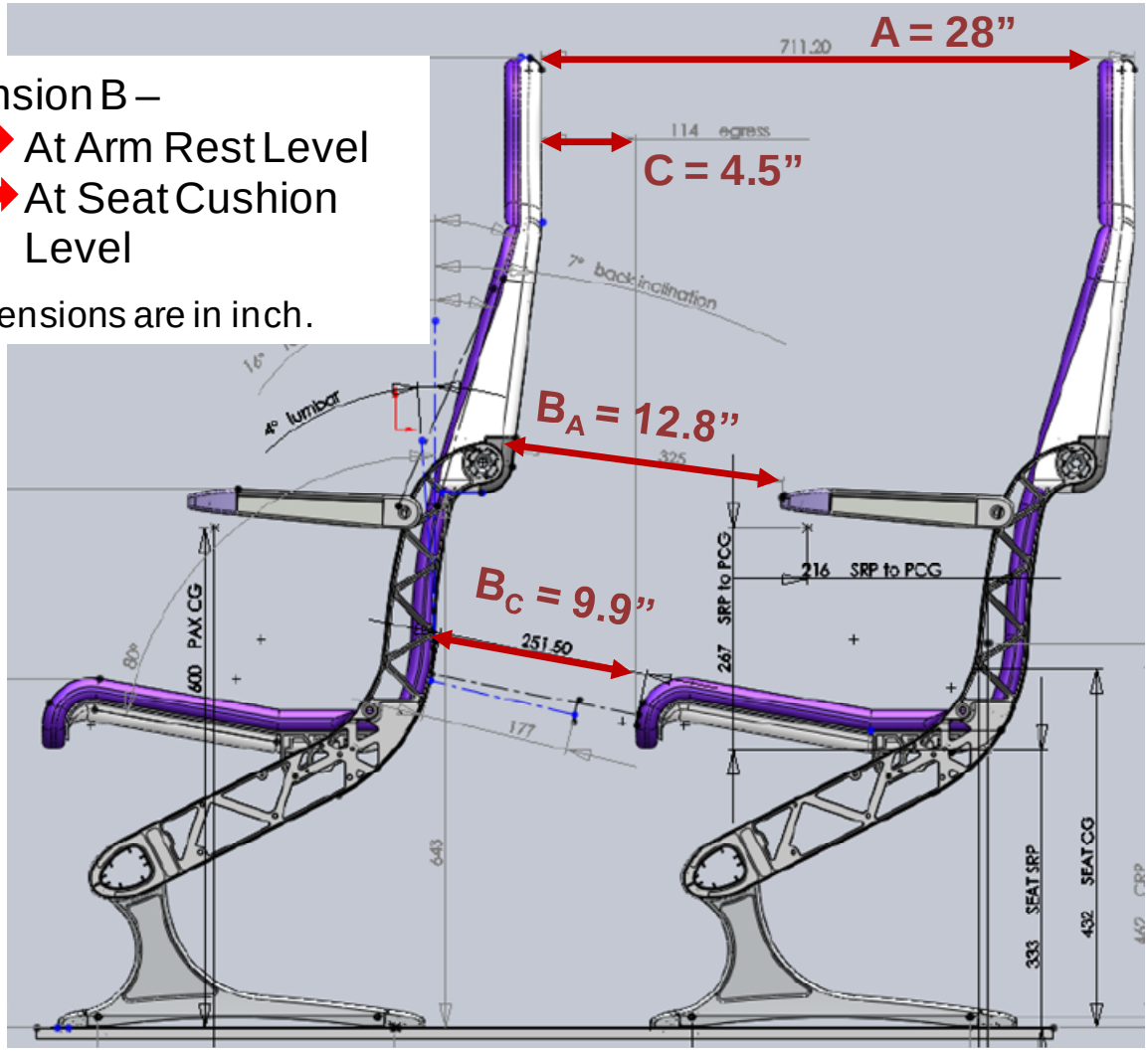

Figure 10-4 Sleep Seat satisfies Dimensions A, B and C (GR2)

Appendix C Analytical calculations for FWD beam

Simplified Free Body Diagram (FBD) of primary load path (considering

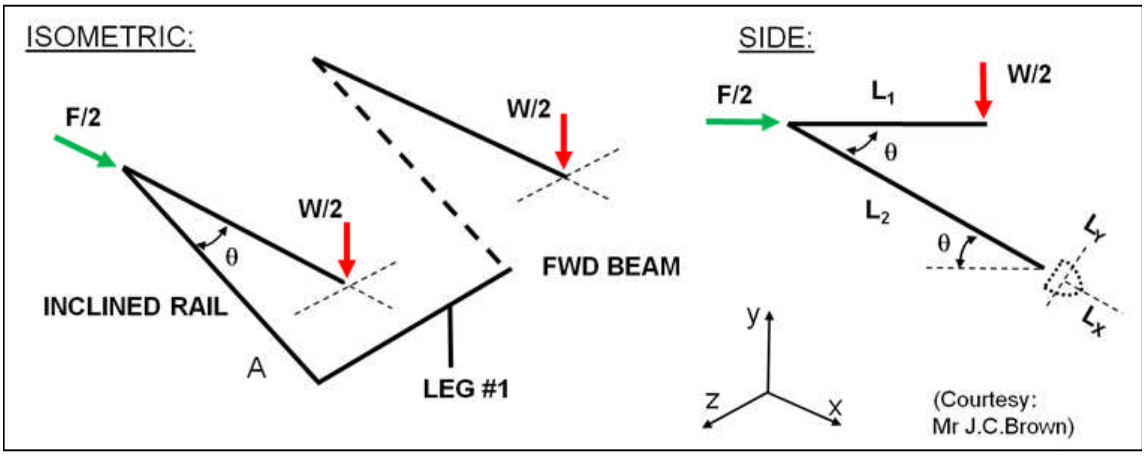

symmetry),

Figure 10-5 Simplified FBD for beam and leg assembly, Courtesy- CISM, Cranfield

C.1 Bending Moment Calculations for FWD beam

Considering the side view and solving for force and moment equilibrium,

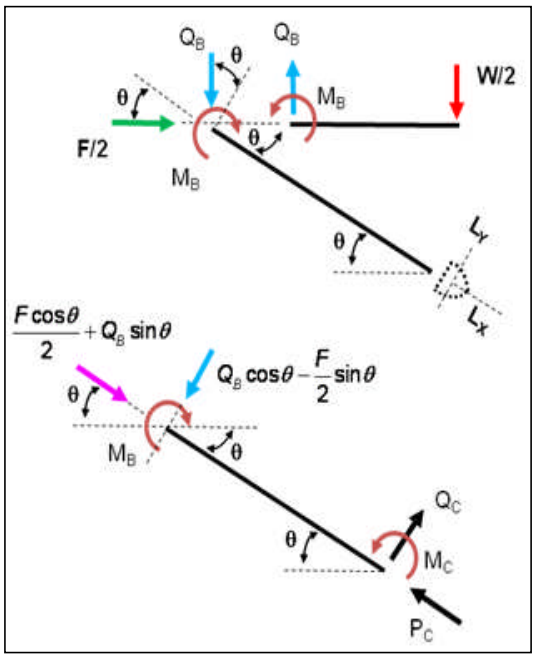

Figure 10-6 Side View and FBD of members, Courtesy- CISM, Cranfield

Resolving the applied force components the active Forces/Moments in Member AB can be calculated as,

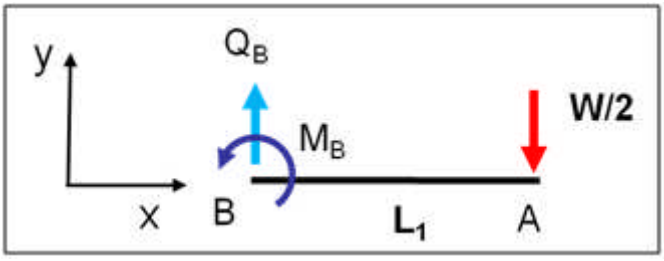

Figure 10-7 FBD of Member AB

For Member AB to be in static equilibrium it should satisfy following conditions,

All the forces acting on the member must balance each other i.e. ∑ F = 0.

All the moments acting on the member must balance each other i.e. ∑M = 0

By applying force and moment equilibrium conditions for member AB,

Qb = (W/2) and Mb = (W*L1)/2

Solution for active Forces/Moments in Side beam Member BC (Figure 10-8),

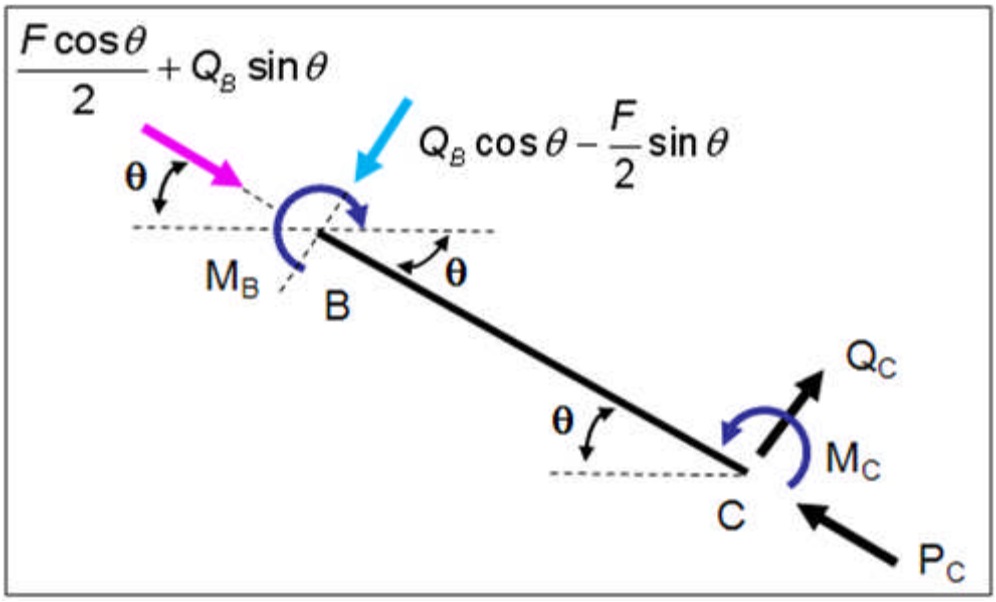

Figure 10-8 FBD of Member BC

Applying force equilibrium condition,

∑ Fx (along BC axis) = 0.

Therefore, ((F*cosΘ)/2) + (Qb *sinΘ) – Pc = 0

∑ Fy (normal BC axis) = 0.

Therefore, ((F*sin Θ)/2)-(Qb *cos Θ) + QC = 0

Applying moment equilibrium condition,

Mb – Mc + ((F*sin Θ)/2)-(Qb *cos Θ) = 0.

Hence, we get,

Pc = ((F*cosΘ)/2) + ((W*sinΘ)/2)

Qc = ((W*cosΘ)/2) - ((F*sinΘ)/2)

Mc = (W*L1)/2 – L2 * ((W*cosΘ)/2) - ((F*sinΘ)/2)

Hence, FBD for FWD beam can be given as shown in Figure 10-9,

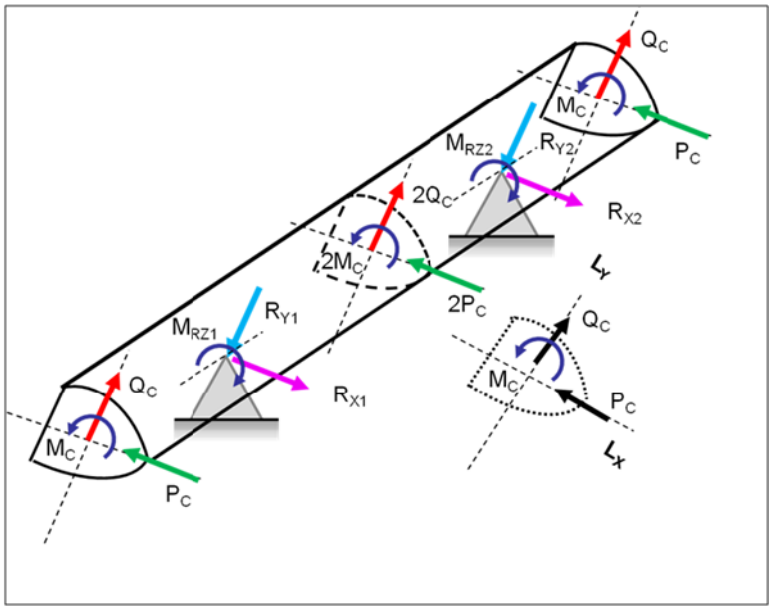

Figure 10-9 FWD beam–Complete FBD (Reaction forces / moments resolved in local axes of cross-section)

Once the FBD for FWD beam is available, next task is to determine the SF and BM distribution along the beam. In order to monitor the SF and BM in detail, beam has been subdivided in four sections (Figure 10-10).

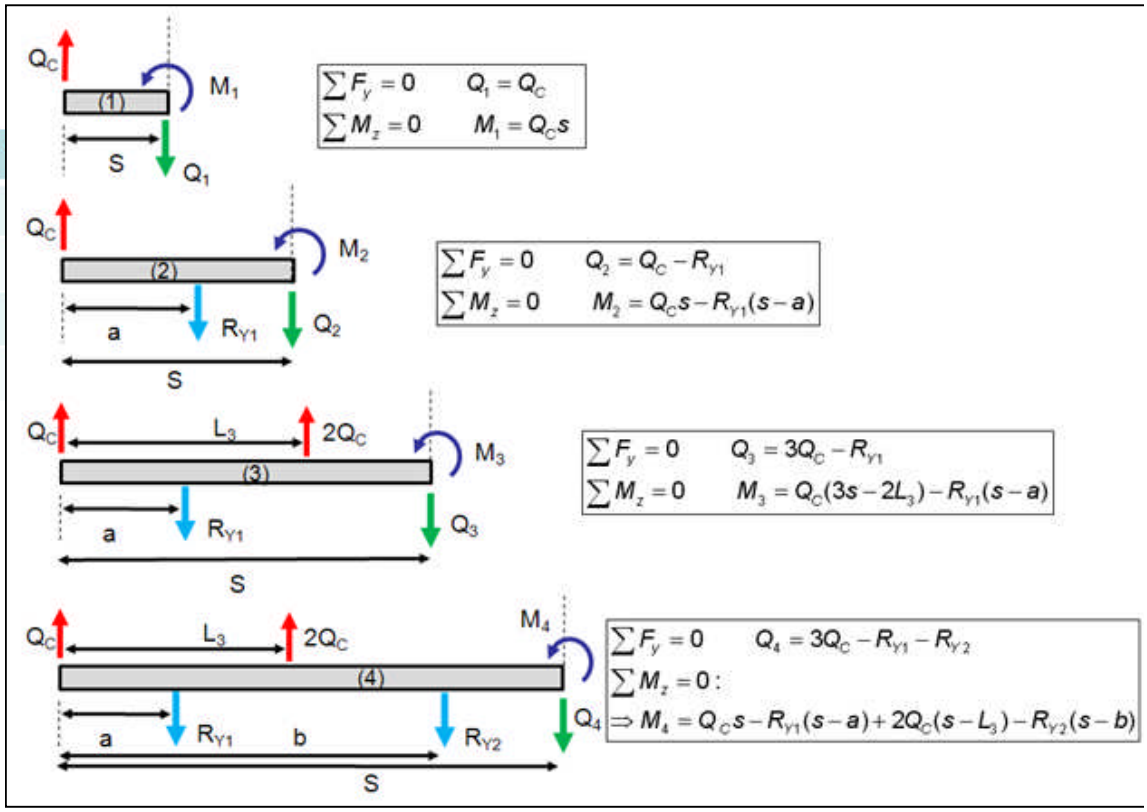

Figure 10-10 SF and BM diagram for FWD beam in YZ plane

Summary of shear force and bending moments acting at each section can be given as,

Member	Shear Force	Bending Moment
1	Q_C	$Q_C s$
2	$Q_C - R_{Y1}$	$(Q_C - R_{Y1})s - R_{Y1}a$
3	$3Q_C - R_{Y1}$	$(3Q_C - R_{Y1})s - (2Q_C L_3 - R_{Y1}a)$
4	$3Q_C - R_{Y1} - R_{Y2}$	$(3Q_C - R_{Y1} - R_{Y2})s - (2Q_C L_3 - R_{Y1}a - R_{Y2}b)$

Figure 10-11 Summary SF and BM (bending about X axis)

For Side beam (2) i.e. bending about y-axis (reactions) i.e. Forces in XZ plane. Loads in this plane have a similar geometry to YZ plane. Hence by doing same equilibrium calculations as above we get,

Member	Shear Force	Bending Moment
1	P_C	$P_C s$
2	$P_C - R_{X1}$	$(P_C - R_{X1})s - R_{X1}a$
3	$3P_C - R_{X1}$	$(3P_C - R_{X1})s - (2P_C L_3 - R_{X1}a)$
4	$3P_C - R_{X1} - R_{X2}$	$(3P_C - R_{X1} - R_{X2})s - (2P_C L_3 - R_{X1}a - R_{X2}b)$

Figure 10-12 Summary SF and BM (bending about Y axis)

After estimating the Shear force and Bending moments in each of the members, spreadsheet was extended to identify the normal stresses in the FWD Beam, that result from in-plane Bending loads, MX and MY around Local beam Axes.

Snapshot of Spreadsheet (Figure 10-13)

- Items in YELLOW – USER Changeable Parameters
  - Calculates FWD Beam loads and Reactions loads at Supports

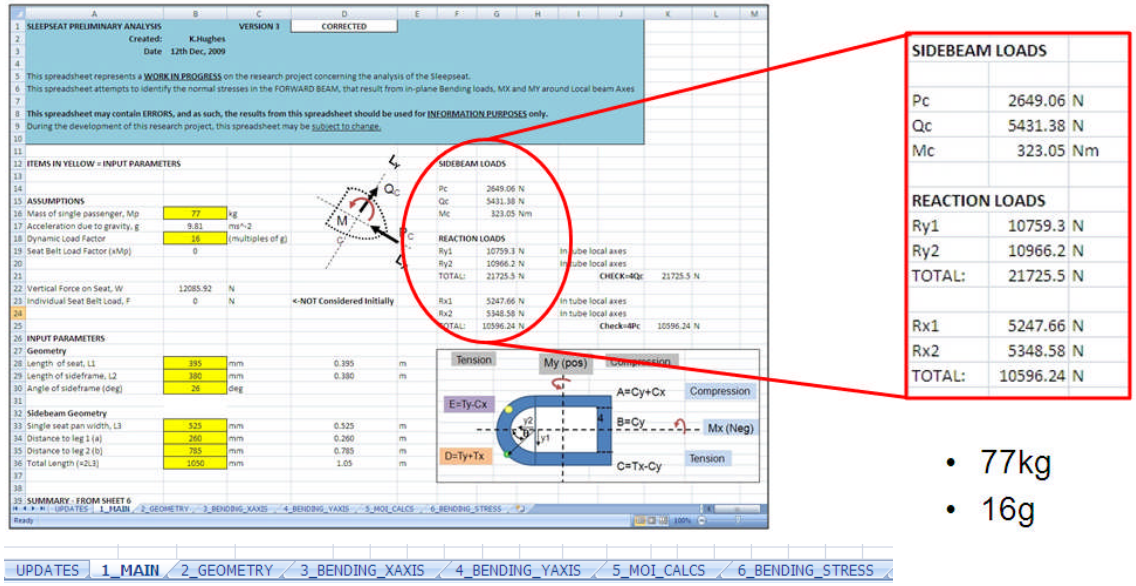

- 77kg
- 16g

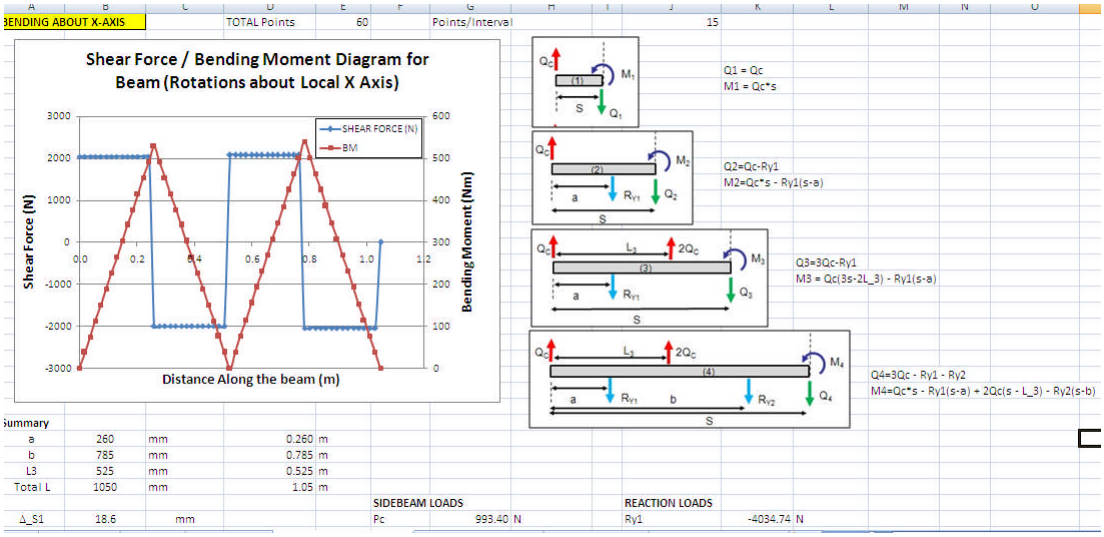

Figure 10-13 Snapshots of the Spreadsheet developed (Courtesy – CISM, Cranfield [21]

Appendix D Effect of Non-ordered node numbering scheme on Solution time of Non-Linear FEA

Effect of Node numbering on Non-Linear Static Analysis (all other conditions same)			
Serial Number	**Parameter**	**Ordered Numbering**	**Non-ordered Numbering**
1	Solution time, (Hour.Minute)	16.10	17.42
2	Memory (RAM) , MB	3307	3609
3	Disc space for Scratch files,GB	12	12.3
Leg V#9, Forward 9g Load. **Nodes = 354862, Elements = 285679 4 Processors**	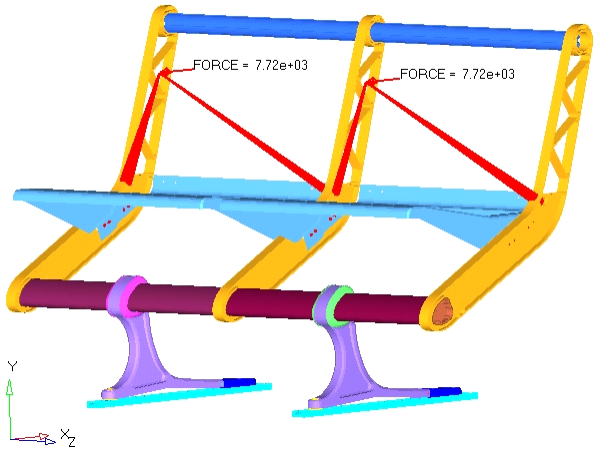		

Figure 10-14 Increase in the solution time and disc space due to non-ordered node numbering for non-linear FEA of complete seat – Forward 9g

Solution algorithm used – Abaqus 6.9.3.

It can be seen that, when the node-numbering scheme is not in order, solution time increases by about 10%.

Appendix E Comparison of FE Solvers

Parameter	Optistruct	Ansys	Abaqus
Compatibility with Hypermesh / HyperView	Best	Good	Good
Special Elements	Standard element library	Standard element library	Incompatible mode elements, Modified second order elements
Suitability for linear static analysis	Good	Good	Good
Suitability for non - linear static analysis	Under development stage	Good	Best
Tools to handle non – convergence issues	Under development stage	Standard	Automatic Stabilisation, Contact diagnostic tool
Model size (based upon type of license available)	No limitation	Elements < 32k	No limitation
Decision	Selected for linear static analysis for quick estimations	Dropped due to limited model size handling capability	Selected for non – linear structural analysis

Table 10-1 Comparison of FE Solvers [24], [29], [30]

Appendix F Bolt Preload Calculator

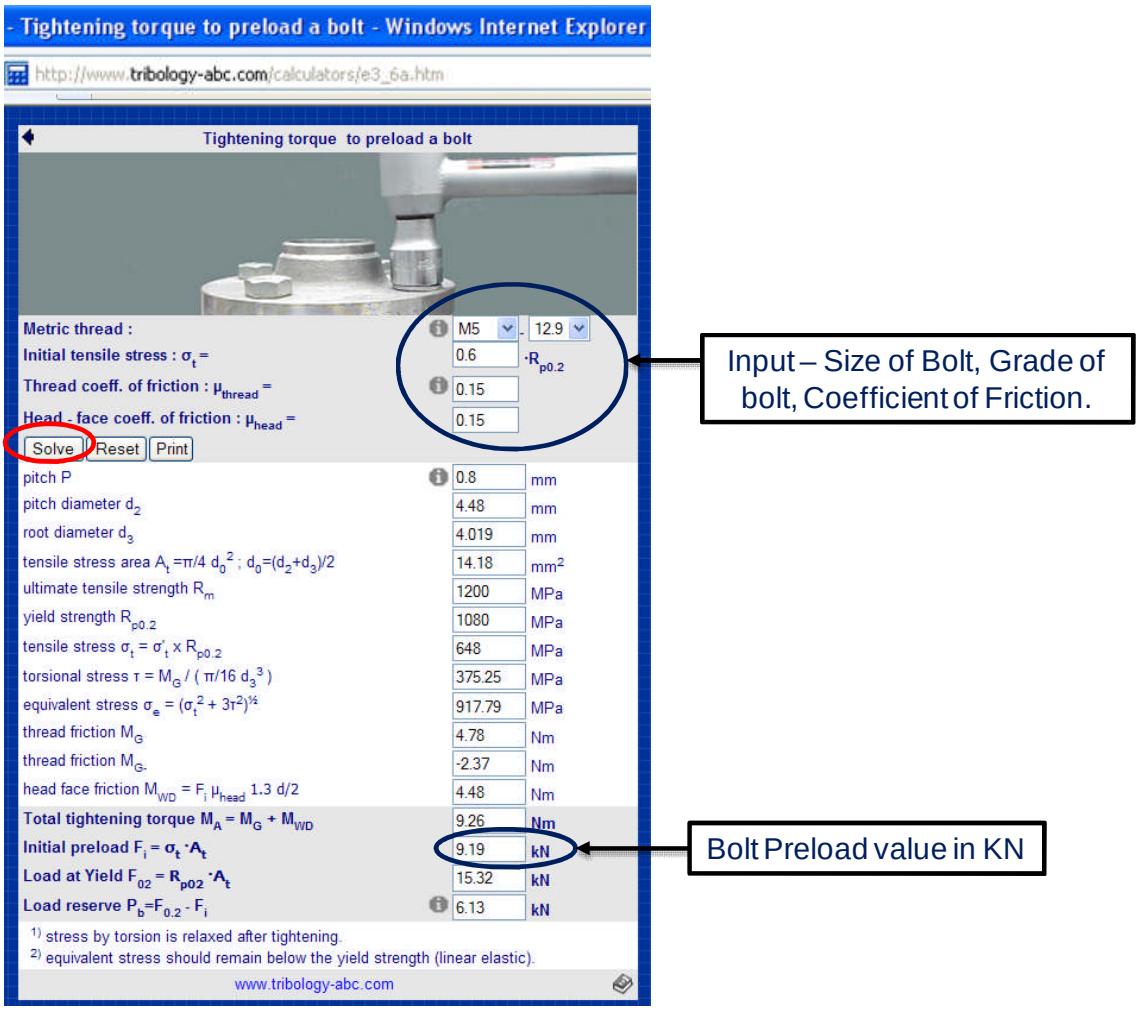

Figure 10-15 Bolt Preload Calculator used

Reference -http://www.tribology-abc.com/calculators/e3_6a.htm [34]

Inputs required for this calculator are: Size of the bolt, Grade of the bolt and Coefficient of Friction.

Upon hitting “Solve” button, a range of outputs such as pitch, tensile stress area, initial tightening torque and initial pre-load is obtained.

Figure 10-15 shows, for a M5, 12.9 stud to be used in FWD beam a initial pre-load of 9 KN is obtained, which is used in present thesis.

Appendix G Why FEA was used to extract Seat Interface Loads

"Boeing Specifications" provided a conventional procedure for interface load calculations (called as "Standard Analysis Method - SAM"), which is based on "linear continuous beam and fastener" type load distribution method [35]. However, there were limitations in applying this procedure for Sleep seat. The problems are as listed below,

G.1 Unconventional Seat design

Conventional design consists of a separate front and aft leg as shown in Figure 10-16. Hence, it is possible to use SAM to estimate seat-track interface loads. However, Sleep seat has only one leg that incorporates all studs and shear pin (Figure 10-16).

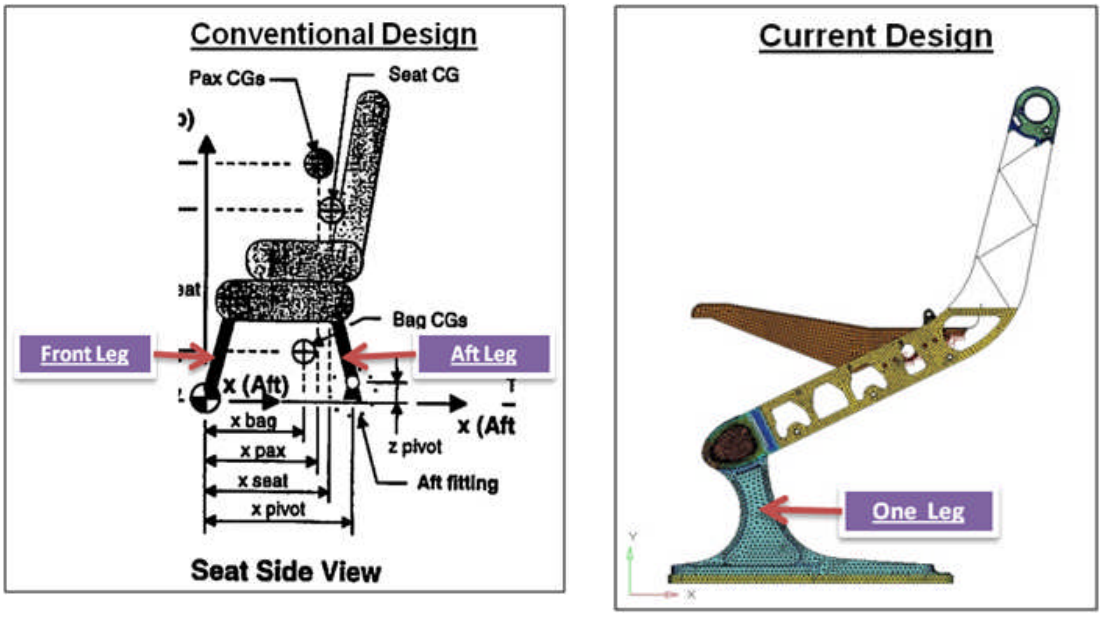

Figure 10-16 Un-conventional Design of the Sleep Seat

It has been observed from previous (i.e. with different leg variants) FEA results that "FWD beam and leg assembly" subjected to" Forward 9g" results in; leg rotating about front lower throat (REGION A - Figure 10-17) causing the fore

part of the leg to separate from the seat track (i.e. lift upwards), pivoting at “REGION A”. Therefore, instead of front stud; interface between bottom of leg and crown (top surface) of track will offer a reaction in vertically upward direction. This will form a reacting couple, together with the vertically downward force in the mid stud (Figure 10-18). This type of arrangement has not been considered in the SAM, supporting the recommendation to use FEA to calculate interface loads.

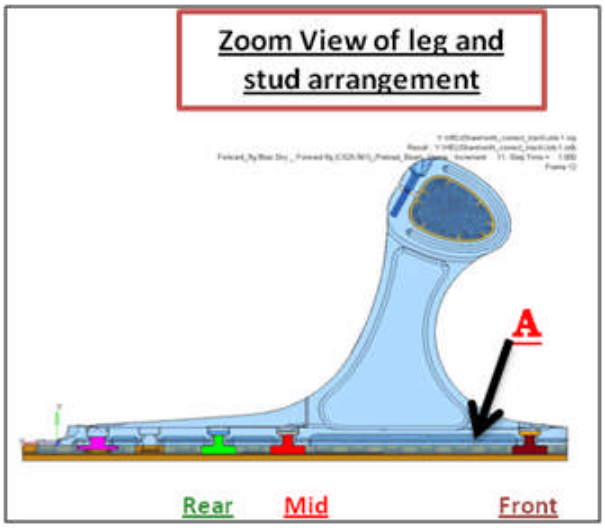

Figure 10-17 Stud arrangement in the leg of "Sleep Seat"

With reference to Section 5.0 “Seat Interface Loads – Standard Analysis Method” from document “Aircraft manufacturer Seat data REV C D6-36238” paragraph 2 [35], “Cases of unusual seat geometry or features, may require special treatment such as finite element analysis (FEA)”.

G.2 Reduction in interface loads

Reaction loads may be reduced by increasing the separation between the studs (called as footprint). The SAM supports this general line of thinking. However, in “Sleep Seat”, the reacting couple is provided by the reaction forces R1 (stud) and R2 (seat-track interface load), multiplied by the separation between these reaction forces, L. (Figure 10-18 setup for a 2-stud configuration).

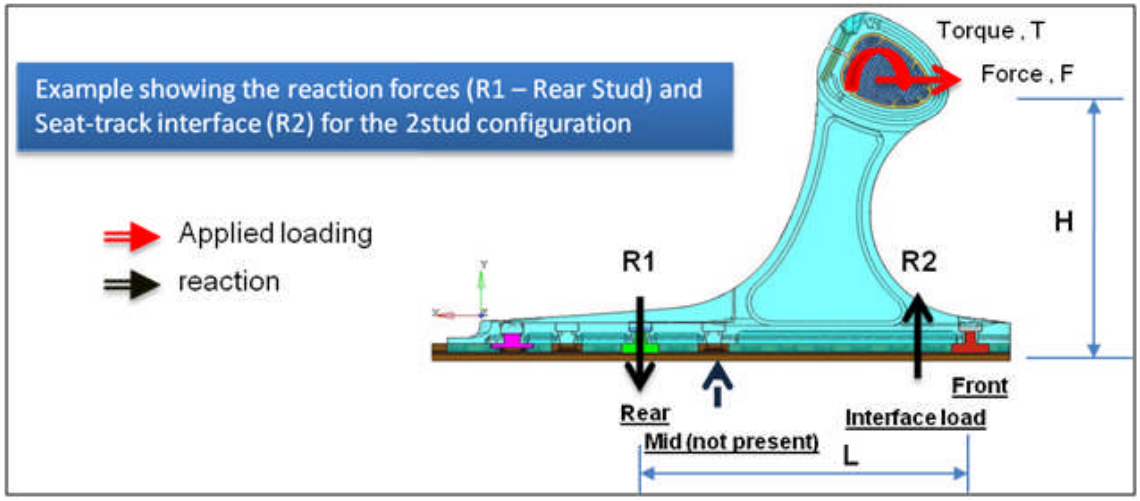

Figure 10-18 Reacting couple offered by the Track-leg Interface and Rear Stud

As the front stud does not offer any vertical reaction for the “Forward 9g” Load case, moving front stud in front direction will not be useful.

SAM does not account for frictional forces developed between mating components due to their relative movement e.g., between seat track and “Aft Stud Housing”. Whereas, coefficient of friction is an important input while defining contact pairs in FEA. In addition, SAM does not offer any information regarding the change in stress pattern as stud location is changed. With the help of FEA, sensitivity studies can be performed (has been actually done in present research for Leg V#8 as explained in Appendix H.3) to assess the changes in distribution of the resulting stress due to different stud configurations.

Therefore, it was decided to use FEA to calculate seat track interface loads.

Appendix H Leg Designs from V#1 – V#8

As seen in Section 8.3, first eight design concepts for leg (Leg V#1 – V#8) were directly attached to the seat track. However, “Boeing Specifications” (received after seven months from initial start date of this research) insisted that leg should not be directly attached to the track; instead, a separate bock should be used [35]. Therefore, basic idea with which leg was designed (V#1 – V#8) was changed. However, FE models developed for these leg variants and design modifications done for strength improvement were directly applicable for the new leg design (V#9). This appendix takes an overview of activities done for three base models of leg (V#1, V#3 and V#8). Remaining leg variants were based on these designs with little modifications (e.g. increase in wall thickness).

H.1 Leg V#1

BlueSky provided this design. Preliminary FE model of “FWD beam and leg” was used for analysing “Forward 9g”. Loads and support conditions as explained in Section 5.2.1. Von Mises stress levels observed in the leg (Figure 10-19) were very high.

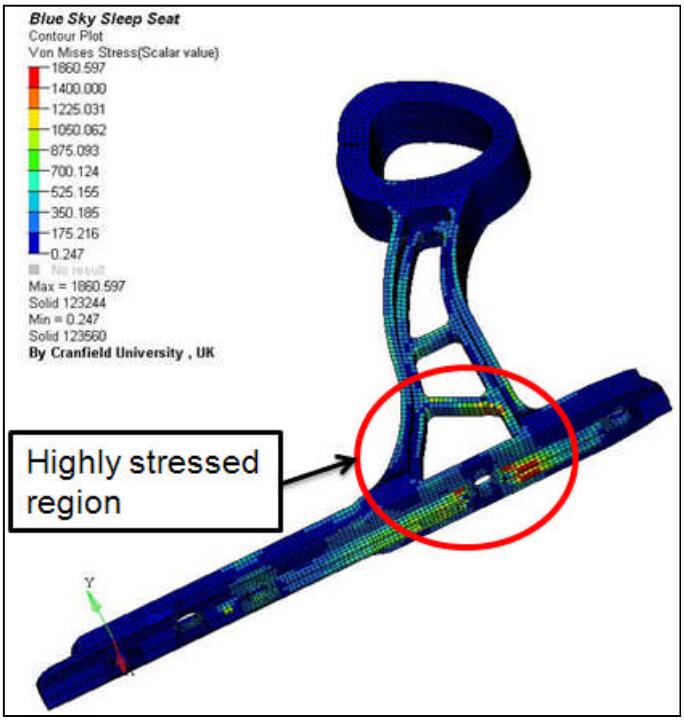

Figure 10-19 Von Mises stress contour for the leg V#1 without nodal averaging (Forward 9g)

It can be inferred from Figure 10-19 that,

- Maximum von – Misses stress of 1800 MPa is observed at the underside of the foot section near the mid bolt. Though it is unrealistic (since elastic material model has been considered), it is well above the yield point of a general aluminium alloy (375 MPa). This indicates that present design is very weak and needs substantial design modifications.

- Upper foot-section that is near the front web is a weak section (Highly Stresses region in Figure 10-19). Leg bends about this section inducing very high von Mises stress. Hence, this region should be a solid region. Thickness of the foot section of the leg is 4 mm, which should be increased to its upper limit fixed by manufacturing constraints.

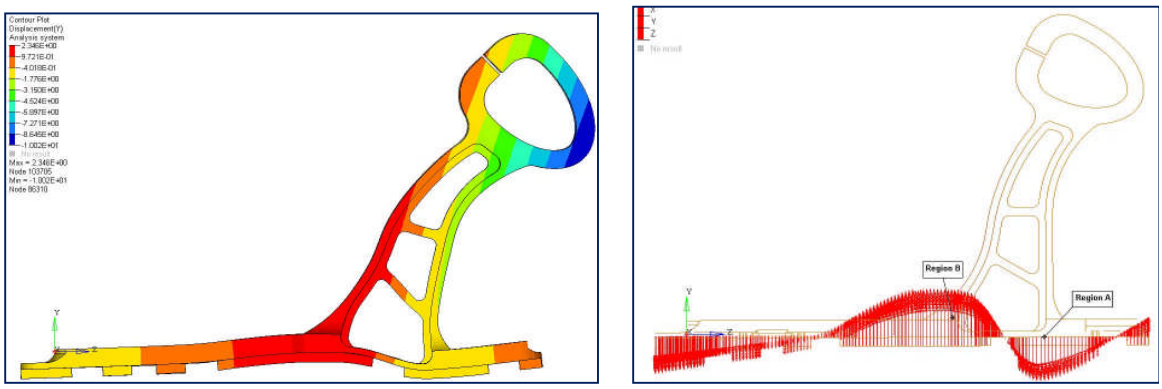

Figure 10-20 Vertical (Y) displacement behaviour of the leg V#1 – FWD 9g

It is interesting to note that the displacement behaviour of the leg V#1 is pivoted at the mid bolt (Figure 10-20). Portion of the leg in fore of mid bolt, moves in downward direction whereas aft portion moves in upward direction. Because of this, region around mid bolt is subjected to high von Misses stress. Therefore, mid bolt should be shifted in aft direction i.e. towards “region B” so as rear (aft) part of leg starts contributing in terms of load carriage.

Relocation of mid bolt to further aft direction can be further justified by carefully studying the Table 10-2, which gives vertical reaction forces for each of the bolt. Vertical reaction force (F_Y) in the mid bolt is about 3.5 KN as compared to that

of 12.8 KN observed in the rear bolt. Therefore, mid bolt is “ineffective” in terms of offering resistance to the applied “Forward 9g” loads. Relocation of mid bolt to more rearward direction will offer more reacting moment, which will reduce F_Y observed in the front bolt and in rear bolt.

Forward 9g load (CS 25.561) - Leg #V1	
Bolt Location	**Vertical Reaction Force, F_Y (KN)**
Front	**-16.2**
Mid	**3.5**
Rear	**12.7**

Table 10-2 Reaction forces at the Front, Mid and Rear bolts for leg V#1 (Forward 9g)

H.2 Leg V#3

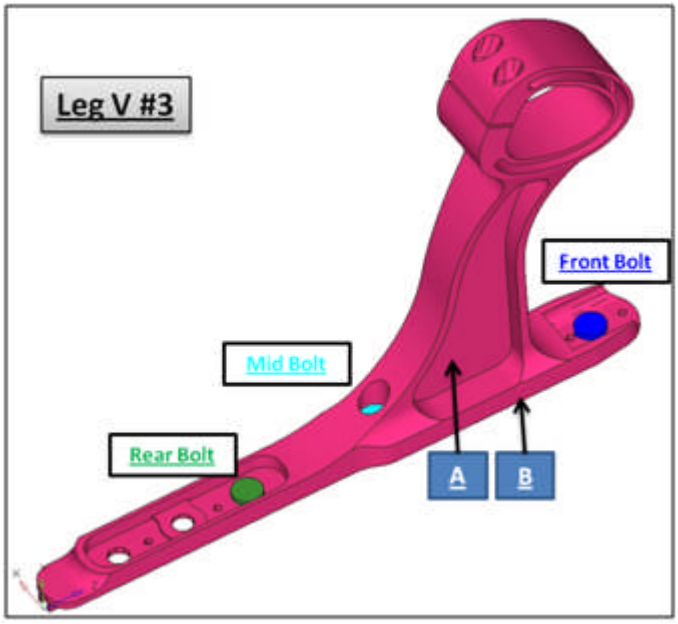

Figure 10-21 Design of the leg variant #3

A list of design changes made over LegV#1 can be put as follows (Please refer Figure 10-21),

- “A” indicates that the Central web has been completely filled.
- “B” indicates that thickness of central base plate has been increased from 4mm to 12.5 mm.
- Mid bolt has been moved rearward.

Maximum von Misses stress has come down from 1800 MPa to 560 MPa (Figure 10-22). Please note that as non–linear material properties have not been considered actual value of stress is unrealistic. Location of maximum stress has changed from foot-section (in Leg V #1) to upper aft throat area. Upper forward throat area experiences von Mises stress of 440 MPa.

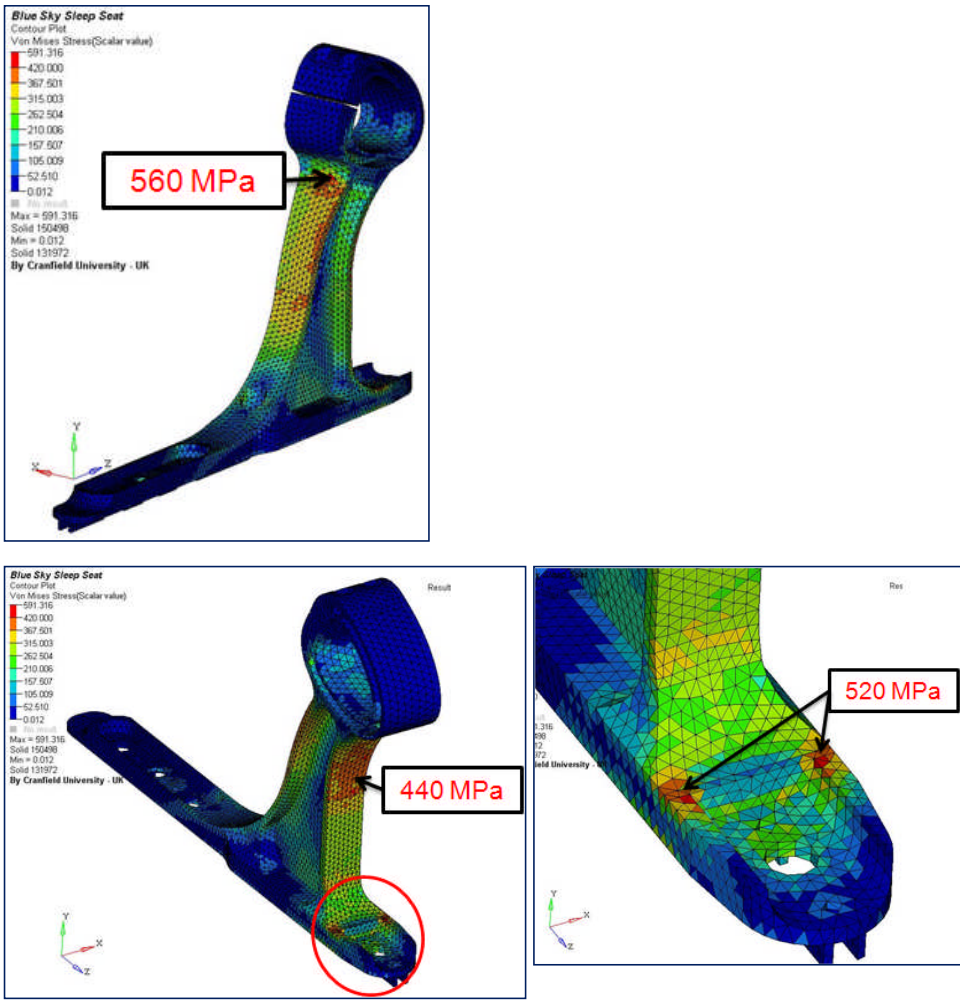

Figure 10-22 von Mises stress plot for the leg variant # 3 without nodal averaging (Forward 9g)

Mid solid web has proven to be beneficial as it has increased second moment of area. Relocation of mid stud in aft direction has lowered the F_Y observed in front and rear studs (Table 10-3).

Forward 9g load (CS 25.561) - Leg #V3/#V1		
Bolt Location	Vertical Reaction Force, FY (KN)	
	Leg #V1 (previous)	Leg #V3 (latest)
Front	-16.2	-14
Mid	3.5	8.1
Rear	12.7	5.9

Table 10-3 Lower reaction forces at Front, Mid and Rear bolts for leg V#3 (Forward 9g) compared to those in Leg V#1

Hence, both the proposed design modifications proved to be beneficial. An important point to note here is that, the decisions to modify the designs were taken considering all components of stress (e.g. principle stress, bending stress). The details are present in internal deliverables. In order to keep the number of pages of this report under control, only von Mises plots have been provided.

Maximum von Mises stress (560 MPa) observed in Leg V#3 was still above the yield limit (375 MPa). In addition, von Misses stress of magnitude 520 MPa was observed in the lower forward throat area (Figure 10-22) due to abrupt change in geometry. Therefore, curvature in this area was extended in next leg design (V#8), to spread the load across a larger section of seat track.

H.3 Leg V#8

Design changes made in leg V#8 were (Figure 10-23),

- Smoother transition from mid web to foot section in front area.

- In previous leg variants, length of mid bolt is 28 mm where as length of other two bolts i.e. front and rear bolts is 16 mm. In Leg #V8, all the three bolts are of same length (i.e. of 16 mm), so that the land from the seat platform upwards is same, all along the leg (Input from BlueSky).
- Increase flange separation from 30 mm to 50 mm(B- Figure I-5)
- Increase flange thickness from 5mm to 6mm.
- Width of leg head (A–Figure 10-23) increased from 40 mm to 50 mm.

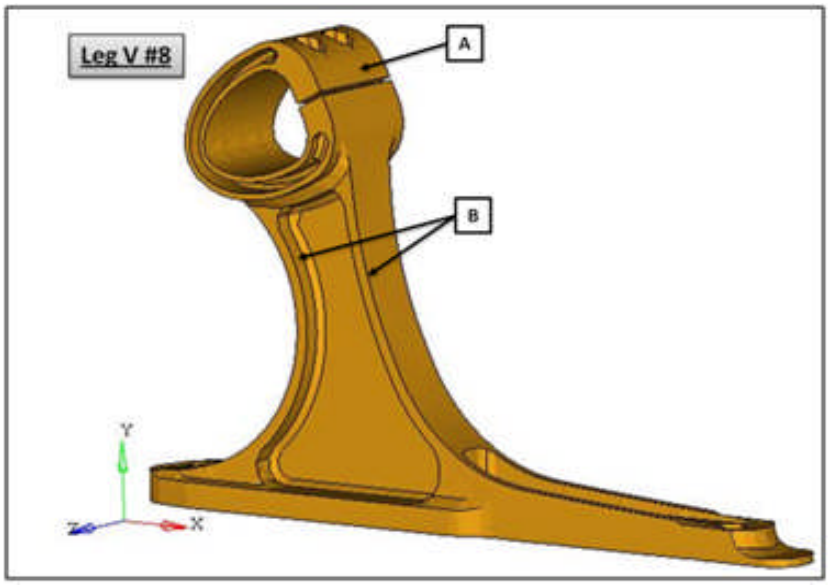

Figure 10-23 Design of the Leg Variant #8

Using intermediate FE model of “FWD beam and Leg V#8” (as explained in Figure 5-1), three different configurations were simulated for “Forward 9g” (Figure 10-24). Outputs extracted from the FEA results were, seat interface loads and stress contours for major components involved in the analysis. In coming Section, results for Configuration 3, have been discussed as it was found to be a better arrangement than other two configurations.

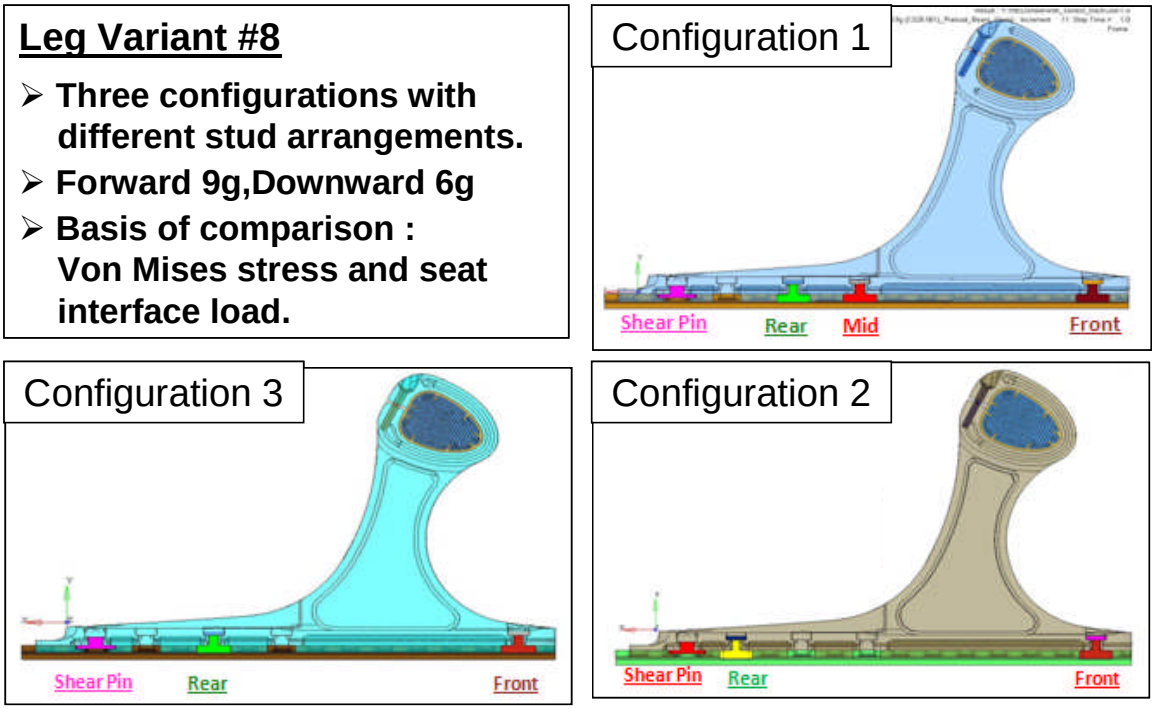

Figure 10-24 Three Different Configurations for the Leg V#8 based on Stud Arrangement

Discussion of FEA results for Leg V#8- Configuration 3

- Maximum von Mises stress of 325 MPa is observed in upper front throat area (Figure 10-25), which is a significant improvement over previous, design (560 MPa in Leg V#3). As the maximum stress is less than the yield limit, design is safe from structural point of view for “Forward 9g” loads.

- As the mid stud is removed, spacing between rear stud and track-leg interface (which provides reacting couple for applied “Forward 9g” load) increases. Therefore, lower seat interface loads were observed in Configuration 3 than those in Configuration 1 (Details are not provided here). Though the interface loads were still lower in Configuration 2 (than those in Configuration 3), higher von Mises stress was observed at the lower aft throat region.

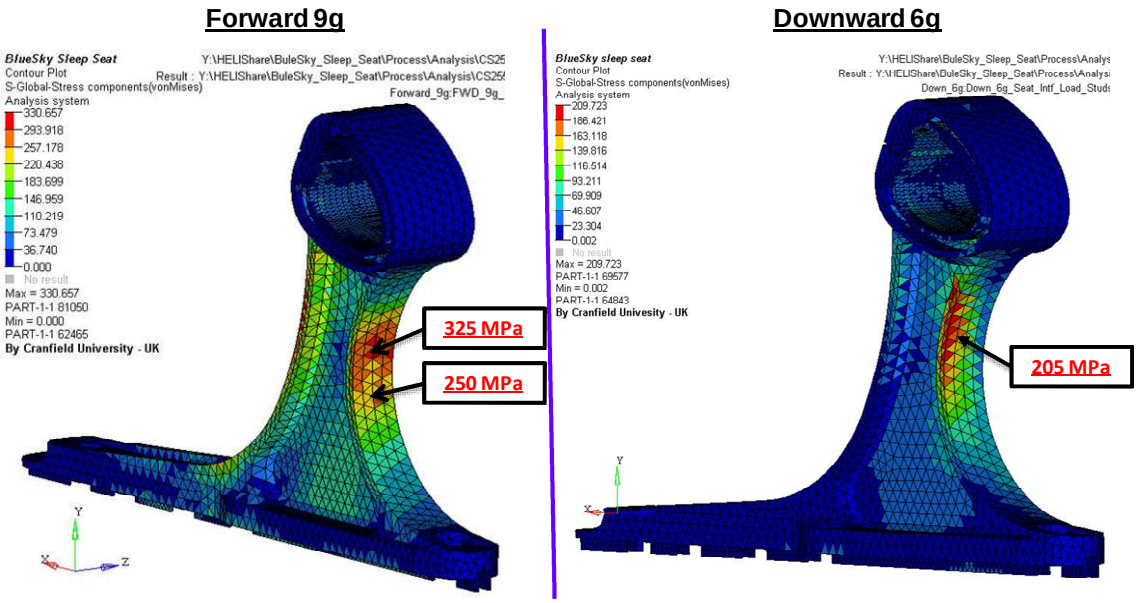

Figure 10-25 von Mises stress plot for Leg V# 8 (Configuration 3) without nodal averaging – Forward 9g and Downward 6g

- For “Downward 6g” load case, the central web in the leg governs the design. Therefore, the von Mises stress contours and values observed for all the three configurations are same.

- Since the maximum von Mises stress observed in the upper front throat area is 205 MPa that is below the yield limit, led design is safe against “Downward 6g” loads.

- It can be concluded that removal of the mid stud does not affect the strength and performance of the leg. Hence, Leg V#8 (Configuration 3) was a promising solution for static loads as per CS 25.561. Unfortunately, at this stage, “Boeing Specifications” were received and it changed the design philosophy of the leg. Learning from these models were absorbing while designing new leg variant V#9 (Section 8.3.1).

Appendix I Non-Linear Material Properties Used

Component name	Material Used	Modulus of elasticity , N/mm^2	Poisson's ratio
Beam, leg, tool-less fittings,C-clamp and beam insert,Track, boomerang,backrest tube,seat pan and connecting blocks	Alloy Aluminum (Al 2024)	7.10E+04	0.34

Al 2024 Input Data (MIL-HDBK-5H 1 Dec. 1998) *		Abaqus/Standard Input format	
Engineering Stress σ_{nom}, MPa	Engineering Strain, ξ_{nom}	True Stress σ_{true}, MPa	Log Plastic Strain $\xi_{pl\ ln}$
360.00	0.00	360.00	0
372.00	0.01	375.72	0.0046585
400.00	0.02	408.00	0.0140561
427.00	0.04	444.08	0.0329661
441.00	0.06	467.46	0.0516850
448.00	0.08	483.84	0.0701464
455.00	0.10	500.50	0.0882609

***** http://www.grantadesign.com/userarea/mil/mil5.htm

$$\sigma_{True} = \sigma_{nom}(1 + \varepsilon_{nom})$$

$$\varepsilon_{\ln}^{pl} = \ln(1 + \varepsilon_{nom}) - \frac{\sigma_{True}}{E}$$

Reference: http://129.25.22.58:2180/v6.7/books/usb/default.htm

Note - For current simulation, non-linear stress-strain relationship has been considered only for, leg, FWD beam, insert, C- Clamp, Boomerang.

Appendix J “Forward 9g” load from Spreadsheet

ASSUMPTIONS		
Mass of single passenger, Mp	77	kg
Acceleration due to gravity, g	9.81	ms^-2
Seat Belt Load Factor (xMp) - FWD 9g	9	(multiples of g)
Dynamic Load Factor - DOWN	0	(multiples of g)

SIDEBEAM LOADS				
Pc	**1490.10**	**N**	**4*Pc**	**12220.60**
Qc	**3055.15**	**N**	**4*Qc**	**5960.38**
Mc	**181.71**	**Nm**		

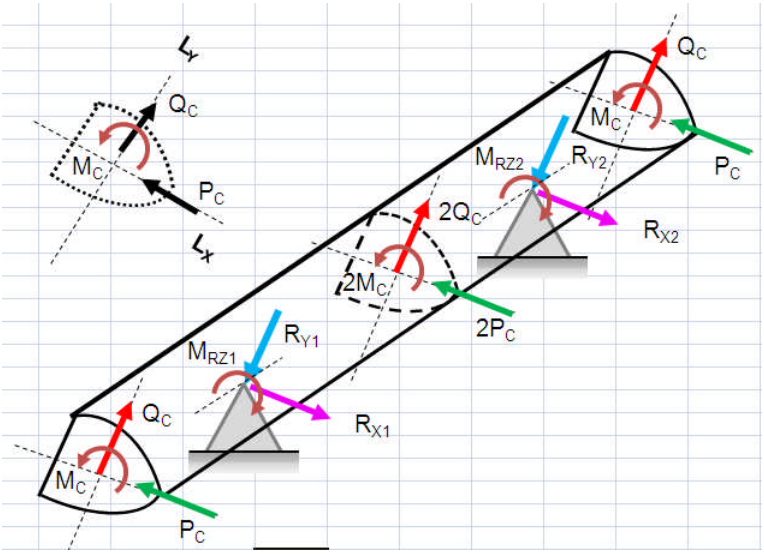

Figure 10-26 Converting "Forward 9g (CS 25.561)" load into the equivalent force and moment to be applied to the FWD beam, using Spreadsheet. Courtesy: CISM, Cranfield